Distribution Agreement

In presenting this thesis or dissertation as a partial fulfillment of the requirements for an advanced degree from Emory University, I hereby grant to Emory University and its agents the non-exclusive license to archive, make accessible, and display my thesis or dissertation in whole or in part in all forms of media, now or hereafter known, including display on the world wide web. I understand that I may select some access restrictions as part of the online submission of this thesis or dissertation. I retain all ownership rights to the copyright of the thesis or dissertation. I also retain the right to use in future works (such as articles or books) all or part of this thesis or dissertation.

Signature:

Rick Bienkowski	Date

The polyadenosine RNA-binding protein dNab2 interacts with the fragile X protein homolog and regulates gene expression in *Drosophila* neurons

By
Rick Stephen Bienkowski
Doctor of Philosophy

Graduate Division of Biological and Biomedical Sciences
Genetics and Molecular Biology

_____ _____

Kenneth H. Moberg, Ph.D.
Co-Advisor

Anita H. Corbett, Ph.D.
Co-Advisor

_____

Yue Feng, Ph.D.
Committee Member

_____

Gary J. Bassell, Ph.D.
Committee Member

_____

Andreas Fritz, Ph.D.
Committee Member

_____

Carlos Moreno, Ph.D.
Committee Member

Accepted:

_____

Lisa A. Tedesco, Ph.D.
Dean of the James T. Laney School of Graduate Studies

_____

Date

The polyadenosine RNA-binding protein dNab2 interacts with the fragile X protein homolog and regulates gene expression in *Drosophila* neurons

By

Rick Bienkowski
B.S., Cornell University, 2006
B.S., SUNY Stony Brook University, 2009

Advisors: Kenneth Moberg, Ph.D.
Anita H. Corbett, Ph.D.

An abstract of
a dissertation submitted to the Faculty of the
James T. Laney School of Graduate Studies of Emory University
in partial fulfillment of the requirements for the degree of
Doctor of Philosophy
in Genetics and Molecular Biology
2016

Abstract:

ZC3H14 is an evolutionarily conserved, ubiquitously expressed polyadenosine RNA-binding protein that is lost in an inherited form of non-syndromic intellectual disability (ID). Studies of ZC3H14 orthologs have revealed a conserved role for ZC3H14 in the restriction of poly(A) tail length, but the molecular function of this protein in neurons has not been defined. To further our understanding of ZC3H14 function in neurons we have utilized *Drosophila melanogaster* to model ZC3H14-associated ID. The *Drosophila melanogaster* ortholog of ZC3H14, dNab2, is required for viability in flies, and is critical for normal neuronal function and axon projection. Here we describe a network of physical and genetic interactions between dNab2 and the fragile X protein homolog dFMRP that link dNab2/ZC3H14 to translational repression. The dNab2 and dFMRP proteins co-precipitate from neurons and can be co-localized to cytoplasmic foci distributed along the neurites of cultured brain neurons. Two well-characterized dFMRP mRNA targets, *futsch* and *CamKII,* are repressed in a dNab2-dependent manner, providing strong evidence that dNab2 functions as a translational repressor in conjunction with dFMRP. In parallel, we find murine ZC3H14 enriched in axons of cultured primary hippocampal neurons and associated with the translational machinery, implying a conserved role for dNab2/ZC3H14 in the control of gene expression. These data suggest that dNab2/ZC3H14 contributes to dFMRP-mediated translational regulation of mRNAs trafficked to distal neuronal compartments, a process that is critical in neurons and may underlie brain-specific defects in ZC3H14-associated ID patients.

The polyadenosine RNA-binding protein dNab2 interacts with the fragile X protein homolog and regulates gene expression in *Drosophila* neurons

By

Rick Bienkowski
B.S., Cornell University, 2006
B.S., SUNY Stony Brook University, 2009

Advisors: Kenneth Moberg, Ph.D.
Anita H. Corbett, Ph.D.

A dissertation submitted to the Faculty of the
James T. Laney School of Graduate Studies of Emory University
in partial fulfillment of the requirements for the degree of
Doctor of Philosophy
in Genetics and Molecular Biology
2016

Table of Contents

List of Figures:

List of Tables:

Chapter 3:

Chapter 1: General Introduction

Introduction

The central dogma of molecular biology, originally proposed in 1958 by Francis Crick, describes the normal flow of genetic information within the cell: information encoded in DNA is transcribed into mRNA, and mRNA then directs the translation of protein (*1*). In this paradigm, it may seem that the only role of mRNA is to act as a physical intermediary between the nucleotide sequences of DNA and the amino acid sequences of protein. However, mRNA is a very highly regulated molecule that must be precisely processed and carefully controlled in order to maintain proper gene expression (*2*). These critical processing events are necessary for the control of gene expression and coordinated by a collection of RNA-binding proteins. The post-transcriptional regulation of mRNA by RNA-binding proteins profoundly affects the expression of downstream protein products.

The importance of post-transcriptional regulatory events *in vivo* is highlighted by the finding that inactivating mutations that disrupt RNA binding proteins are often associated with human disease (*3*). One such example is the *ZC3H14* gene, which encodes a ubiquitously expressed polyadenosine RNA-binding protein predicted to bind to all polyadenylated mRNAs (*4, 5*). Mutations in the *ZC3H14* gene are associated with a form of non-syndromic intellectual disability (*5*). This linkage raises a critical question: how can a defect in a ubiquitously expressed polyadenosine RNA-binding protein cause a brain-specific disorder? This dissertation investigates this question by utilizing a *Drosophila melanogaster* model of ZC3H14-associated disability. Here, I present data showing the fly homolog of ZC3H14, dNab2, is required for the proper neurodevelopment of the brain in flies (Chapter 2). I show that dNab2 physically

interacts with the *Drosophila* homolog of the fragile X mental retardation protein (FMRP), a protein that is lost in the most common form of inherited intellectual disability (Chapter 3). Furthermore, I show that dNab2 regulates the expression of an enzyme that controls actin polymerization, providing a molecular basis for how loss of dNab2 can lead to neurodevelopmental defects in the brain (Chapter 4). These data provide a foundation to understand the role of ZC3H14 in neurons, and elucidates how loss of this protein contributes to intellectual disability.

I. RNA-binding proteins are the Key Mediators of Post-transcriptional Regulation in Eukaryotes

A. Post-Transcriptional Processing of mRNA in the Nucleus

Proper mRNA biogenesis relies on a network of RNA-binding proteins that govern the production and processing of mRNA (*6*) (Figure 1-1). Some RNA-binding proteins interact generally with all mRNAs, while other are recruited to specific sequence motifs within target mRNAs. Before an mRNA can be exported from the nucleus, it must undergo a series of post-transcriptional modifications, including capping, splicing, cleavage and polyadenylation (*7*). In this processing, both ends of the RNA are substantially modified: a methylguanosine cap is added to the 5' end of the transcript (*8*), and a polyadenosine (poly (A)) tail is added to the 3' end (*9*). These features are specifically recognized and bound by RNA-binding proteins that increase the stability of the transcript and help facilitate translation (*10, 11*).

The 5' end processing of mRNA begins concurrently with transcription by RNA polymerase II, where a methylguanosine cap is added to 5' end of the nascent RNA. This cap serves to stabilize the transcript, and the first step of a major RNA degradation

pathway requires the cap to be removed before it can be degraded by a 5' to 3' exonuclease (*12*). The methylguanosine cap also facilitates translation, as the translation initiation factor eIF4e interacts directly with the cap (*11*). Processing of the 3' end of RNA begins when the transcript is cleaved at a polyadenylation signal found within the 3' UTR by an endonuclease, and a non-templated polyadenosine tail is then added to the end of the cleavage site. Older methods of quantifying poly(A) tail length suggest the poly(A) tail is about 250 nucleotides (nts) long in mammalian cells (*13*), while more sophisticated methods have estimated the poly(A) tail to have a median length of 70 nts (*14*). The proper regulation of poly(A) tail length is clearly important for proper gene expression (*14, 15*); however, the median length of poly(A) tails and the distribution of lengths during the life cycle of an mRNA transcript is currently unclear.

Polyadenylation allows mRNAs to recruit poly(A) RNA-binding proteins (Pabs), which in turn can increase the stability of the RNA transcript and facilitate translation (*16*) (Figure 1-2). One such Pab, PABPC1, is required to initiate translation, and participates in the circularization of mRNA and the formation of polysomes, which serve to enhance translational efficiency (*2*). In addition, longer poly(A) tails are thought to protect RNAs from degradation by the exosome, because this degradation occurs in a 3' to 5' manner and begins with the shortening of poly(A) tails by the CCR4/Not complex (*17, 18*). Traditionally, the poly(A) tail has been associated with translational efficiency, and it was generally thought that a longer poly(A) tail would lead to more robust translation (*19*). Although a minimal poly(A) tail is absolutely required for translation (*20*), the idea that poly(A) tail length universally correlates with translational efficiency has been challenged in recent years. Firstly, Gawky-182 (GW182), an RNA binding

protein associated with microRNA (miRNA)-mediated repression and deadenylation, binds to mRNA in a PABPC1- and poly(A) tail-dependent manner (*21, 22*). This suggests that a longer poly(A) tail can lead to translational repression and degradation in certain cases. More generally, transcriptome-wide sequencing and profiling of poly(A) RNA in a number of model systems including *Drosophila* (*14*) has shown the increased translation paradigm only holds true in the early stages of development; at later stages, and in cell lines, the length of the poly(A) tail does not correlate with translational efficiency, but with the stability of the transcript (*14*). Thus, the developmental and cellular context dictates whether poly(A) tail length affects translational efficiency or transcript stability. Both ZC3H14 and dNab2 act to limit the length of poly(A) tails *in vivo* (*5, 23*), suggesting that ZC3H14/dNab2 function could be linked to poly(A) dependent RNA regulation.

In addition to the 3'-end and 5'-end processing of mRNA, transcripts must be spliced before they can be exported out of the nucleus. Metazoan mRNA contains large sections of non-coding RNA termed introns interspersed between the coding exons that must be removed before the transcript is translated by a ribosome (*2*). Splicing is the process by which these non-coding introns are removed by the spliceosome. mRNAs can also undergo alternative splicing, in which variable inclusion of certain exons can generate distinct polypeptides from a single RNA transcript. In this process, the controlled removal of certain exons, coupled with the ligation of non-adjacent exons, leads to the production of different mRNA isoforms or non-functional mRNAs that are degraded by nonsense-mediated decay (*24*). When genes are alternatively spliced, different isoforms of proteins may be made, creating functional variants of proteins. This

process must be tightly controlled, as certain mRNA transcripts are required at certain stages in development (*25*) and in a tissue-specific manner (*26*). RNA binding proteins in the nucleus are important for the processing of a pre-mRNA into a mature mRNA transcript, which must pass several quality control measures to be exported into the cytoplasm. Once the mRNA transcript is exported, it immediately associates with a number of cytoplasmic RNA-binding proteins that act to regulate the expression of the transcript.

B. RNA-binding Proteins in the Cytoplasm regulate gene expression

The terminal non-coding regions (or untranslated regions; UTRs) at the 3' and 5' ends of an mRNA contain regulatory information that allows the transcript to be targeted and regulated by specific sets of RNA binding proteins (*27*). Throughout the life cycle of an mRNA, transcripts associate with a wide range of RNA-binding proteins that contribute to transcript localization, stability and translational efficiency. These RNA-binding proteins act in concert with one another, and coalesce to form ribonucleoprotein particles (RNPs). RNPs are dynamic structures; the mRNA and protein constituents that form RNPs are continually shuttled in, out, and between granules, consequently effecting the RNA processing properties and stability of these mRNPs.(*28*). Distinct classes of RNPs are classified according to the individual RNA-binding protein components of the RNP and the overall function of the RNP. Here I will discuss three types of RNPs that contain Pabs and may be relevant to the role of dNab2 in cells: processing bodies (P-bodies), stress granules, and neuronal transport granules.

P-bodies are centers of mRNA turnover in the cytoplasm, and consist of aggregated non-translating mRNA, decapping enzymes, activators of decapping, and exonucleases. Many different RNA degradation pathways are mediated through P-bodies, including decapping enzyme-mediated-5' to 3' mRNA decay, CCR4/Not complex deadenylation, nonsense-mediated mRNA decay and miRNA-induced silencing (*29*).

Stress granules form a distinct class of RNP thought to be sites of temporary translational repression. RNAs found in stress granules are stalled in translation and co-localize with a subset of translation initiation factors, the 40S ribosomal subunit, and the cytoplasmic poly(A) binding protein PABPC1 (*30*). Additionally, a number of RNA-binding proteins that contain low-complexity domains (also referred to as prion-like domains, or self-aggregation domains) can be localized to stress granules (*28*). In budding yeast, stress granules formation is promoted by a number of environmental stresses, including nutrient deprivation, heat shock, and cold shock (*29*). Interestingly, the inhibition of translational initiation alone is sufficient to form stress granules (*29*). Mounting evidence suggests that mRNAs and RNA-binding proteins can dynamically move between P-bodies, stress granules, and polysomes, and suggest an "mRNA Cycle" of translation, inhibition, and decay (*29*).

A third type of granule, the neuronal transport granule, appears exclusively in neuronal tissue. These specialized RNPs are critical in neurons. Neurons are highly polarized cells that require specific RNAs to be silenced and transported to the distal dendrites or axon terminals where they are locally translated; in some cases, the site of translation of RNA can be on the order of a meter away from the nucleus. The localization of the β–actin mRNA is a paradigm for the importance of correct mRNA

localization, as correctly localized β–actin mRNA is required for the function of growth cones (*31*). Neuronal transport granules are responsible for this translational repression and localization of RNAs to specific locations within the neuron (*32*). Evidence suggests that these RNPs are first formed in the nucleus, then exported into the neuronal cytoplasm (*33*). Neuronal transport granules contain many of the same RBP components that are found within P-bodies and stress granules (*30*), and contain eIF4e and inhibitors of translation, including the RNA binding protein Fragile X Mental Retardation Protein (FMRP) (*33*).

FMRP is a negative regulator of translation (*34, 35*) that is essential for local protein translation. FMRP can localize to axons terminals, dendrites and dendritic spines, where it binds and represses the translation of mRNAs (*36, 37*). FMRP can be phosphorylated in response to local signals, such as mGluR activation (*38*), thus relieving the repression and allowing translation to occur. Local protein translation in dendrites mediates synaptic plasticity, the process that is thought to underlie learning and memory (*39, 40*). Importantly, the loss of FMRP dysregulates the local translation of protein in neurons and leads to fragile X syndrome (discussed in section II).

II. Mutations in the *ZC3H14* Gene Cause Intellectual Disability

A. Mutations in Genes that Encode RNA-binding Proteins Cause Human Disease

The post transcriptional regulation of RNA is vital for proper cellular function, and is underscored by the fact that many mutations in genes encoding RNA-binding proteins are associated with human disease (*41*). Disease-causing mutations can be found in genes that operate at every step of RNA processing and regulation. For example, loss of expression of SMN1, a factor that has been implicated in the regulation of splicing and in

the neuronal transport of mRNAs (*42*), gives rise to Spinal Muscular Atrophy. Mutations in *PABPN1*, a gene which encodes a nuclear RNA-binding protein essential for proper mRNA polyadenylation and export from the nucleus, is associated with Oculopharyngeal Muscular Dystrophy (*43*). Additionally, loss of FMRP, a negative regulator of translation, is the cause of Fragile X Syndrome, the most common cause of inherited intellectual disability (*44, 45*). One interesting observation drawn from the examples provided above is that defects in ubiquitously expressed RNA-binding proteins can nonetheless give rise to tissue-specific pathology: mutations in *SMN1* and *FMR1* primarily affect neuronal tissue, and *PABPN1* mutations affect muscle. This theme has been reinforced in our analysis of the ubiquitously expressed *Drosophila* polyadenosine RNA binding protein dNab2, which we find is specifically required in neurons and supports axonogenesis.

B. Fragile X Syndrome is Caused by the Loss of Expression of FMRP

Fragile X syndrome (FXS) is the most commonly inherited form of intellectual disability and represents a significant fraction of autism spectrum disorder (ASD) cases, with an incidence of about 1 in 4000 live births (*37*). Patients diagnosed with FXS suffer from severe cognitive impairment, autism-associated behaviors, and stereotyped physical features, including elongated faces and macroorchidism (*37*). FXS is caused by the loss of function of a single gene, *FMR1,* and the associated protein product Fragile X mental retardation protein (FMRP) (*44*). The loss of expression of FMRP in FXS patients is most commonly due to a CGG nucleotide expansion found in the 5’ UTR of the *FMR1* gene. Once this CGG expansion reaches a critical threshold of 200 repeats, the gene is targeted

by chromatin modifying enzymes and is epigenetically silenced, leading to the complete loss of the FMRP expression (*37*).

FMRP interacts with a subset of cellular mRNAs and represses their translation (*35*) via three distinct RNA-binding domains: two hnRNP K homology domains (KH domains) and a single RGG domain (rich in arginines and glycines) (Figure 1-3). FMRP is thought to play a number of critical roles in mRNA regulation within neurons, including translational repression of mRNAs, transport and localization of mRNAs to pre- and post-synaptic sites, and the activity-dependent local translation of target mRNAs (*45*). FMRP is an exceptionally well-studied protein, and the physical and functional consequences of loss of FMRP have been studied in a number of model systems, including fly and murine models (*45*). Loss of FMRP leads to a number of defects in neuronal architecture, including aberrant synaptic development (*46*), excessive dendritic branching (*47*), increased dendritic spine density (*48*), and defects in growth cone mobility (*49*). Loss of FMRP also has functional consequences in neurons, impairing synaptic plasticity (*50*), long-term depression (*51, 52*), and activity-dependent translation (*53, 54*).

dFMR1 encodes the *Drosophila* Fragile X-protein (dFMRP). dFMRP regulates translation by binding directly its target mRNAs and the 80S subunit of the ribosome (*55*). *dFMR1* mutant flies display a number of neurological defects including inappropriate development of the mushroom bodies (*56*), a neuropil structure in the brain, and deficits in learning and memory (*45*). These *dFMR1* null phenotypes are proposed to arise due to the dysregulation of dFMR1-bound mRNAs; however, the full range of transcripts regulated by dFMR1 is not well defined. Multiple labs have attempted to

identify FMRP-target RNAs through a variety of transcriptome-wide methods, but these endeavors have produced largely non-overlapping datasets (*57, 58*). However there is a small subset of validated dFMR1-repressed mRNAs targets in *Drosophila*, including *fustch* (*59*), *CaMKII* (*60*), and *chickadee (profillin)* (*61*). Depletion of these dysregulated targets is able to partially rescue *dFMR1* null phenotypes, supporting the hypothesis that phenotypes observed in *dFMR1* null flies are due to excessive translation of mRNAs normally repressed by dFMR1 *in vivo*.

While the *Drosophila* genome encodes only one fragile X gene, *dFMR1*, the mouse and human genomes contain three fragile X related genes. In addition to *FMR1*, mice and humans possess the autosomal *fragile X related 1* and *2* genes (*Fxr1, Fxr2)* (*62*). FXR1 and FXR2 are paralogs of FMRP, sharing about 60% of amino acid identity with FMRP (*63*). FXR1 and FXR2 are highly expressed in the brain comparably to FMRP, though these paralogous proteins are differentially expressed in non-neuronal tissues, including skeletal and cardiac muscle.(*64, 65*).

FMRP, FXR1, and FXR2 can coalesce into structures known as fragile X granules (FXGs) in neurons (*66*). FXR2 is absolutely required for FXG formation and is observed as a component of all FXGs (*67, 68*), while FMRP and FXR1 can only detected in FXGs found in specific neuronal subtypes (*66*). FXR2 displays a distinct subcellular distribution in neurons and is preferentially expressed in axons and in pre-synaptic terminals (*67, 69*). FXR2 is essential for the axonal and pre-synaptic localization of FMRP, and this requirement suggests that the axonal and presynaptic functions of FMRP are dependent on FXR2 (*69*). Given that *Drosophila* only express one fragile X protein, dFMRP may serve the role encompassed by all three paralogs in mammals, and loss of dFMRP

expression in *Drosophila* may uncover phenotypes not observed when mammalian FMRP is lost due to redundant functions of FXR1 and FXR2.

C. ZC3H14 is an Evolutionarily Conserved RNA-binding Protein

ZC3H14 (also termed mSut2; (*70*)) encodes a Cys_3His (CCCH) tandem zinc finger (ZnF) polyadenosine RNA-binding protein. ZC3H14 is evolutionarily conserved, and orthologs can be found in a number of model organisms including *S. cerevisiae* (Nab2), *C. elegans* (Sut2), and *D. melanogaster* (dNab2) (*71*). The domain structure of these proteins is well-conserved, including an N-terminal PWI (proline/tryptophan/isoleucine)-like domain that is thought to facilitate export from the nucleus (*71*), a centrally located nuclear-localization sequence, and a C-terminal domain of five CysCysCysHis (CCCH)-type zinc fingers that mediates RNA binding (*4, 5*) (Figure 1-4). ZC3H14 protein is found predominantly in the nucleus at steady-state, and is widely expressed in many tissues, including the brain (*4, 5*).

While *ZC3H14*-related genes from a number of different species encode a single protein isoform (e.g. yeast Nab2 and fly dNab2), mammalian *ZC3H14* encodes at least four protein isoforms that are generated by alternative RNA splicing and use of an alternative first exon (*4*). The mammalian isoforms 1, 2, and 3 encode a full-length protein that contains all functional domains (PWI-like, NLS, and CCCH), while isoform 4 utilizes a unique first exon and lacks the PWI-like and NLS domains, but retains the RNA-binding CCCH-domain. Isoform 4 is found primarily in the cytoplasm, suggesting that it may serve a unique, divergent molecular function from isoforms 1-3. Accordingly,

the full-length ZC3H14 isoforms 1-3 are evolutionarily conserved, while the truncated isoform 4 is not (*71*).

The best studied ortholog of *ZC3H14* is the *S. cerevisiae* Nab2 protein. Nab2 is an abundant nuclear protein that binds polyadenosine RNA with high affinity and restricts poly(A) tail length and export of mRNA from the nucleus (*72-74*). Mammalian ZC3H14 also preferentially binds to polyadenosine RNA *in vitro*, and depletion of ZC3H14 leads to the extension of poly(A) tail length (*5, 23*). However, no nuclear export defect has been observed in ZC3H14-depleted mammalian cells, which suggests that mammalian cells might have evolved a redundant mechanism for nuclear export

D. Mutation of *ZC3H14* Causes Non-syndromic Intellectual Disability

Intellectual disability, formerly referred to as mental retardation, is a neurodevelopmental disorder defined by general impairments in adaptive functioning and intelligence quotient (IQ) scores below 70 (*75*). Patients diagnosed with intellectual disability often display substantial deficits in self-management and personal care, relying on others to accomplish everyday tasks. The reliance on others comes at a great personal cost for the individual family caregivers, and significant economic costs for the healthcare system as a whole; the lifetime healthcare cost for an individual with intellectual disability can exceed 2.2 million dollars in the United States (*76*). With an estimated prevalence of intellectual disability between 1%-2% in the US (*77*), caring for those with intellectual disability creates a significant economic burden.

Although intellectual disability is a relatively common disease, the underlying causes are not well understood. Many well-defined environmental and genetic factors can increase the risk of intellectual disability (*78-80*); however, there is no clear cause for

intellectual disability in up to 60% of cases (*81*). By furthering our understanding of the molecular pathways that are dysregulated in intellectual disability, we may one day be able to develop treatments that ameliorate the symptoms of intellectual disability. One strategy to elucidate the root causes of intellectual disability is to focus on forms of intellectual disability that are caused by single gene mutations. Studying the monogenic causes of intellectual disability allows for characterization of the molecular dysfunctions that occur in intellectual disability and identify the particular pathways that support proper brain function.

Recently, mutations in *ZC3H14* were identified that cause an inherited form of autosomal recessive, non-syndromic intellectual disability (*5*). Mutations in *ZC3H14* were first identified in an autozygosity mapping performed on a cohort of patients diagnosed with non-syndromic intellectual disability in rural Iran. This analysis identified a large region of homozygosity on chromosome 14, and sequencing of this region revealed homozygosity for inactivating mutations within the *ZC3H14* locus that segregated with the occurrence of non-syndromic intellectual disability (*5*). *ZC3H14* homozygous mutant individuals display IQ scores between 30-50. One of the identified mutations, R154X, creates a nonsense mutation in exon 6 predicted to yield a truncated ZC3H14 protein lacking any capacity for RNA binding. Lymphoblast cell lines generated from patient cells confirm the R154X mutation completely ablates expression of the evolutionarily conserved ZC3H14 isoforms 1-3, while expression of ZC3H14 isoform 4 remains intact (*5*).

Importantly, patients homozygous for deleterious mutations in the *ZC3H14* lack any associated dysmorphic features (*5*), suggesting a specific role for the ZC3H14 protein

in nervous system development or function. Consistent with a putative role in neuronal function, ZC3H14 is enriched in mammalian hippocampal neurons relative to glia (*5*), and ZC3H14 co-localizes with poly(A) RNA puncta in the pyramidal cell layer of the hippocampus in mice(*5*). These data suggest a critical role for ZC3H14 in the central nervous system. Because of the small number of patients and limited availability of tissue, studying the function of ZC3H14 directly in human cells is not feasible. However, it is possible to study the neuronal role of *ZC3H14* in model organisms with a functioning nervous system. This rationale led us to generate a *Drosophila* model of *ZC3H14*-associated intellectual disability.

III. The polyadenosine RNA-binding protein dNab2 is the *Drosophila melanogaster* homolog of ZC3H14

A. *Drosophila melanogaster* as a model system to study human neurological disease

Drosophila melanogaster makes an ideal model system for the study of ZC3H14. First and foremost, ZC3H14 is evolutionarily conserved in *Drosophila*, and the major RNA-processing pathways are well conserved from *Drosophila* to humans. This means that findings from experiments in *Drosophila* could be conserved in humans and possibly be directly relevant to the pathology and etiology of *ZC3H14*-associated non-syndromic intellectual disability in human patients.

Second, *Drosophila* has many practical advantages over other model systems. The fast generation time of *Drosophila* is ideal for the rapid screening of many candidate alleles. *Drosophila* also has the most diverse genetic "tool kit" available to manipulate gene expression with temporal and spatial precision at all stages of development and in all tissues. The core of this tool kit is the yeast-derived *UAS-Gal4* system (*82*), which allows for the precise spatiotemporal control of gene expression or RNAi knockdown of

transgenes, and allows for the tissue-specific overexpression and knockdown of target genes. Additionally, the large community of *Drosophila* researchers readily and enthusiastically shares key reagents and resources between laboratories.

Third, *Drosophila* has been utilized as a model system to study learning and memory since the 1970's (*83*), and evolutionarily conserved genes that contribute to learning and memory were first identified in *Drosophila* genetic screens (*84*). A number of learning and memory paradigms have been developed in *Drosophila,* including visual, and olfactory learning, although olfactory learning and classical conditioning have shown to be the most robust forms of learning for the laboratory setting (*85, 86*).

In addition to learning and memory paradigms, fly models of human intellectual disability have been developed prior to our *ZC3H14/dNab2* model. The most well characterized model of human intellectual disability in *Drosophila* is the model of Fragile X syndrome (FXS). In humans, FXS is caused by the loss of the FMRP protein. The *Drosophila* model of FXS utilizes a null allele of *dFMR1(87)*, the fly equivalent of the gene that encodes FMRP. Flies lacking dFMRP show impaired learning and memory, developmental defects in neuronal architecture, and deficiencies in neuronal plasticity (*46, 47, 88, 89*). Importantly, findings made in the *Drosophila* model of FXS are conserved in Fragile-X pathology across a number of model systems: for example, the overactivation of pathways downstream of the mGluR receptor (*90*) and the overactivation of the PI3K pathway (*91*) occur in flies and mammals. In Chapter 3 of this dissertation, we characterize genetic and functional interactions between the *dNab2* and *dFMR1* genes, and identify a physical interaction that occurs between the proteins encoded by these two genes.

B. The *Drosophila melanogaster* model of ZC3H14-associated intellectual disability

dNab2 encodes the *Drosophila melanogaster* ortholog of the ZC3H14 protein *(5).* Although the dNab2 protein only shares ~41% amino acid identity with ZC3H14 isoform-1 (iso1) (BLASTP, NCBI), their domain structure is remarkably well conserved: each contain an N-terminal PWI-like domain, a predicted NLS, and five tandem CCCH-type Zinc fingers within a C-terminal RNA-binding domain (*5*). To model the *ZC3H14* loss in *Drosophila,* mutant alleles of *dNab2* were created through the imprecise excision of the P-element *EY08422* (*5*) found at the 5' end of the *dNab2* gene locus (*92*). The $dNab2^{ex3}$ excision allele removes a large portion of the gene, including the transcription start site, and creates a complete RNA and protein null (*5*). The $dNab2^{ex3}$ allele has been used for all subsequent studies, and flies homozygous for the $dNab2^{ex3}$ allele are referred to as "dNab2 null" throughout this dissertation.

dNab2 is required for normal development and viability in *Drosophila*: zygotic loss of dNab2 leads to a high rate of pupal lethality with only 3%-5% of $dNab2^{ex3}$ homozygotes surviving to adulthood, and further loss of the maternal supply of *dNab2* deposited in the oocyte leads to very early embryonic lethality (*5, 23*). $dNab2^{ex3}$ zygotic mutants that survive to adulthood have a number of phenotypes that are consistent with neuronal dysfunction and are absent from their isogenic control counterparts (*dNab2 precise-excision#41* or $dNab2^{pex41}$). Adult *dNab2* null flies have a severe locomotor defect and cannot fly. These flies also have a wings-held-out phenotype and cannot fold their wings behind their back, which is a phenotype commonly found in flies with neuronal dysfunction. Additionally, the adults exhibit a bristle defect in which the bristles are disordered and kinked.

Though the phenotypes described above could arise through defects in a number of different tissues, including neurons, muscles, or glia, all of the above-described phenotypes are due to loss of dNab2 specifically in neurons. This was shown using two complementary approaches. First, RNAi-mediated knockdown of *dNab2* with a neuronal *Gal4* driver is sufficient to elicit locomotor and flight defects (*5*), whereas knockdown of *dNab2* with muscle- or glial-specific drivers did not recapitulate these phenotypes. In the second line of experimentation, *dNab2* null phenotypes were efficiently rescued through the re-expression of transgenic *dNab2* only in neurons (*5*). Expression of a *UAS-Flag-dNab2* transgene in the neurons of flies otherwise null for dNab2 rescues all of the defects associated with $dNab2^{ex3}$ allele homozygosity. These experiments definitively show that *dNab2* expression is required for normal neuronal function, and that behavioral and developmental phenotypes in a *dNab2* null fly are specifically due to a loss of dNab2 expression in neurons. Importantly, recent work has shown that expression of human ZC3H14 isoform-1 in the neurons of *dNab2* null flies is also sufficient to rescue a subset of *dNab2* null-associated phenotypes; *dNab2* null flies that express transgenic *ZC3H14-iso1* in neurons show markedly better rates of survival and enhanced locomotor activity (*23*). These pivotal findings provide evidence that ZC3H14 is a true functional ortholog of dNab2.

C. The development of the mushroom bodies provides a paradigm for axon guidance

Chapters 2, 3, and 4 of this dissertation describe defects in the development of the mushroom bodies (MB) within the brains of flies that lack *dNab2.* The mushroom bodies are bilateral neuropil brain structures found in the *Drosophila* brain (*93*). Each lobe is

composed of a group of about 2500 neurons known as Kenyon cells (*94*). The cell bodies of these neurons are situated at the dorsal posterior surface of the central brain, and the dendrites form the *calyx,* directly below the cell bodies (*93*). Kenyon cell axons project ventrally to form the *peduncle* and eventually split to form the α, α', β, β', and γ lobes (*93*). These lobes originate from three separate groups of mushroom body cells; α and β lobes originate from a single group of bifurcated axons, α' and β' lobes are formed from a second distinct group of bifurcated axons, and the γ lobes from a separate third group (*93*). These structures of the MB arise sequentially, with the γ lobes forming in the early larval stages, the α' and β' lobes forming in late larval development, and the α and β lobes forming during pupal development.

The mushroom bodies are required for learning and memory and are thought of as an analog to the mammalian hippocampus (*94*). Chemical or genetic ablation of the mushroom bodies severely impairs learning and memory in olfactory assays (*95*). Additionally, many fly mutants with defective mushroom body structure are also impaired in olfactory learning (*96*) . The role of the mushroom bodies in learning and memory has been genetically dissected with a temperature sensitive *shibire* allele, allowing for the inactivation of individual MB lobes in a temporal manner (*85*). The α, α', β, β', and γ lobes all play a role in the learning and memory process, and it is thought that the α and β lobes function specifically in memory retrieval (*85*). Accordingly, *Drosophila* mutants with defects in the structure of the α and β lobes commonly have coincident deficits in learning and memory (*85*). In Chapter 2, we will discuss mushroom body defects observed in *dNab2* null flies in greater detail and describe learning and

memory deficits that arise in adult flies when *dNab2* is knocked down in the mushroom bodies.

IV. Summary and scope of the dissertation

ZC3H14 encodes an evolutionarily conserved, polyadenosine RNA binding protein required for the proper control of poly(A) tail length. ZC3H14 is required for normal cognition in humans, and patients homozygous for inactivating mutations in *ZC3H14* are afflicted with a form of non-syndromic intellectual disability. Previous studies in model systems have revealed a critical role for ZC3H14 in restricting poly(A) tail length *in vivo.* In *Drosophila melanogaster,* the ZC3H14 ortholog dNab2 is essential in neurons for viability. Despite these findings, there has been very little insight into the molecular functions of ZC3H14/dNab2, or why these functions are especially critical in neurons.

The overarching goal of the research described in this dissertation is to further the understanding of the molecular basis of ZC3H14-associated intellectual disability, and to elucidate how loss of dNab2/ZC3H14 expression leads to cognitive defects in flies and humans. To this end, we have utilized our *Drosophila melanogaster* model of ZC3H14-associated non-syndromic intellectual disability to study the molecular and developmental consequences of *dNab2/ZC3H14* loss in flies. In **Chapter 2** of this dissertation, we describe a brain defect found in the mushroom bodies of flies that are depleted for dNab2. We establish that this is a cell-autonomous defect, and that loss of dNab2 specifically in the mushroom bodies is sufficient to cause this phenotype, and that expression of transgenic *dNab2* in the mushroom bodies of a fly otherwise null for *dNab2* is sufficient to rescue this phenotype. Additionally, this chapter provides the first evidence that depletion of *dNab2* in the mushroom bodies is sufficient to impair learning

and memory and to alter axon projection patterns within the mushroom bodies, establishing a role for dNab2 in the normal development and function of this critical brain structure. In **Chapter 3**, we describe genetic and functional interactions between *dNab2* and *dFMR1*, as well as physical interactions between the dNab2 and dFMR1 proteins. This observation links the function of dNab2 to dFMR1, the fly homolog of the fragile X protein, and connects the fly model of *ZC3H14*-associated disability to fragile X syndrome, the most commonly inherited form of intellectual disability and autism-spectrum disorder. This chapter also describes the discovery of a pool of dNab2 in the cytoplasm of fly and mouse neurons with an apparent role in translational regulation; this finding alters previous models that dNab2/ZC3H14 localize exclusively to the nucleus and suggests that its key role in neurons may be based on a role in cytoplasmic mRNA processing. An ultimate goal of these studies is to identify the mRNA transcripts that are normally regulated by dNab2, and to determine which of these dysregulated transcripts are responsible for dNab2 null phenotypes. In **Chapter 4**, we briefly describe a role for dNab2 in regulating the *still life (sif)* mRNA transcript, a putative Rho/Rac GEF, which my preliminary data show is required for mushroom body axon projection. Evidence suggests that *dNab2* normally represses this transcript, and upon loss of *dNab2,* the overexpression of *sif* can lead to axon guidance defects. This dissertation thus significantly extends our understanding of the molecular and cellular roles of *Drosophila* dNab2 and in doing so contributes to the body of knowledge regarding *ZC3H14*-associated intellectual disability. **Chapter 5** concludes by providing an overall context for the findings introduced in this dissertation, and discussing future directions and goals to move these studies forward.

Figures:

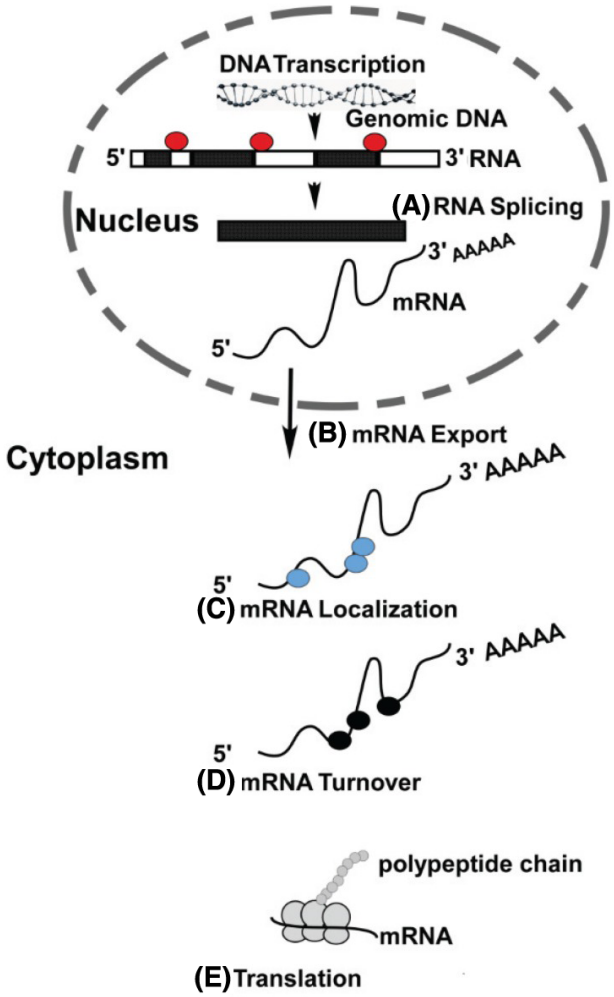

Figure 1-1. The role of RNA-binding proteins (RBPs) in the maintenance of gene expression and in RNA metabolism. RNA is transcribed in the nucleus, using genomic DNA as a template. RBPs mediate the (**A**) splicing and alternative splicing of RNA. mRNAs are exported from nucleus into the cytoplasm (**B**). In the cytoplasm, RBPs are responsible for the trafficking and localization of mRNAs to distal sites in the cell (**C**) RBPs regulate the stability and the eventual degradation of mRNA in the cytoplasm (**D**). The translation of mRNAs by ribosomes is modulated by RBPs that selectively bind to mRNAs (**E**). Adapted from: "**Guardian of Genetic Messenger-RNA-Binding Proteins",** Anji A and Kumari M.

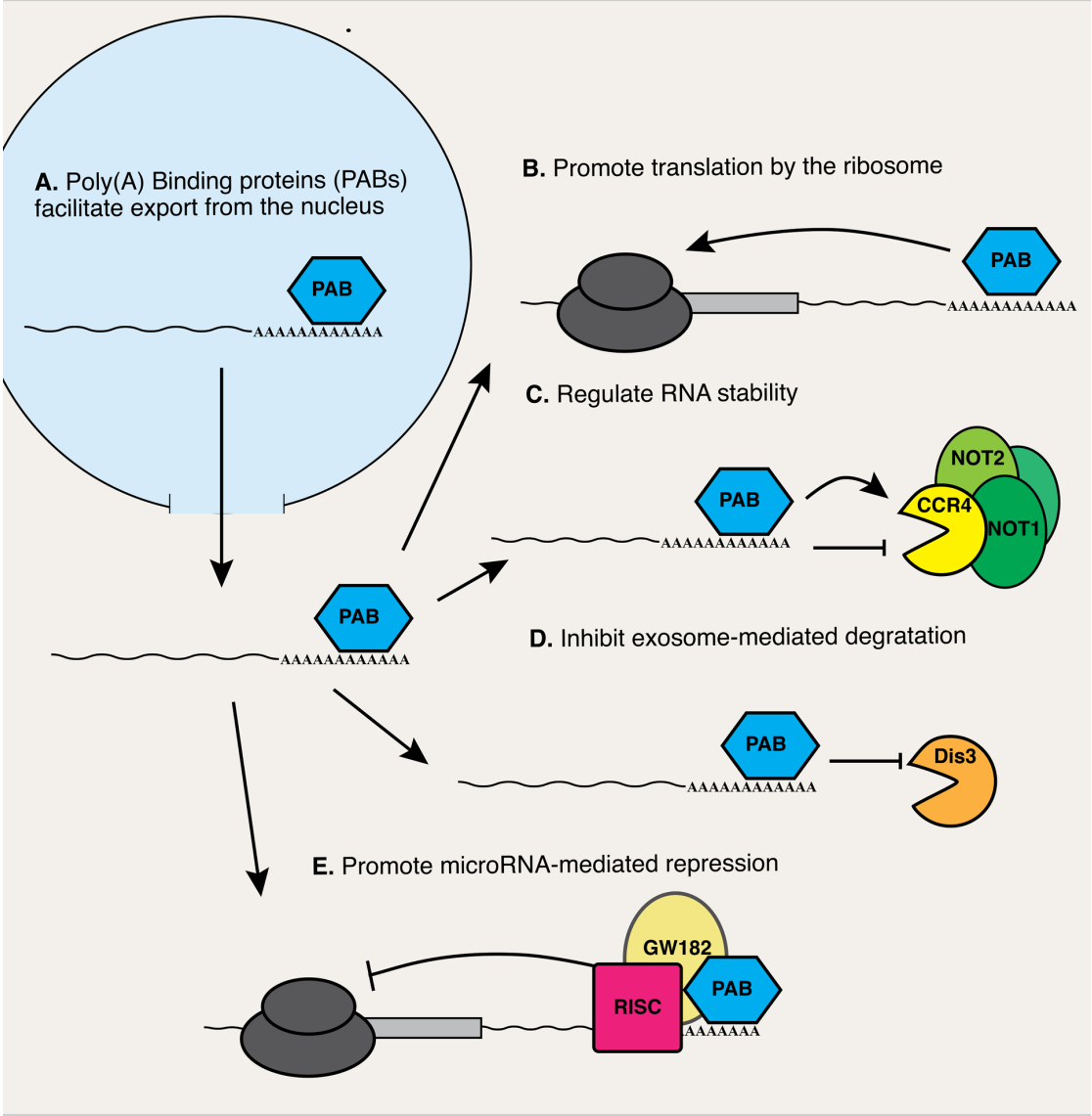

Figure 1-2. Polyadenosine RNA-binding proteins (PABs) regulate mRNA expression. The addition of poly(A) tails to the 3' end of mRNA allows the transcripts to be bound and regulated by PABS. PABs serve many functions, including: **(A)** facilitating export from the nucleus, **(B)** promoting translation, **(C)** allowing for the stabilization or destabilization by other RNA-binding proteins, **(D)** protecting the transcript from 3' to 5' degradation by the exosome, and (**E)** enabling miRNA-induced silencing.

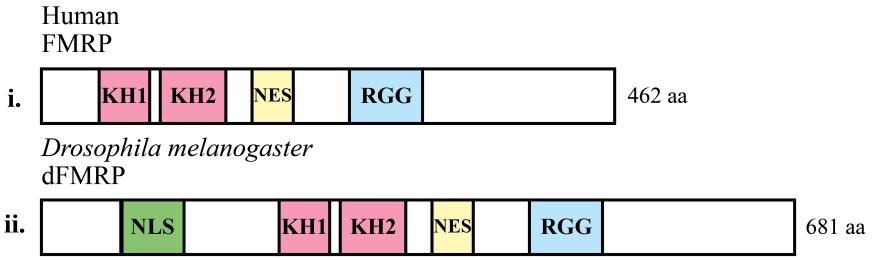

Figure 1-3. Domain structures of FMRP homologs are conserved between Drosophila melanogaster and humans. Human FMRP contains two RNA-binding KH1 domains, a nuclear export signal, and an RNA-binding RGG domain **(i)**. This general domain structure is conserved in *Drosophila,* with the addition of an N-terminal nuclear localization signal (NLS).

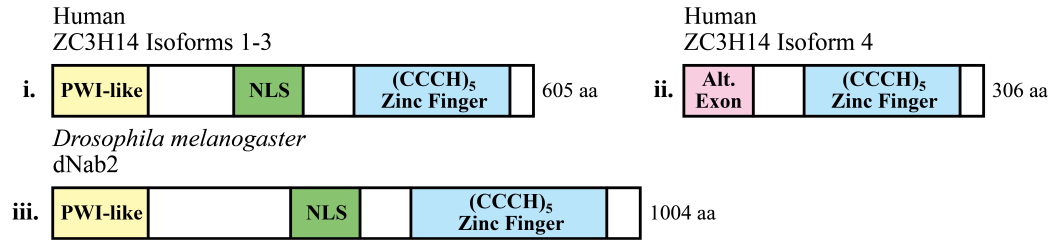

Figure 1-4. Domain structure of human ZC3H14 is conserved in *Drosophila melanogaster* dNab2. *(*A) ZC3H14 isoforms 1-3 and dNab2 contain a PWI-like fold, nuclear localization signal (NLS), and a CCCH-type Zinc finger RNA binding domain **(i,iii)**. Isoform 4 is an alternatively spliced with an alternate first exon, and leads to a truncated protein with only the CCCH-type Zinc finger RNA binding domain **(ii)**. Note that the order and relative spacing of the functional domains between Human ZC3H14 Isoforms 1-3 **(i)** and *Drosophila melanogaster* dNab2 **(iii)** are conserved.

Chapter 2: The Drosophila ortholog of the ZC3H14 RNA binding protein acts within neurons to pattern axon projection in the developing brain

This chapter is adapted from the following published paper:

The Drosophila ortholog of the ZC3H14 RNA binding protein acts within neurons to pattern axon projection in the developing brain. *Developmental Neurobiology 2015*

Kelly, S.M.[1], Bienkowski, R.[2,3,4], Banerjee, A.[3], Melicharek. D.J.[5], Brewer, Z.A.[1], Marenda, D.R.[5,6], Corbett, A.H.[3,†], and Moberg K.H.[2,†]

Department of Biology, College of Wooster [1];
Departments of Cell Biology [2] and Biochemistry [3]
Emory University School of Medicine;
Graduate Program in Genetics and Molecular Biology, Emory University [4], 30322
Departments of Biology [5] and Neurobiology &
Anatomy [6], Drexel University College of Medicine, 19104

* In this chapter, Rick Bienkowksi contributed to the experiments and the associated text for imaging and quantifying the rates of NP7175 defects in Figure 2-2D, imaging the 24h APF pupae in Figure 2-3B, and performing the qPCR experiments in Figure 2-4C.

All other experiments were performed and associated text written by the remaining co-authors, primarily Seth Kelly, Kenneth H. Moberg, and Anita Corbett.

Abstract

The dNab2 polyadenosine RNA binding protein is the *D. melanogaster* ortholog of the vertebrate ZC3H14 protein, which is lost in a form of inherited intellectual disability (ID). Human ZC3H14 can rescue *D. melanogaster* dNab2 mutant phenotypes when expressed in all neurons of the developing nervous system, suggesting that dNab2/ZC3H14 performs well-conserved roles in neurons. However, the cellular and molecular requirements for dNab2/ZC3H14 in the developing nervous system have not been defined in any organism. Here we show that dNab2 is autonomously required within neurons to pattern axon projection from Kenyon neurons into the mushroom bodies, which are required for associative olfactory learning and memory in insects. Mushroom body axons lacking dNab2 project aberrantly across the brain midline and also show evidence of defective branching. Coupled with the prior finding that ZC3H14 is highly expressed in rodent hippocampal neurons, this requirement for dNab2 in mushroom body neurons suggests that dNab2/ZC3H14 has a conserved role in supporting axon projection and branching. Consistent with this idea, loss of dNab2 impairs short-term memory in a courtship conditioning assay. Taken together these results reveal a cell-autonomous requirement for the dNab2 RNA binding protein in mushroom body development and provide a window into potential neurodevelopmental functions of the human ZC3H14 protein.

Introduction

Nascent RNA transcripts in eukaryotic cells associate with RNA binding proteins that regulate gene expression via effects on splicing, 3'-end cleavage, polyadenylation, export, trafficking, translation and ultimately destruction (*6*). The importance of these interactions is underscored by the prevalence of diseases linked to defects in RNA binding proteins (*97*). The frequency of neurological impairments among these diseases suggests that post-transcriptional regulatory mechanisms are particularly important in neurons. For example, the most common form of inherited intellectual disability, Fragile-X Syndrome, is caused by loss of the Fragile X Mental Retardation Protein (FMRP) RNA binding protein (*98*).

One key family of proteins that contributes to post-transcriptional regulation interacts with the 3'-polyadenosine (poly(A)) tails of mRNAs in both the nucleus and cytoplasm. These polyadenosine RNA binding proteins (Pabs) modulate transcript export from the nucleus as well as stability and translation in the cytoplasm (*99, 100*). The human PABPN1 protein (called Pabp2 in flies) localizes to the nucleus, enhances poly(A) polymerase activity, and modulates alternative polyadenylation (*43*). The most abundant human Pab, cytoplasmic PABPC1 (called Pab1 in *D. melanogaster*), enhances translation by bridging an interaction between 3' poly(A) tails and initiation factors at the 5'-mG cap (*100, 101*). While these Pab proteins recognize polyadenosine RNA via RNA Recognition Motif (RRM) domains, a recently described Pab protein termed ZC3H14 (Zinc finger CysCysCysHis domain-containing protein 14) does so via zinc finger motifs and thus constitutes a new class of Pab proteins (*23, 102*).

The biological importance of ZC3H14 is highlighted by the recent finding that mutation of the *ZC3H14* gene causes an autosomal recessive form of intellectual disability **(*5*)**. Patients homozygous for *ZC3H14* loss-of-function mutations have very low IQs ranging from 30-50 compared to the average of 100 (*103*), indicating that ZC3H14 plays a critical role in the brain (*5, 23*). ZC3H14 [also termed mSut2; (*70*)] is expressed highly in the brain and co-localizes with poly(A) mRNA speckles in hippocampal neurons **(*5*)**. Consistent with a critical role for ZC3H14 in the brain, adult *Drosophila* lacking the ZC3H14 homolog, dNab2, have extended poly(A) tails on a subset of brain mRNAs, impaired motor response in a negative geotaxis assay, and reduced survival that is specifically rescued by neuronal expression of dNab2 or human ZC3H14 (*5, 23*).

We have previously found that expression of human ZC3H14 in the developing nervous system rescues multiple defects in dNab2 null flies, including extended poly(A) tails, reduced adult eclosion, and impaired locomotor responses in a negative geotaxis assay (*23*). These effects of ZC3H14 expression is indicative of a significant level of functional overlap between the Nab2 and ZC3H14 proteins in developing neurons, providing strong justification for the use of *Drosophila* to model ZC3H14 function. The role of Nab2/ZC3H14 in the developing nervous system has not yet been explored. However, work on Nab2/ZC3H14 in neuronal disease is accelerating and has linked Nab2 homologs to a Tau-induced model of Alzheimer's pathology in *C. elegans* and cultured vertebrate cells (*70, 104*). Thus there is significant interest in uncovering the role of the Nab2/ZC3H14 family in both neurodevelopment and disease.

Here we exploit the *Drosophila* model to assess requirements for dNab2 in the developing brain. We find that dNab2 loss disrupts development of the mushroom bodies (MBs), twin neuropil structures required for learning and memory (*94*). dNab2-deficient MBs develop two highly penetrant defects in axonal development: the first is overgrowth of axons across the brain midline, and the second is a distinct defect in which these same axons apparently fail to branch along developmentally stereotyped paths. These neuronal defects in dNab2 zygotic mutants imply a role for the dNab2 protein in regulating neuronal RNAs within MB neurons. Consistent with this hypothesis, we find dNab2 to be expressed highly in the cell bodies of MB neurons. Complementary RNAi-depletion and single-cell tracing experiments confirm that dNab2 acts within brain neurons to control axon morphology and short-term memory. In sum, these genetic and cellular data reveal a key role for the dNab2 RNA binding protein in supporting developmental axonogenesis in MB neurons. Given the conserved nature of many neurodevelopmental mechanisms, our data provide a potential paradigm for understanding roles of dNab2/ZC3H14 in development and disease.

Materials and Methods

Drosophila stocks and genetics. All crosses and stocks were maintained in standard conditions unless otherwise noted. The *dNab2*^{ex3} strong loss-of-function mutant and *dNab2*^{pex41} precise excision isogenic control stocks were described previously (*5*). The following Gal4 stocks were used to drive expression in various subsets of mushroom body neurons: *c739-Gal4* (α/ß lobes; BL #7362), *NP7175-Gal4* (core α/ß lobes; DGRC #114120), *201Y-Gal4* (enriched in γ-lobes; BL #4440), *OK107-Gal4* (all MB lobes; BL #854), *c305a-Gal4* (α'/ß'-lobes; BL #30829). *C155-Gal4* (all neurons commencing at embryonic stage 12; BL #458) was used to drive expression in all neurons. The following transgenic stocks were used in this study: *UAS-CD8-GFP* (*105*) and *UAS-dNab2:Flag* (*5*). Single-cell marking of MB neurons was achieved using the 3R MARCM stock (BL #44408) in combination with *OK107-Gal4* and *dNab2*^{ex3}.

Brain dissections and immunohistochemistry. Brain dissections and staining were performed as described previously (*106*). Briefly, brains of anesthetized animals were dissected in PTN buffer (0.1M $NaPO_4$, 0.1% Triton X-100), fixed in 4% paraformaldehyde (Electron Microscopy Sciences), and then stained overnight with primary antibodies diluted in PTN. Following several washes, brains were incubated with the appropriate fluorescently conjugated secondary antibody (1:250) in PTN for 3 hours at room temperature, washed in PTN, and then mounted in Vectashield (Vector Labs). The polyclonal antibody recognizing dNab2 has been described previously (*5*) and was preabsorbed on fixed *Drosophila* embryos. The 1D4 anti-FasII hybridoma (1:20) developed by C. Goodman (*107*) was obtained from the Developmental Studies Hybridoma Bank (DSHB). GFP polyclonal antibody (1:500) was obtained from Aves

Labs. Quantitation of MB phenotypes was performed as described in Michel et al., 2004 (see text for detailed explanation).

Conditioned Courtship Behavior. For courtship behavioral training, virgin males of the appropriate genotype were collected between 0 and 6 hours after eclosion and transferred to individual food vials (*108*). All flies were maintained at 25°C in a 12:12 light:dark cycle at 50% humidity. Behavioral tests were performed in a separate room maintained at 25°C and 50% humidity and illuminated under a constant 130 V white light Kodak Adjustable Safelight Lamp mounted above the courtship chambers. Behavior was digitally recorded using a Sony DCR-SR47 Handycam with Zeiss optics. Subsequent digital video analysis of male courtship behavior was quantified using iMovie software (Apple). The male Courtship Index (CI) was calculated as the total time each male was observed performing courting behavior divided by the total time assayed, as described in (*109*). Virgin female wildtype (Canton S) flies were collected and kept in vials in groups of 10. Male flies were aged for 3 days prior to behavioral training and testing. All tests were performed during the relative light phase. Five-day old mated Canton S females were used for training. Virgin female Canton S targets used were 4 days old. Male flies were assigned to random groups the day of training, and assays were set up and scored blind. Male flies were transferred without anesthesia to one half of a 15mm partitioned mating chamber from Aktogen (aktogen.com) that contained a previously mated Canton S female in the other partitioned half. Males were allowed to acclimate for 1 minute, and then the partition between the male and female was removed. Male flies were then trained for 60 minutes. After 60 minutes, male flies were transferred within 2 minutes without anesthesia to one half of a clean partitioned mating chamber that contained a

virgin Canton S female in the other partitioned half. The partition was removed and the flies were recorded for 10 minutes. A total of 20 flies were scored for each genotype, both trained and sham. To determine significance among individuals of the same genotype for the learning phase of this assay, a two-tailed paired t-test was performed. A two-tailed unpaired t-test was performed to determine significant differences between sham and untrained male flies of the same genotype.

Statistics: All statistical analyses were performed in IBM SPSS statistics, version 22.0.0.0. To determine whether there was a significant difference in the number of brains displaying β-lobe fusion defects in the rescue experiment shown in Figure 5, all categories of fusion were collapsed in a single 'fusion' category and the total number of brains in this fusion category was compared to the number of brains showing no fusion using the non-parametric Mann-Whitney U test.

Results

dNab2 loss disrupts structure of the mushroom bodies

To begin to assess the neurodevelopmental functions of proteins in the ZCH14 family, we exploited our *Drosophila* model (*5*). As ZC3H14 is highly expressed in hippocampal neurons and patients show cognitive defects(*5*), these analyses focused on the structure of the mushroom bodies (MBs) due to their roles in specific forms of learning and memory (*94*). As shown in Fig. 1A, each mushroom body (MB) is divided into α/α', β/β' and γ-lobes composed of bundled axons that project from a dorsally located group of ~2000 Kenyon cells, with later growing axons following a path through the central core of earlier pioneer axons (*110, 111*). The ß/ß' branches and γ-lobes project medially toward the ellipsoid and fan-shaped bodies of the midbrain, while the α/α' branches project dorsally. The neuronal adhesion protein Fasciclin-II (FasII) is enriched on α and ß axon branches and to a lesser extent on the γ-lobes and regions of the *Drosophila* central complex (*93, 112*) and was thus used as a marker to assess the effect of dNab2 loss on MB structure. This analysis used $dNab2^{ex3}$ homozygous null flies, which contain an RNA and protein null deletion of the *dNab2* gene caused by imprecise excision of a nearby P-element that removes the transcriptional start site and approximately half of the coding sequence (*5*), and control precise excision $dNab2^{pex41}$ homozygotes (Fig. 1A,B). The *pex41* allele was generated by a precise excision of the original P-element found in stock *EY08422* that was used to generate the $dNab2^{ex3}$ allele (*5*).

Serial optical sectioning of FasII-stained $dNab2^{ex3}$ brains reveals thinned or missing MB α and ß lobes (arrows in **1B)** and overgrowth of ß lobes across the midline of the brain (asterisks in **1B**). By contrast, loss of dNab2 has no discernable effect on the

structure of the MB γ-lobes. We also noted subtle defects in the pattern of FasII staining of the ellipsoid body (EB) in *dNab2*^{ex3} homozygous null brains and those with dNab2 depleted from neurons using an RNAi transgene co-expressed with the Dicer2 protein (*elav-Gal4/Y;UAS-dNab2*^{RNAi}) (**Supplemental Fig. S1**). Ellipsoid body neurons normally project axons medially towards the midline and eventually form a closed ring structure (*113*). *dNab2*^{ex3} homozygous null brains and dNab2-RNAi depleted neurons lack this completely closed ring structure and leave an opening along the ventral side of the ring (**Fig. S1**). Thus, dNab2 loss affects the morphological development of a subset of structures within the brain, with a particularly discernable effect on the MB α and ß lobes.

The effect of dNab2 loss on β-lobe development was quantitated according to the parameters used by Michel et al (2004) for analysis of MB defects in adult brains lacking the *Drosophila* Fragile-X protein, dFmr1. Briefly, extreme fusion was defined as a FasII-positive neuron bundle crossing the midline that was of equal or greater thickness than the adjacent β lobes; moderate fusion was defined as a substantial FasII-positive fiber bundle crossing the midline that was less than the width of the β-lobes; mild fusion was defined as a thin strand of FasII-positive fibers crossing the midline. β-lobe crossing in *dNab2*^{ex3} homozygous null brains is often symmetric, but in some cases only one β-lobe crosses the midline; this phenotype is more apparent when the contralateral lobe is missing (e.g. the *dNab2* mutant brain in middle panel **Fig. 1B**). By these scoring criteria, ß-lobe defects occur in slightly more than 80% of *dNab2*^{ex3} homozygous brains while α-lobe defects occur in approximately 65% of *dNab2*^{ex3} homozygous brains. Each of these lobe defects occurs in less that 10% of control (i.e. *dNab2*^{pex41}) brains (**Fig. 1C,D**). More

than half of *dNab2*^{ex3} homozygous null brains with ß-lobe fusion fall into the 'severe' class (approximately 45% of all brains), and in all cases tested, single transverse optical sections confirm that opposing ß-lobes in this group are merged at the midline (**Fig. 1B, midline**).

The FasII antigen marks bundled groups of axons and thus does not provide sufficient resolution to track the path of single axons or subsets of axons within the MBs. To more directly examine axon projection patterns, specific subsets of *dNab2*^{ex3} homozygous null or control *dNab2*^{pex41} MB neurons were marked by Gal4/UAS-driven expression (*82*) of a membrane-tethered fluorescent protein CD8-GFP (**Fig. 2**). This technique illuminates the axon projection paths of the marked neurons. Two Gal4 transgenes were used for this analysis: *c739-Gal4*, which marks MB α/ß neurons, and *NP7175-Gal4*, which is expressed in adults in approximately 45-70 late-born Kenyon neurons whose axons track through the central core of the α/β lobes (*114*). In control brains, GFP-positive α and ß axons (*c739>CD8-GFP*) substantially overlap with the region of FasII expression in the dorsally projecting α-lobes and medially projecting ß-lobes. Importantly, all control ß-lobes examined (*c739>CD8-GFP*; *n=4*) terminate appropriately short of the brain midline (**Fig. 2A** and **Fig. 2C**). By contrast, one-third of *dNab2*^{ex3} homozygous null brains examined (*n=3*) contain GFP-positive ß-lobe neurons (*c739>CD8-GFP*) that project contralaterally across the brain midline (arrows, **Fig. 2A** and **Fig. 2C)**. Similarly, all control (*Nab2*^{pex41}) brains examined (*n=8*) contain GFP-positive core ß-lobe axons (*NP7175>CD8-GFP*) that terminate at the midline while ~80% of homozygous *dNab2*^{ex3} brains (*n=6*) contain core ß-lobe axons that cross the midline (**Fig. 2B** and **Fig. 2C**). *dNab2*^{ex3} null flies expressing CD8-GFP in all α/β

mushroom body neurons (*c739>CD8-GFP*) or in just the core α/β mushroom body neurons (*NP7175>CD8-GFP*) also have a dramatically increased rate of missing α or β lobes (75% and 100%, respectively) (**Fig. 2C**). Thinned FasII-positive α-lobes in $dNab2^{ex3}$ homozygous null brains often lack *NP7175*-expressing core axons, as revealed by the lack of CD8-GFP fluorescence in merged projections of FasII-positive α-lobes in the *NP7175>CD8-GFP* background (white asterisk, **Fig. 2B**). As *NP7175* is expressed in late-born Kenyon neurons (*114, 115*), these data suggest that dNab2 loss could impair both projection and branching of developing MB axons.

The FasII and Gal4 techniques label groups of cells but do not provide conclusive, single-cell resolution of the effects of Nab2 loss on axonal morphology. To carry out fine-scale analysis of individual Kenyon cells in either control $dNab2^{pex41}$ brains or $dNab2^{ex3}$ null brains, a membrane bound CD8-GFP marker was used in combination with a MB-specific MARCM system (using the MB driver *OK107-GAL4*) which allows visualization of one or a few axons within intact MB lobes (*115-117*). Individual ß-lobe axons in $dNab2^{pex4}$ control brains project medially but arrest short of the brain midline (**Fig. 2D**, arrow in left panel). By contrast, individual ß-lobe axons in $dNab2^{ex3}$ homozygous null brains project medially but fail to stop, forming a meshed network of axons across the brain midline (**Fig. 2D**, arrow in right panel). This MARCM data is consistent with the α/ß lobe and core driver (*c739* and *NP7175* respectively) data and strongly support a model in which dNab2 is required for proper projection and branching patterns among developing MB axons.

dNab2 is a cell-autonomous regulator of axon branching and growth

Although the dNab2 protein is expressed in all cell types examined throughout the organism, the viability, locomotor, and wing-posture phenotypes that occur in *dNab2*^{ex3} homozygotes can be rescued by pan-neuronal re-expression of wildtype dNab2 protein (*5, 23*). The MB defects in *dNab2*^{ex3} homozygous null adults suggest a similar autonomous requirement for dNab2 within Kenyon cells. To examine dNab2 expression in the cell bodies of adult Kenyon cells, the plasma membranes of control *dNab2*^{pex41} and mutant *dNab2*^{ex3} homozygous MB neurons were marked by expression of a membrane-tethered GFP driven by the *201Y-Gal4* driver (*201Y>CD8-GFP*) and co-stained with the anti-dNab2 polyclonal antibody (*5*). In the adult, the *201Y* driver labels γ neurons and core neurons of the α and ß lobes (*114*). dNab2 protein is readily detected in both *201Y*-positive and *201Y*-negative cells within cell bodies of control *dNab2*^{pex41} Kenyon cell clusters (**Fig. 3A**, top panels; see asterisk). The intensity of the dNab2 signal in these cells is not uniform across the plane of section, suggesting that there may be differences in dNab2 protein levels between adult Kenyon cell subgroups. Within each Kenyon cell, dNab2 localizes primarily to the nucleus in foci reminiscent of nuclear speckles (**Fig. 3A**, zoom), which resembles the localization of the dNab2 ortholog ZC3H14 in adult mouse hippocampal neurons and cultured mammalian cells (*4, 5, 70*). Importantly, anti-dNab2 fluorescence signal is largely eliminated in *dNab2*^{ex3} homozygous adult Kenyon cells (**Fig. 3A**, bottom panels). The low level of residual staining in *dNab2*^{ex3} MB cells is likely due to background reactivity of the anti-dNab2 sera (*5*). These fluorescence data confirm that dNab2 is highly expressed in Kenyon neurons and is absent in *dNab2*^{ex3} null adult α/β neurons. However, as α/β lobes begin to develop in the pupal stage (~12 hours after pupal formation, APF), we also sought to test whether dNab2 is expressed in pupal

Kenyon cells as they extend α/β axons towards the midline. Brains from 24 hour pupae in which MB cells were marked by CD8-GFP driven by the *OK107-Gal4* driver (*110*) were stained with the dNab2 antiserum (Pak et al., 2011). As shown in **Figure 3B**, dNab2 is expressed widely in the 24 hour pupal brain, including in the cell bodies of CD8-GFP+ developing mushroom body neurons, which is consistent with dNab2 playing a role in MB development.

The broad expression of dNab2 in the pupal brain suggests that dNab2 could act in other cell types to non-autonomously control aspects of Kenyon cell pathfinding. To assess the role of dNab2 within specific groups of mushroom body neurons, we exploited the *Gal4/UAS* system in combination with a *dNab2* RNA-interference transgene (*UAS-dNab2*^{RNAi}) (*5*) to knockdown dNab2 expression in the developing brain. To assess the efficiency of dNab2 knockdown, *dNab2* mRNA transcript levels were examined by quantitative real-time PCR on samples isolated from heads of adult flies with dNab2 knocked down in all neurons (*elav-Gal4,UAS-dNab2*^{RNAi}) (**Fig. 4C**). Levels of *dNab2* mRNA in these samples were decreased relative to *dNab2*^{pex41} controls but less so than in *dNab2*^{ex3} homozygous null heads, consistent with the RNA-null nature of the *ex3* allele (*5*). Inclusion of a *UAS-dicer2* transgene in combination with the *UAS-dNab2-RNAi* transgene (*elav-Gal4,UAS-dNab2*^{RNAi}*,UAS-dcr2*) significantly enhanced knockdown efficiency, but did not lower *dNab2* expression to the level observed in *dNab2*^{ex3} homozygous null heads, which is consistent with dNab2 being widely expressed in neuronal and non-neuronal cells (*5*). Neuronal expression of Dcr2 alone (*elav-Gal4,UAS-dcr2*) also significantly lowered levels of *dNab2* mRNA in adult heads (**Fig. 4C**),

although not to the level achieved with the *dNab2* RNAi transgene, suggesting that Nab2 levels may be regulated by a Dcr2-dependent mechanism *in vivo*.

Pan-neuronal depletion of dNab2 led to an increase in MB defects relative to the control pan-neuronal expression of Dcr2 alone (*elav-Gal4, UAS-dcr2, UAS-dNab2^{RNAi}*, vs. *elav-Gal4,UAS-dcr2*) (**Figs. 4A,B**), which resemble those seen in *dNab2^{ex3}* null brains. These defects include thinned or absent α and ß-lobes, and variable degrees of ß-lobe fusion (see magnified insets in **Fig. 4A**). In females, *elav-Gal4, UAS-dcr2, UAS-dNab2^{RNAi}* β-lobe phenotypes vary from unaffected, to 'mild' (white arrow in bottom inset of **Fig. 4A**) or 'severe' fusion (*56*), while males show a mixture of complete fusion and an intermediate defect in which the ß-lobes are very closely apposed over the brain midline (**Fig. 4A**). Overall, the percentage of *elav-Gal4, UAS-dcr2, UAS-dNab2^{RNAi}* males and females showing fused β lobes, thinned α/β lobes, or completely missing lobes is 73% and 65%, respectively (**Fig. 4B**). The enhanced frequency of MB defects in dNab2-depleted males could be due to sex-specific differences in transgene expression (e.g. dosage compensation) and consistent with this hypothesis, approximately 20% of males overexpressing Dcr2 alone (*elav-dcr2*) show α/β lobe defects while no females show this effect (**Fig. 4B**). These data are consistent with enhanced transgene expression in males and further suggest that a Dcr2-dependent micro-RNA might play a role in MB development [e.g. *let-7*; (*118*)] that is independent of dNab2.

To more precisely characterize the spatial and temporal requirement for dNab2 within subsets of developing MB neurons, a *UAS-dNab2* transgene was used in combination with Gal4 drivers to rescue the α/ß-lobe axon defects in *dNab2^{ex3}* null brains. Representative examples of each genotype are shown in **Figure 5**. Re-expression

of dNab2 in all neurons (*elav-Gal4*) (**Fig. 5A**, right panel) significantly rescued ß-lobe fusion defects in a majority of $dNab2^{ex3}$ null brains (Mann-Whitney test, $p<0.05$); the *elav-Gal4* driver alone had no effect on ß-lobe defects in d$Nab2^{ex3}$ null brains **(Fig. 5A**, left panel; penetrance ~75%, n=8). Importantly, *dNab2* re-expression from the pan-MB driver *OK107* (*114*) also significantly rescued the $dNab2^{ex3}$ null ß-lobe fusion defect; while 87.5% of $dNab2^{ex3}$ homozygous null flies containing just the *OK107-Gal4* driver alone (n=8) showed extreme, moderate, or slight fusion defects, only 25% of flies re-expressing dNab2 (n=16) in all mushroom body neurons (*OK107>dNab2*) showed some level of β-lobe fusion (**Fig. 5B**, right panel; Mann-Whitney test, $p<0.05$). Gal4 transgenes with enriched expression in either the adult γ-lobe (*201Y*) or the α'/ß'-lobes (*c305a*) (*114*) were also used in conjunction with the *UAS-dNab2* transgene. Neither of these genotypes conferred significant rescue of the *dNab2* mutant MB structural defects as assessed by FasII staining (Mann-Whitney test, $p>0.05$), **Fig. 5C,D**). The *c739-Gal4* driver, which is expressed mainly in the α/ß-lobe neurons (*114*), produced an observable but not significant degree of rescue to the β-lobe fusion defect (**Fig. 5E**) when in combination with the *UAS-dNab2* transgene (Mann-Whitney test, $p=0.226$, *c739>dNab2* [n=18] vs. *c739* alone [n=10]). In sum, these RNAi and Gal4 rescue experiments support a model in which the dNab2 RNA binding protein is required cell-autonomously within Kenyon cells to control the branching and projection of their axons into the α and β-lobes.

dNab2 loss impairs short-term memory

dNab2 is the fly ortholog of a protein, ZC3H14, which is lost in an inherited form of human intellectual disability (*5, 23*). To extend our analysis of dNab2 function, we

tested whether dNab2 is required for proper cognitive function in adult flies. To assess the pan-neuronal requirement for dNab2 in supporting cognitive behavior, a courtship-conditioning assay (*108*) was used to test the effect of pan-neuronal dNab2 loss on learning and short-term memory (**Fig. 6**). Briefly, in this assay individual adult male flies are placed in courtship chambers with single mated wildtype adult females for one hour. The amount of time each male engages in courtship activity during the first and last ten minutes of this "training session" is recorded and analyzed in order to derive a courtship index (CI). Previously mated females reject courtship advances of males, whose consequent decrease in CI between the first and last 10 minutes indicates learning. The durability of this CI suppression is indicative of memory.

Three separate genotypes were tested in the courtship conditioning assay: the pan-neuronal driver alone (*elav-Gal4/Y*), the dNab2 RNAi transgene alone (+/Y;*UAS-dNab2*^{RNAi}/+), or combined driver and RNAi (*elav-Gal4/Y;UAS-dNab2*^{RNAi}/+). We omitted the *UAS-dcr2* transgene from these experiments due to its independent effects on dNab2 levels (see **Fig. 4C**). All three test groups show statistically significant suppression of CI across the training period (**Fig. 6A**), indicating that they are able to learn and adapt their behaviors to a continuous training regimen. Following the conditioning period, trained males (Trained) were transferred to a new courtship chamber containing a single virgin female to measure the durability of the learned CI suppression. Untrained flies (Sham) were included in this assay as negative controls. While Sham males display robust courtship of virgin females, control Trained males (*elav-Gal4* or *UAS-dNab2*^{RNAi} alone) maintained suppressed CI values, indicative of intact short-term memory. By contrast, the CI value of Trained males with pan-neuronal depletion of

dNab2 (*elav-Gal4>dNab2*^{RNAi}) was comparable to that of Sham trained flies (**Fig. 6B**). This difference is not due to a difference in motor activity as Nab2-depleted (*elav-Gal4>dNab2*^{RNAi}) and control (*elav-Gal4*) adult males show similar frequencies of beam breaks per waking minute over the course of a 24-hour period in a Trikinetics *Drosophila* activity monitor (independent t-test, p=0.682; **Fig. S2**). These behavioral data are consistent with the hypothesis that the dNab2 polyadenosine RNA binding protein regulates pathways involved in short-term memory in addition to its role in axon branching and guidance.

Discussion

Here we present an analysis of the cellular and cognitive requirements for the *Drosophila* polyadenosine RNA binding protein dNab2, an ortholog of the ZC3H14 protein, which is lost in an inherited intellectual disability (*5*), in brain development. The data show that dNab2 is required for proper development of the mushroom bodies, a brain region that supports learning and memory (*111*), and that this defect is due to a cell-autonomous role for dNab2 within subsets of mushroom body neurons. Furthermore, evidence also shows that pan-neuronal knockdown of dNab2 results in a defect in short-term memory, possibly paralleling cognitive defects produced by ZC3H14 loss in humans.

The analysis of dNab2 reveals a number of parallels to another RNA binding protein, dFmr1, which is also an ortholog of a protein lost in heritable intellectual disability, FMRP. As with ZC3H14, FMRP is a ubiquitously expressed protein whose loss leads to defects in brain function (reviewed in Santoro et al., 2011). Strikingly, *dFmr1* mutant flies show adult MB defects very similar to those described here for *dNab2* mutant flies, including thinned/missing α lobes and fused ß lobes (*56*). Human and *Drosophila* FMRP/dFmr1 are well-established translational repressors (*55, 59, 119, 120*), and while the precise molecular role of ZC3H14 and dNab2 have yet to be determined, the role of these proteins in limiting poly(A) tail length (*5, 23*) suggests that they could impact the fate of mRNAs in the cytoplasm, perhaps via effects upstream of translation. Finally, the dNab2 ortholog ZC3H14 is highly expressed in hippocampal neurons (*5*), which are also an important site of FMRP action (reviewed in Santoro et al., 2011). These similarities between dNab2/ZC3H14 and dFmr1/FMRP are suggestive of potential links between these RNA binding proteins that warrant further investigation.

Given its proposed molecular role as a Pab, dNab2 is likely to support neurodevelopment and memory via effects on the stability and/or translation of neuronal mRNAs. These roles could be linked such that defects in regulation of RNAs supporting axon projection lead to corresponding defects in memory circuits. Alternatively these phenotypes could reflect a requirement for dNab2 in regulating distinct pools of RNAs involved in each process. Our observations that neuronal RNAi-mediated depletion of dNab2 elicits penetrant effects on locomotor behavior (*5*) and short-term memory (this study), but comparatively mild effects on α/ß-lobe structure (approximately 65% of brains affected), suggests these two phenotypes could stem from effects in different cells and perhaps different target RNAs. Indeed some proteins required for courtship memory act in γ-lobe neurons (*121*) whose structure is unaffected by dNab2 loss, while other proteins are only required in the α/ß-lobes (*122*). Future studies will need to define dNab2 target RNAs in groups of brain neurons and assess their roles in axon projection and STM phenotypes that arise upon dNab2 loss.

The RNAs responsible for axonal defects in dNab2 mutant Kenyon cells whose projections the α/ß MB lobes are as yet undefined. Although dNab2 is localized to the nucleus at steady-state, the budding yeast Nab2 protein shuttles between the cytoplasm and nucleus, presenting the possibility that dNab2 could impact RNA regulatory processes beyond nuclear processing. Studies have implicated a diverse set of molecules in MB development, including the cell-cell adhesion proteins N-cadherin (*123*), Down-syndrome cell adhesion molecule (Dscam) (*124-126*), and L1CAM (*127*), as well as signaling cascades from Ephrin (*128*) and Wingless/Wnt signals (*129-131*), providing a number of candidate pathways. Coordinated control of these signals during axon

outgrowth, bifurcation, and synapse formation likely requires precise temporal and spatial control of mRNA stability, transport, and translation. The dNab2/ZC3H14 Pab restricts poly(A) tail length *in vivo* (*5, 23*). Thus, the required role in MB axon development could stem from effects on one or more transcript(s) involved in axonal projection and branching. Identifying these target RNAs will require functional assays that define dNab2-regulated transcripts in neurons and physical interaction screens that recover transcripts bound by dNab2. The identity of these transcripts will provide important clues as to how dNab2 influences cellular processes in the fly brain. However, equally important will be determining the fate of these RNAs once bound by dNab2, and testing whether dNab2 primarily influences neuronal gene expression by controlling the nuclear export, stability, transport, or translation of cytoplasmic RNAs, even if its role is primarily restricted to controlling poly(A) tail length in the nucleus. This combined analysis of dNab2 targets and how each is regulated by dNab2 will likely shed considerable light on the role of the dNab2/ZC3H14 protein family in brain development and function.

Figures:

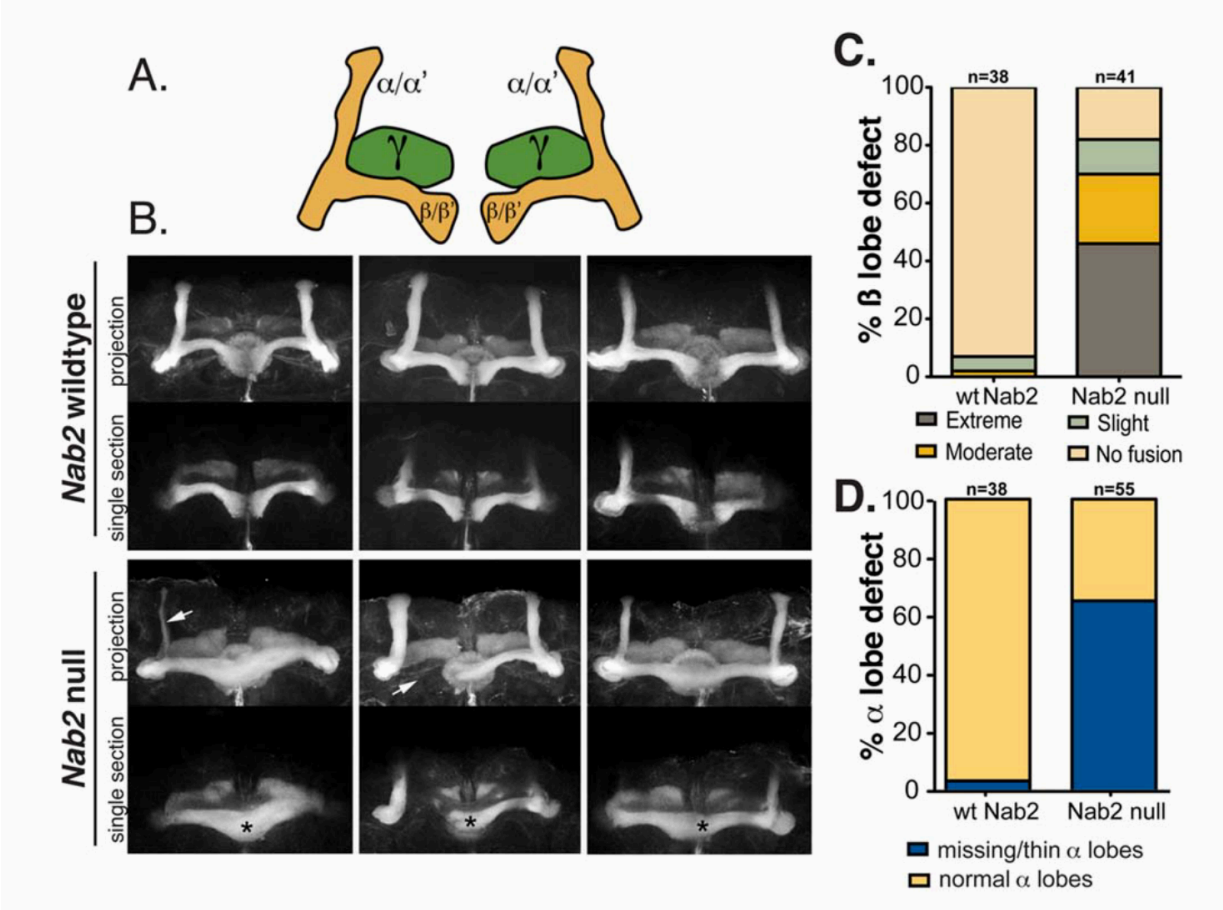

Figure 2-1. dNab2 is required for proper development of the *Drosophila* mushroom body neurons. ***A***, Diagram of the adult *Drosophila* mushroom body lobes depicting the axons of the medially projecting gamma (γ) neurons (green), the vertical alpha (α) and alpha prime (α') neurons, and the medially projecting beta (β) and beta-prime (β') neurons. ***B,*** Fasciclin II (FasII) antibody staining of three control ($dNab2^{pex41}$) brains or three *dNab2* null ($dNab2^{ex3}$) brains. Maximum intensity Z-stack projections (projection) as well as single 1.5µm sections in the transverse plane of the β-lobes are shown. β-lobes of control brains rarely cross the mid-line and these brains have well-formed α-lobes, while $dNab2^{ex3}$ null brains have β-lobes that often project to the contralateral hemisphere

and appear to fuse (black asterisks) or have missing α or β lobes (white arrows). ***C,*** Quantification of the frequency of the *dNab2*^{ex3} null β-lobe defect according to the scoring system described in the text (defined by Michel, Kraft and Restifo (*56*). ***D,*** Quantification of the frequency the *dNab2*^{ex3} null α-lobe defect for missing or thinned lobes.

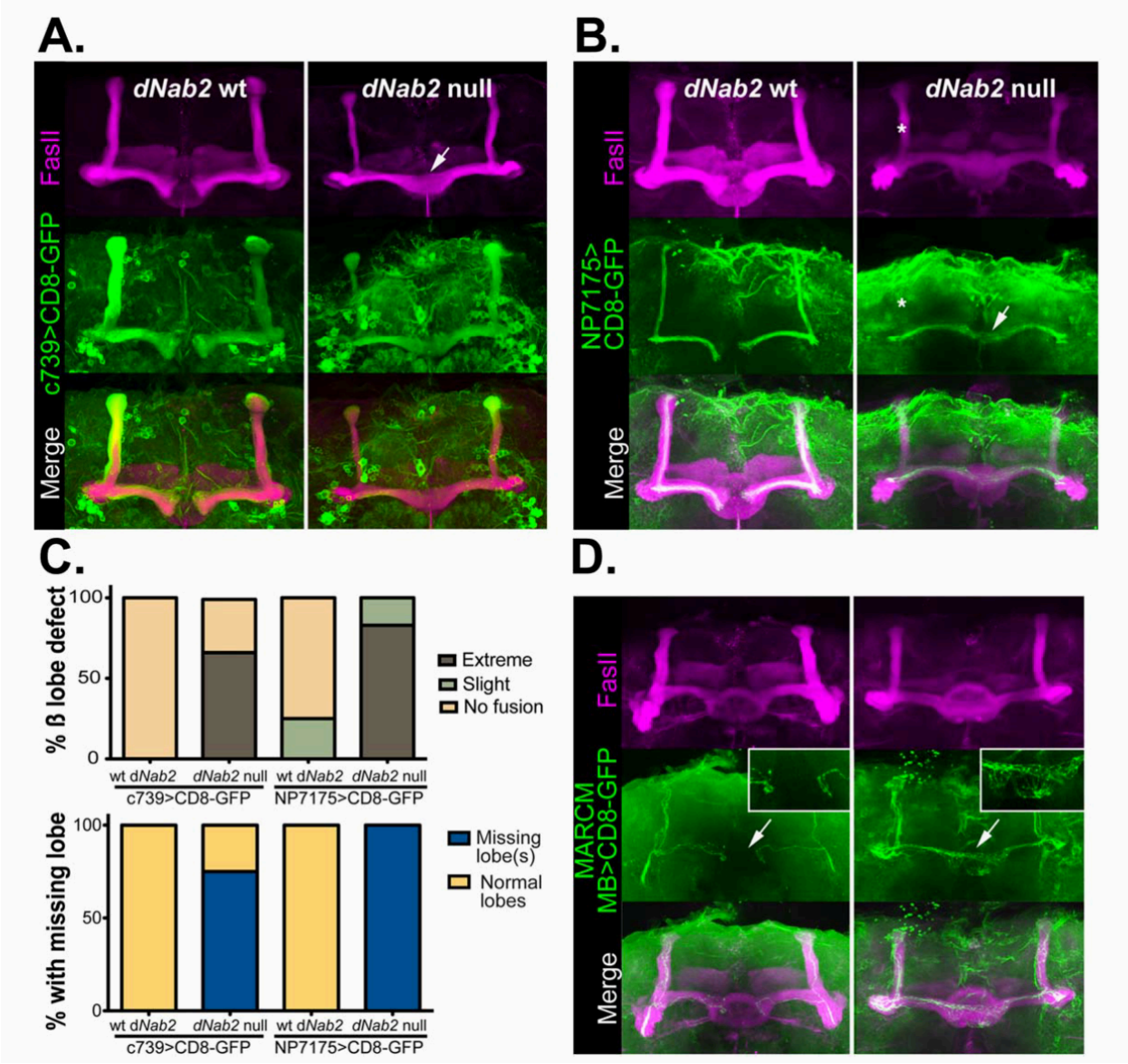

Figure 2-2. Loss of *dNab2* disrupts the morphology of *Drosophila* mushroom body neurons. *UAS-CD8-GFP* (green) was used in combination with cell-type specific Gal4 drivers to mark either all α/β neurons (***A*****;** *c739*) or "core" α/β neurons (***B*****;** *NP7175*) of the MBs in $dNab2^{pex41}$ control or $dNab2^{ex3}$ null brains. Brains are co-stained with FasII (magenta) to mark of the α/β lobes. Control β-lobes terminate at the brain midline but lobes from $dNab2^{ex3}$ null brains overextend into the contralateral hemisphere (white

arrows). α-lobe core axons are often absent in *dNab2*^{ex3} null brains (white asterisk). Genotypes shown are: **(A)** *C739-Gal4/UAS-CD8-GFP;+/+* or *C739-Gal4/UAS-CD8-GFP;dNab2*^{ex3}*/dNab2*^{ex3} and **(B)** *NP7175-Gal4/Y;UAS-CD8-GFP/+;+/+* or *NP7175-Gal4/Y;UAS-CD8-GFP/+; dNab2*^{ex3}*/dNab2*^{ex3}. ***C***, Quantification of the frequency of the β-lobe midline fusion defects (top) and the missing α- or β-lobe defects observed in **A** and **B**. Phenotypes were scored according to the criteria outlined in (*56*). Mushroom body β lobes show 'extreme fusion' when lobes cross the midline with similar or increased thickness to the rest of the β-lobe (white arrows in A and B). Brains showing thin β-lobes crossing the midline in comparison to the thickness of β-lobes of either side of the midline are scored as having 'slight fusion.' ***D,*** MARCM analysis of individual neurons (green) in *dNab2* control and *dNab2*^{ex3} null brains co-stained with FasII (magenta). Wildtype β-axons terminate at the midline but Nab2 mutant axons project to the contralateral side (white arrows). Insets show a magnified regions of the midline in each genotype. Control genotype: *hsFLP/+;FRTG13,UAS-CD8-GFP/FRTG13, tubulin-GAL80;dNab2*^{pex41}*/dNab2*^{pex41}*;OK107-Gal4/+*. Mutant genotype: *hsFLP/+; FRTG13,UAS-CD8-GFP/FRTG13,tubulin-GAL80;dNab2*^{ex3}*/dNab2*^{ex3}*;OK107-Gal4/+*.

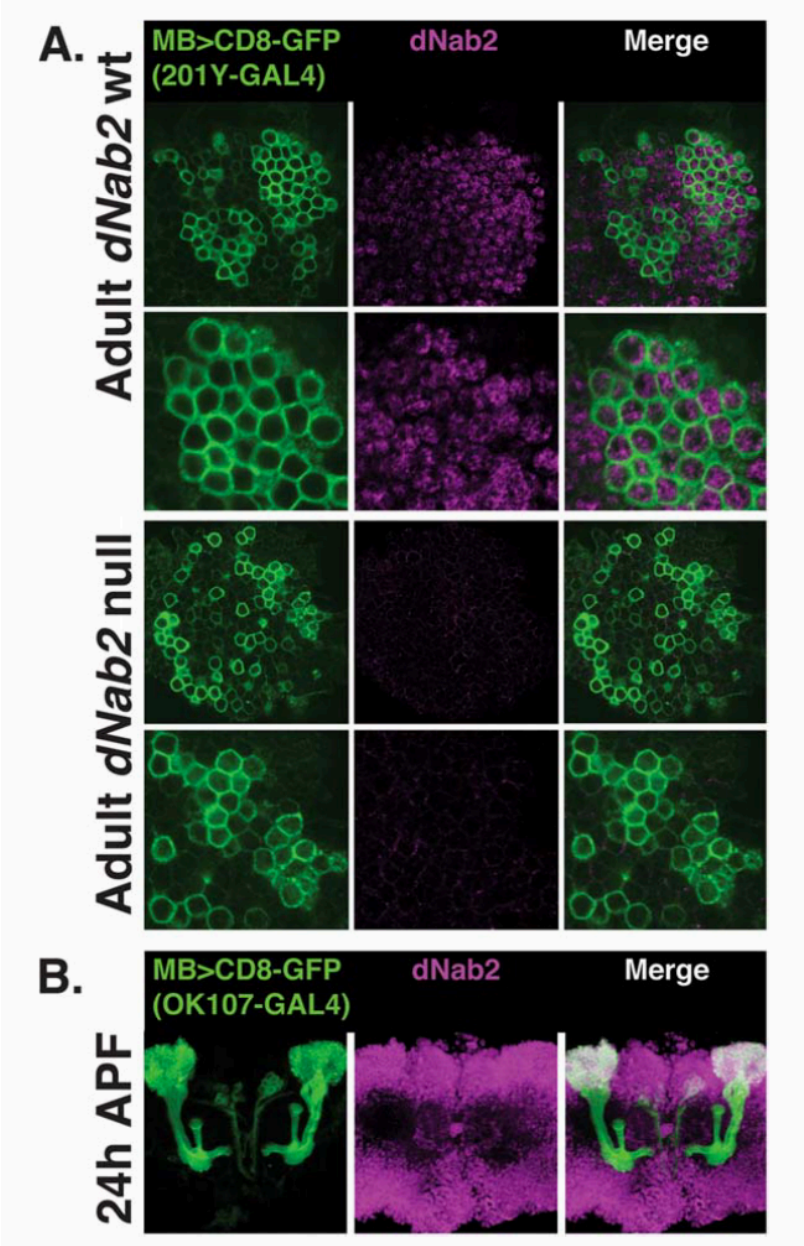

Figure 2-3. dNab2 is expressed in the cell bodies of adult and pupa mushroom body neurons. ***A,*** Anti-dNab2 staining (magenta) in Kenyon cells labeled by *201Y*-driven expression of *UAS-CD8-GFP* (green) in wildtype or $dNab2^{ex3}$ homozygous null flies. dNab2 is readily detected in wildtype Kenyon cell bodies (top panels) but absent in Kenyon cells from $dNab2^{ex3}$ homozygous null flies (bottom panels). ***B,*** dNab2 staining in pupal brains 24 hours after pupal formation (24APF). All MB lobes (γ, α'/β', and α/β)

are present at this time point (*110*) and are labeled by *OK107-GAL4* driven expression of *UAS-CD8-GFP*. dNab2 is present (white overlap in the merged image) in the cell bodies of mushroom body neurons during pupal development.

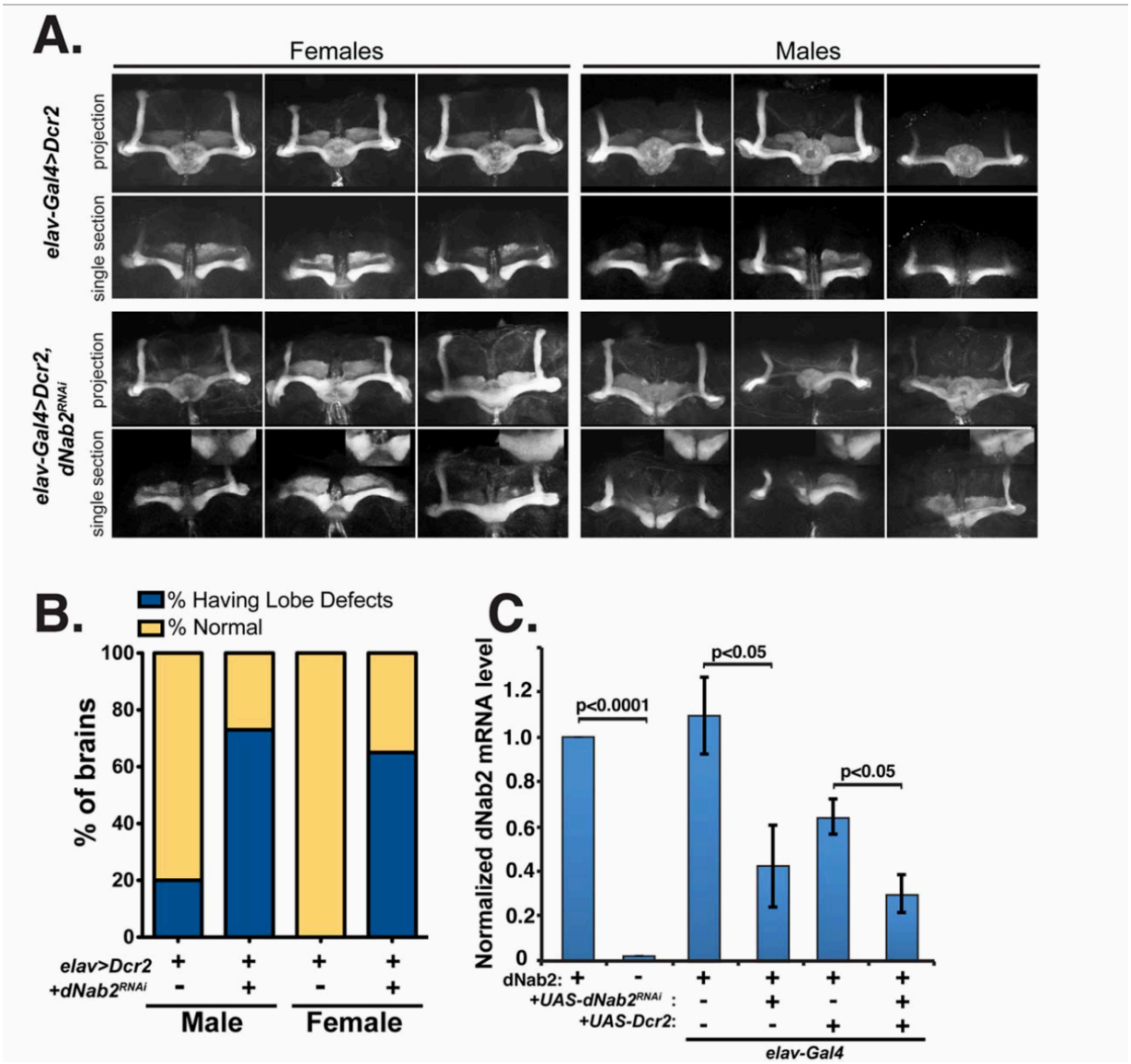

Figure 2-4. dNab2 is required in neurons for mushroom body development. ***A,*** Merged projections (projection) and single 1.5μm transverse slices (midline) of FasII-positive α/β-lobes of Dcr2 control flies (top, genotype: *elav-Gal4/+ or Y; UAS-dcr2*/+) or flies with RNAi knockdown of dNab2 in all neurons (bottom, genotype: *elav-Gal4/+ or Y; UAS-dcr2*/*UAS-dNab2*^{RNAi}). dNab2-depleted neurons show evidence of mushroom body fusion (arrow). ***B,*** Quantification of missing/thin α-lobes or missing/over-extending β-lobes as observed in ***A*** (*Drc2* alone: males n=20, females n=14; *Dcr2+dNab2-RNAi*:

males n=15, females n=14) . All flies contain *elav-Gal4>UAS-Dcr2*. ***C,*** qPCR analysis of *dNab2* levels in the indicated genotypes (as in ***A***). Data represents an average of three biological replicates of ~50 adult fly heads for each genotype. Precise excision control ($dNab2^{pex41}/dNab2^{pex41}$) flies and $dNab2^{ex3}$ homozygous null flies ($dNab2^{ex3}/dNab2^{ex3}$) were used as positive and negative controls, respectively. Statistical significance values via two-tailed independent t-test are shown between indicated samples.

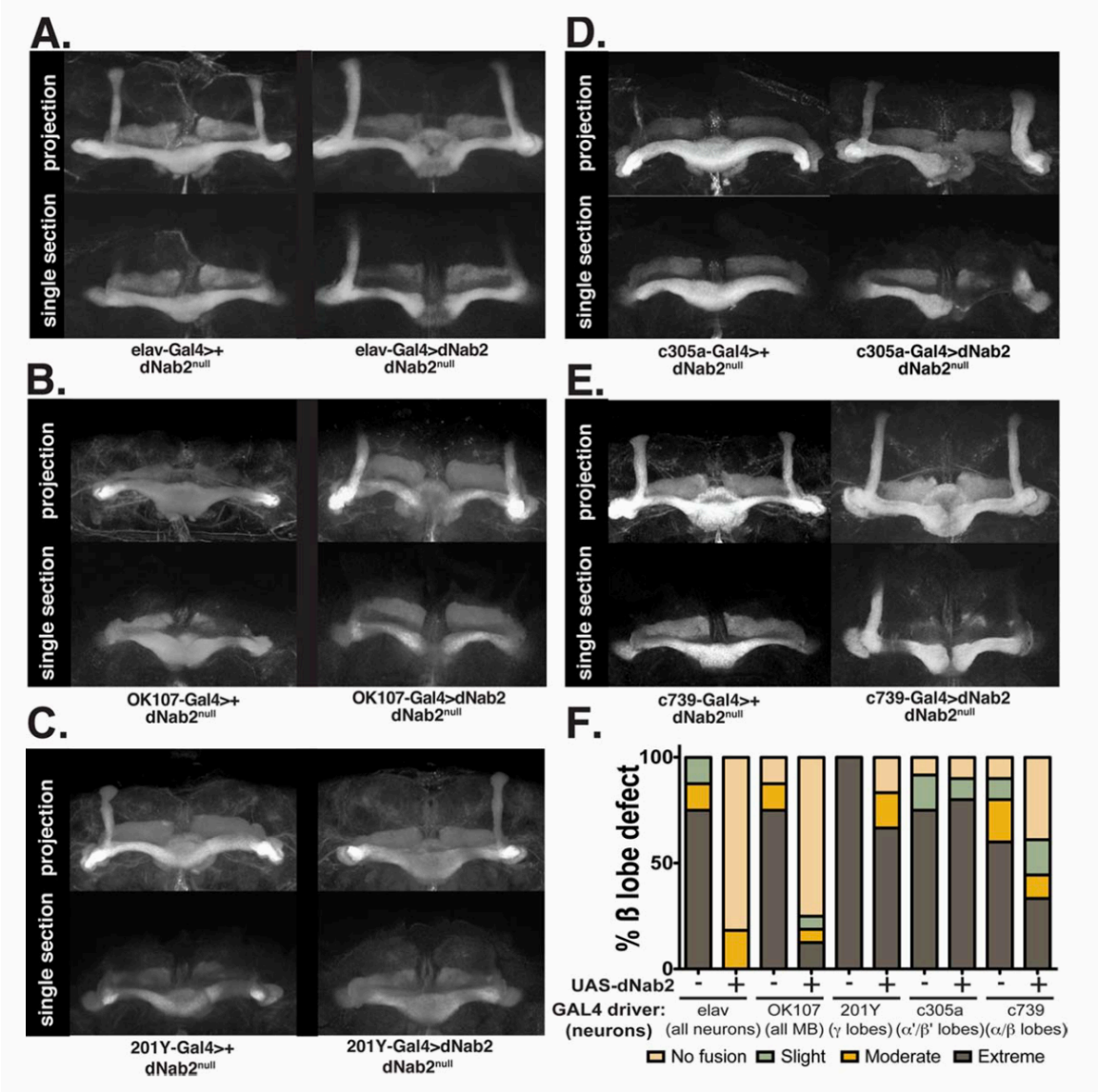

Figure 2-5. Mushroom body-specific expression of dNab2 rescues the β-lobe morphology defects in *dNab2^{ex3}* homozygous null mushroom bodies. Representative images of anti-FasII staining of *dNab2^{ex3}* homozygous null brains expressing a suite of Gal4 drivers with or without a *UAS-dNab2* transgene. The following *Gal4* drivers were used: (***A***) the pan-neuronal driver *elav-Gal4* (genotype: *elav-Gal4/+;;dNab2^{ex3}/dNab2^{ex3}*, n=8, or *elav-Gal4/UAS-dNab2;; dNab2^{ex3}/dNab2^{ex3}*, n=11); (***B***) the pan-MB driver *OK107-Gal4* (genotype: d*Nab2^{ex3}/dNab2^{ex3};OK107-Gal4/+*, *n=8*, or *UAS-*

dNab2/+;;dNab2^{ex3}/dNab2^{ex3};OK107-Gal4/+, n=16); (***C***) the γ-lobe driver *201Y-Gal4* (genotype: *201Y-Gal4/+; dNab2^{ex3}/dNab2^{ex3}*, n=4, or *UAS-dNab2/+;201Y-Gal4/+; dNab2^{ex3}/dNab2^{ex3}*, n=6); (***D***) the α'/β'-lobe driver *c305a-Gal4* (genotype: *c305a-Gal4/+; dNab2^{ex3}/dNab2^{ex3}*, n=12, or *UAS-dNab2/+;c305a-Gal4/+; dNab2^{ex3}/dNab2^{ex3}*, n=10); or (***E***) the α/β-lobe *c739-Gal4* driver (genotype: *c739-Gal4/+; dNab2^{ex3}/dNab2^{ex3}*, n=10, or *UAS-dNab2/+;c739-Gal4/+; dNab2^{ex3}/dNab2^{ex3}*, n=18). (***F***) Quantification of the frequency of β-lobe fusion defects according to the scoring system used in Michel, Kraft and Restifo (*56*). Note that re-expression of dNab2 in all neurons (Mann-Whitney U=80, $p<0.05$) or in all mushroom body neurons (Mann-Whitney U=104, $p<0.05$) significantly rescued the *dNab2^{ex3}* homozygous null β-neuron midline fusion phenotype.

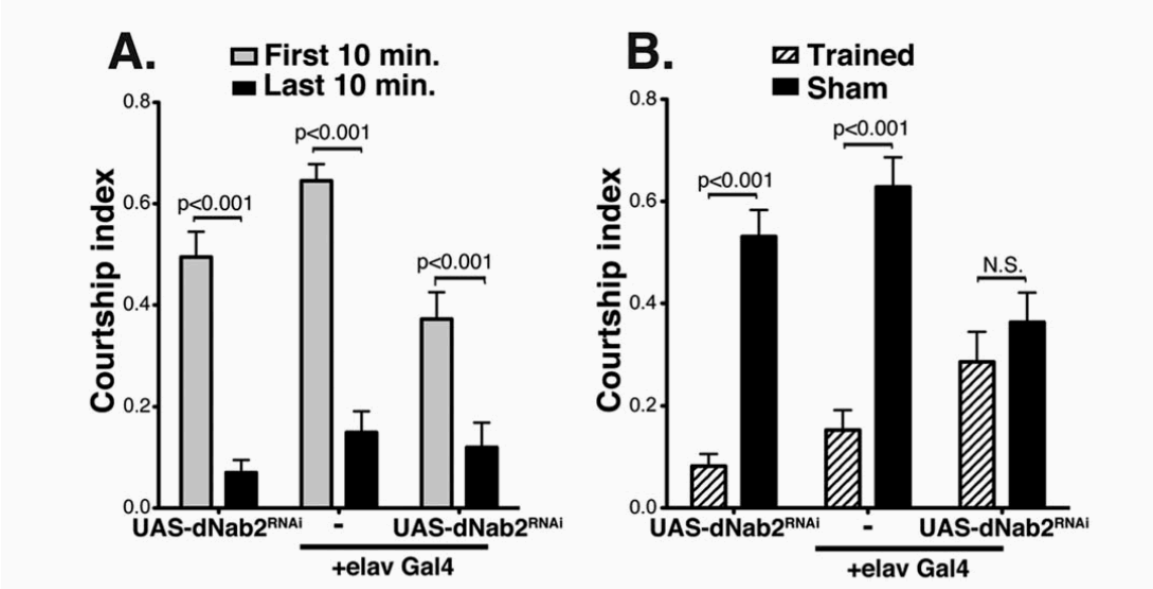

Figure 2-6. **dNab2 is required for short-term memory**. Courtship indices among two-day old males of the indicated genotypes during the training/learning phase (***A***) or the retesting/memory phase (***B***) of the courtship conditioning assay. While Trained males carrying the Gal4 driver or RNAi cassette alone show robust CI suppression in the retesting phase, flies with dNab2 knockdown specifically in neurons (*UAS-dNab2*^{RNAi}+neuronal-Gal4) showed no significant CI suppression upon retesting and were indistinguishable from mock treated controls. For each genotype, n=20. Statistical significance determined by two-tailed t-test.

Chapter 3: The evolutionarily conserved RNA-binding protein dNab2 interacts with the fragile X protein homolog and mediates translational repression in *Drosophila* neurons

This chapter has been submitted for review as:

The evolutionarily conserved RNA-binding protein dNab2 interacts with the Fragile-X protein homolog and mediates translational repression in *Drosophila* neurons

Rick S. Bienkowski[a,b], Jennifer Rha[b], Ayan Banerjee[b], J. Christopher Rounds[a,b], Julia Omotade[a], Christina Gross[c], ChangHui Pak[a,b], Kevin J. Morris[b], Stephanie K. Jones[b], Michael R. Santoro[e] , James Zheng[a], Stephen T. Warren[b,e], Gary J. Bassell[a], Anita H. Corbett[b,*] and Kenneth H. Moberg[a,*]

Departments of [a]Cell Biology, [b]Biochemistry and [e]Human Genetics, Emory University School of Medicine, Atlanta, GA 30322; [c]Division of Neurology, Cincinnati Children's Hospital Medical Center, Cincinnati, OH 45229;

Summary

The evolutionarily conserved, ubiquitously expressed RNA-binding protein ZC3H14 is lost in a heritable form of human intellectual disability. Studies of the *Drosophila* ZC3H14 ortholog, dNab2, have uncovered a critical function in neurons required to support memory and axon projection. However, the molecular function of this protein within neurons has not been defined. Here we discover a network of physical and genetic interactions between dNab2 and the Fragile-X protein homolog dFMRP that link dNab2/ZC3H14 to translational repression. The dNab2 and dFMRP proteins co-precipitate from fly brain neurons and co-localize in cytoplasmic foci distributed along the neurites of cultured brain neurons. Two well-characterized dFMRP mRNA targets, *futsch* and *CamKII,* can be repressed in a dNab2-dependent manner, providing evidence that dNab2 functions as a translational repressor in conjunction with dFMRP. In parallel, we identify mouse ZC3H14 enriched in axons of cultured primary hippocampal neurons and associated with translation machinery, implying a conserved role for dNab2/ZC3H14 in translational control. Our data support a model where dNab2/ZC3H14 contributes to dFMRP-mediated translational regulation of mRNAs trafficked to distal neuronal compartments, a process that is more critical in neurons than other cell types and that may underlie brain-specific defects in patients.

Introduction

RNA-binding proteins play critical roles in the transcription, processing, and translation of mRNAs to ensure proper gene expression (*2*). Consistent with the importance of this class of proteins, mutations in a number of genes that encode ubiquitously expressed RNA-binding proteins have been linked to human disease (*3*), and in many cases, these diseases present with tissue-specific pathology (*3, 41*). Neurological disorders are quite prevalent among diseases linked to RNA-binding proteins (*41*), likely due to the requirement for finely tuned control of gene expression in neurons. The challenge in such cases is to define the tissue-specific requirements and mechanisms of action for these factors that underlie their neuronal roles.

The *ZC3H14* (zinc finger CCCH-type 14) gene encodes an RNA-binding protein that is lost in an inherited form of autosomal recessive, non-syndromic intellectual disability (*5, 23*). Patients homozygous for nonsense mutations in the *ZC3H14* gene have very low IQ but lack dysmorphic features (*5*), suggesting a specific role for the ZC3H14 protein in nervous system development or function. In support of this idea, *Drosophila* lacking dNab2, the functional orthologue of ZC3H14 (*23*), show reduced viability, impaired motor function, and defects in brain morphology (*5, 132*), phenotypes that are rescued upon neuronal re-expression of dNab2 (*23, 132*). Despite evidence indicating an important role in the brain, the function of this protein that is critical in neurons remains largely undefined. *Drosophila* have been used extensively to model tissue-specific human disease (*133*) and provide an excellent system to define molecular roles of the dNab2/ZC3H14 protein family *in vivo*.

The *Drosophila* dNab2 and human ZC3H14 proteins share a domain structure and significant sequence homology, with an N-terminal PWI (proline/tryptophan/isoleucine)-

like domain, a centrally located nuclear-localization sequence, and a C-terminal domain of five CysCysCysHis (CCCH)-type zinc fingers that mediates RNA binding (*4, 5*). Each protein is found predominantly in the nucleus at steady-state and is widely expressed in many tissues, including the brain (*4, 5*). Fly dNab2 and human ZC3H14 each bind with high affinity to polyadenosine (poly(A)) RNA *in vitro* (*5, 74*), suggesting an interaction with the poly(A) tail of mRNAs *in vivo*. Consistent with this model, ZC3H14 colocalizes with poly(A) mRNA speckles in mouse hippocampal pyramidal neurons and cultured rat hippocampal neurons (*5*). In addition, RNAs harvested from the heads of adult *Drosophila* lacking dNab2, or from a mammalian neuronal cell line depleted for ZC3H14, show elongated poly(A) tails among a subset of total cellular RNA (*5, 23*). This elongated poly(A) tail phenotype is also observed in *S. cerevisiae* cells depleted of the Nab2 protein (*72*). The conserved nature of the poly(A) defect implies that dysregulated polyadenylation may drive altered patterns of mRNA stability and/or impact translation within the developing brains of flies and humans lacking dNab2/ZC3H14 that, in turn, impair neural function.

Genetic analysis in *Drosophila* has confirmed a critical and conserved requirement for dNab2 in neurons and specifically in neurons that extend axons into the mushroom bodies (*132*), twin neuropil structures required for associative olfactory learning and memory (*94*). Pan-neuronal dNab2 depletion in otherwise wildtype *Drosophila* is sufficient to replicate almost all phenotypes resulting from organism-wide loss of dNab2, including impaired adult viability, locomotor and flight defects, and a wings-held-out phenotype (*5*). Reciprocally, dNab2 re-expression solely in the neurons of *dNab2* mutants rescues these same phenotypes (*5*). Importantly, pan-neuronal expression

of a major isoform of human ZC3H14 (isoform 1) in *dNab2* mutant *Drosophila* is also sufficient to rescue a number of these defects, demonstrating a high degree of functional conservation between the dNab2 and ZC3H14 proteins in neurons (*23*). Notably, the *dNab2* mutant wing-posture and locomotor defects are not phenocopied by dNab2 depletion from motor neurons that innervate adult muscle (*5*), implying a requirement for dNab2 within central nervous system (CNS) neurons. Consistent with this observation, neuronal depletion of dNab2 impairs short-term memory in a courtship-conditioning paradigm (*132*) and at a structural level, dNab2 loss alters developmentally programmed patterns of axon projection into the α and β lobes of the mushroom bodies: β-lobe axons misproject across the brain midline and α-lobe axons show a high frequency of branching defects (*132*). Selective depletion or re-expression of dNab2 only in Kenyon cell neurons, which give rise to α and β axons, is sufficient to respectively phenocopy or rescue these defects (*23*). These findings confirm a critical and conserved role for dNab2 in neurons.

In aggregate, these genetic data provide strong evidence that dNab2 acts within neurons to control mushroom body morphology and behavior, but do not provide insight into molecular pathways that dNab2 uses to control these processes. The dNab2 protein likely modulates gene expression by binding to target mRNAs, perhaps in cooperation with other RNA-binding proteins. The near ubiquitous expression combined with the steady-state nuclear localization implies that dNab2 may rely on nuclear interactions to regulate mRNA processing. However the yeast Nab2 protein shuttles between the nucleus and cytoplasm (*73*), opening the possibility that dNab2/ZC3H14 could also play a role within the cytoplasm. A number of other RNA-binding proteins play critical roles in the neuronal cytoplasm. For example, the most commonly inherited form of intellectual

disability, fragile X syndrome, is caused by loss of expression of the RNA-binding protein FMRP (Fragile X Mental Retardation Protein). FMRP localizes to axons, dendrites and dendritic spines, and binds to target mRNAs to repress their local translation allowing for finely tuned post-synaptic, local protein translation (*36, 37*). FMRP is also localized to subcompartments within axons where it appears to play an important role in growth cone dynamics (*49, 134*) and presynaptic function during the development of neural circuits (*66, 67*). Thus, FMRP serves as a paradigm for how RNA-binding proteins can perform specialized critical functions within neurons.

Here, we describe a genetic screen for *dNab2* interacting loci in neurons that has uncovered a role for dNab2 as a translational repressor in association with the *Drosophila* FMRP homolog, dFMRP. We find extensive genetic interactions between *dNab2* and *dfmr1* in neuronal development and behavior that are paralleled by a physical interaction between the dNab2 and dFMRP proteins in the neuronal cytoplasm. We also provide evidence that dNab2 can engage in translational repression of specific neuronal mRNAs *in vivo* that are also targets of dFMRP. We extend these studies to demonstrate that murine ZC3H14 is also present in cytoplasmic foci and associated with translational machinery providing evidence that this translational regulatory role in the cytoplasm is conserved for ZC3H14. These data represent a critical first step in defining a molecular role for the conserved dNab2/ZC3H14 protein in neurodevelopment and neurological disease.

Results

dfmr1 is a dominant modifier of *dNab2* overexpression in the eye

To probe the function of *dNab2* in neurons, we exploited our prior finding that dNab2 overexpression in *Drosophila* retinal cells (*GMR-Gal4,UAS-dNab2*, or '*GMR>dNab2'*) leads to an adult rough-eye phenotype that is modified by alleles of the *PABP2* nuclear poly(A) binding protein and the *hiiragi* poly(A) polymerase (*5*). The *GMR>dNab2* rough-eye is characterized by a small adult eye field, loss of pigmentation and disorganized ommatidia (Figure 1A), all of which presumably reflect the ability of exogenous dNab2 to interact with cellular RNAs and engage endogenous RNA regulatory mechanisms. In this candidate-based approach, genes with established roles in neurodevelopment, neuronal function, that encode RNA-binding proteins, or that autonomously regulate axonogenesis in the brain mushroom bodies in a manner similar to dNab2 (*132*) were analyzed for modification of the *GMR>dNab2* rough-eye phenotype. Available alleles for these candidate genes (200 in total) included loss-of-function alleles, RNAi depletion lines, and EP-type overexpression lines (*135*). Each candidate modifier allele was crossed into the *GMR>dNab2* background and evaluated for suppression or enhancement of the rough eye phenotype (Figure 1A). Of 200 alleles tested, 14 enhanced the rough eye phenotype and 30 suppressed (Figure 1A and Table S1); some of these 44 modifiers correspond to loss-of-function alleles and others are EP-type insertions (*135*), confirming that the effect of dNab2 expression in eye cells is readily modified by altering gene-dosage of multiple factors among the selected group of candidates.

Multiple *GMR>dNab2* modifier alleles recovered from the genetic screen correspond to factors that function within translational regulatory pathways that involve *dfmr1*, which encodes the *Drosophila* homolog of the fragile X syndrome mental retardation protein (dFMRP) (Table S1). A null allele of *dfmr1*, $dfmr1^{\Delta 50}$, dominantly

suppresses the *GMR>dNab2* eye phenotype, indicating that a diploid dose of *dfmr1* is required for dNab2 to disrupt eye morphology (Figure 1B). In addition, alleles of the miR pathway components *Argonaute-1* (*Ago1*) and *Gw182*, the *Rm62/dmp68* RNA helicase, the RNA-binding proteins *Staufen* and *Ataxin-2*, and the matrix metalloproteinase *Timp*, also modify the *GMR-dNab2* adult eye phenotype. Each of these genes interacts genetically with *dfmr1* in *Drosophila* (*60, 136-139*). Furthermore, *dNab2* and *dfmr1* transgenes exhibit synthetic lethality when co-expressed in the developing eye. Transgenic overexpression of *dfmr1* in *Drosophila* causes apoptosis and a dominant rough eye phenotype (*87, 140*). Flies that overexpress *fmr1* in the eye (*GMR>dfmr1)* are viable in a wildtype background (*GMR-Gal4,UAS-dfmr1*) but this overexpression is lethal when *dNab2* is also overexpressed (*GMR-Gal4,UAS-dNab2,UAS-dfmr1*) (Table S1). The recovery of *dfmr1* and *dfmr1*-interacting genes as *GMR-dNab2* modifiers led us to explore whether dNab2 and dFMRP function within similar neuronal pathways and/or complexes.

dfmr1 interacts with *dNab2* in locomotor behavior and mushroom body development

To further explore interactions between dNab2 and dFMRP in neurons, we examined neuronally encoded locomotor behavior and development of the mushroom bodies, twin neuropil structures in the brain that are essential for olfactory learning and memory (*94*). Pan-neuronal RNAi-mediated depletion of dNab2 causes a locomotor defect in adult flies that is not replicated by depletion solely in motor neurons (*5*), implying a requirement for dNab2 in central nervous system (CNS) circuits that support locomotion. This dNab2-RNAi locomotor defect is dominantly enhanced by the $dfmr1^{\Delta 113M}$ null allele (*C155-*

Gal4,UAS-dNab2-RNAi;dfmr1$^{\Delta 113M}$/+) (Figure 1F). This effect of a second, independent *dfmr1* allele, *dfmr1*$^{\Delta 113M}$, parallels the suppressing effect of *dfmr1*$^{\Delta 50}$ on the gain-of-function *GMR-dNab2* model and provides additional evidence of a tight link between *dNab2* and *dfmr1* gene dosage.

dNab2 and dFMRP each act cell-autonomously within the Kenyon cell neurons of the mushroom bodies to pattern axon projection (*56, 132*). Loss of either factor elicits similar mushroom body defects, including misprojection of β-lobe axons across the brain midline (ß-lobe fusion) and missing or thinned α-lobes [(*56, 132*) and Figure 2]. These α/β-lobe defects appear with similar severity and penetrance in each homozygous null background (*dNab2*^{ex3} or *dfmr1*$^{\Delta 50}$) ((*56*) and Figure 2A,B), suggesting the potential for shared effects on downstream pathways. Consistent with this idea, heterozygosity for either gene has no detectable effect on mushroom body morphology in isolation, but dominantly modifies mushroom body phenotypes caused by loss of the other gene. *dfmr1* heterozygosity significantly increases the frequency of α-lobe defects (i.e. missing or thinned α-lobes as judged by anti-Fas2 staining) in *dNab2* null brains without a corresponding effect on β-lobe defects (Figure 2D,G,H). Reciprocally, *dNab2* heterozygosity rescues the frequency of α-lobe defects in *dfmr1* null brains with no discernable effect on β-lobes (Figure 2E,H). Thus, although removing dNab2 from otherwise wildtype Kenyon cells leads to highly penetrant defects in α-lobe development (*132*), reducing dNab2 dosage in *dfmr1* null neurons has the opposite effect of rescuing α-lobe development (Figure 2G). This remarkable pattern of opposing effects of *dNab2* alleles on α-lobe structure implies that dNab2 can either promote or disrupt α-lobe

development depending on *dfmr1* status, perhaps via linked roles for dNab2 and dFMRP proteins on an overlapping cohort of transcripts with roles in α-lobe development.

dNab2 co-localizes with dFMRP RNPs in neurites

The abundant and complex genetic links between *dNab2* and *dfmr1* in retinal and CNS neurons suggest that the two RNA-binding proteins may associate with one another within RNA-protein complexes. A dNab2-dFMRP association would be somewhat surprising, given that the majority of each protein localizes to distinct cellular compartments at steady-state: dNab2 is localized to the nucleus at steady state (*5, 71*) while dFMRP is primarily cytoplasmic (*45*). However, orthologs of dNab2 and dFMRP undergo dynamic nucleocytoplasmic shuttling (*141, 142*). Human FMRP binds mRNA transcripts in the nucleus and accompanies them to the cytoplasm (*143*) and *S. cerevisiae* Nab2 also shuttles between the nucleus and the cytoplasm in a manner that depends on poly(A) RNA export (*142*). To examine the subcellular distribution of dNab2 in single neurons, we utilized an anti-dNab2 antibody (*5*) to track dNab2 protein in 3-day old cultured primary *Drosophila* brain neurons (Figure 3). These neuronal cultures were co-stained with an anti-HRP antibody to visualize neuronal membranes and illuminate neurite arbors (Figure 3A). As previously reported (*5*), the dNab2 protein is enriched in the nucleus of all neurons examined; however, two-thirds of these neurons also contain cytoplasmic dNab2 in the form of discrete puncta distributed along the length of neurites (Figure 3A,C). To confirm that the cytoplasmic signal is due to dNab2, we demonstrated that it is lost in cultured neurons derived from dNab2 null brains (Figure 3B). Of the cultured cells examined, only 2/3 have detectable dNab2 in the cytoplasm. This diversity could reflect the fact that the cultured neurons contain a mixture of types of neurons that

are not readily distinguished *in vitro*. We hypothesized that cell-to-cell variation in the presence of dNab2 cytoplasmic puncta in mixed brain cultures could be due to differences in dNab2 localization between specific types of neurons. To test this hypothesis, the distribution of dNab2 protein was examined in neuronal cultures expressing membrane-tethered GFP in Kenyon cells (*OK107-Gal4,UAS-CD8:GFP*), which extend axons into the mushroom body lobes (*114*). This approach labels Kenyon cells with GFP and allows for identification of these cells in the mixed culture. Among these CD8:GFP-positive Kenyon cells examined, 80% (8 of 10) contained dNab2 cytoplasmic puncta (Figure 4E). Thus, even within a single neuronal cell type, there is cell-to-cell variation in whether or not dNab2 can be detected in cytoplasmic puncta. The reason for this variation is not clear, however it could be stochastic or due to Kenyon cell subtype (e.g. α, α', β, β' or γ) or developmental age (e.g. 'early' vs 'late' born mushroom body neurons). In sum, these fluorescence data identify a previously undefined pool of dNab2 present within neurites.

We next tested whether dFMRP co-localizes with cytoplasmic dNab2 puncta in neuronal processes of wildtype brain neurons illuminated by anti-HRP (Figure 4A). As described by others (*137, 138*), dFMRP is detected in the soma cytoplasm and in puncta that distribute along the length of neurites (Fig 4A), which correspond to dFMRP-containing ribonucleoprotein (RNP) granules (*137, 138*). Importantly, when dNab2 localization is analyzed in these same neurites, dNab2 and dFMRP co-localize within a subset of these neurite puncta (Figure 4A, arrows). Mander's Coefficient was used to quantitate dNab2-dFMRP co-localization specifically in neurites distal from the cell body (Figure 4A). By this analysis, approximately 20% of total dNab2 signal in neurites

overlaps with dFMRP-positive puncta and approximately 25% of the dFMRP signal in neurites overlaps with dNab2-positive puncta. This co-localization of subsets of dNab2 and dFMRP protein in neurites suggests that dNab2 may be a component of a subset of dFMRP-containing RNP granules in brain neurons. These data also provide a potential molecular context for the strong genetic interactions between *dNab2* and *dfmr1* in retinal cells and in brain neurons.

The dNab2 and dFMRP proteins physically associate in neurons

To assess whether dNab2 and dFMRP physically interact and corroborate the immunofluoresence data, the RNA-tagging technique (*144*) was used to precipitate N-terminally Flag-epitope tagged Nab2 from brain neurons. Briefly, lysates generated from heads of flies with pan-neuronal expression of Flag-dNab2 (*C155-Gal4;UAS-Flag-Nab2*) were immunoprecipitated with anti-Flag antibody-conjugated agarose beads. This technique effectively enriches for Flag-tagged dNab2 or a control Flag-tagged RNA-binding protein, human PABP (Flag-hPABP) (*144*), from head lysates (Figure 4B). Negative control lysates prepared from flies expressing the *C155-Gal4* driver alone did not immunoprecipitate detectable anti-Flag reactive epitopes. Immunoblot of these anti-Flag precipitates with anti-dFMRP antibody (*145*) specifically detects dFMRP protein only in the Flag-dNab2 sample and not in the Flag-hPABP or Gal4-alone samples, indicating that dNab2 may be part of protein-RNA complex that includes dFMRP.

To biochemically localize the dNab2-dFMRP association within cells, we exploited a muscle-specific driver (*MHC-Gal4*) in order to provide sufficient starting tissue for biochemical fractionation. The immunoprecipitation protocol was repeated with lysate prepared from *MHC>Flag-dNab2* adult flies that was fractionated into nuclear and

cytoplasmic fractions. Immunoblotting these lysates with an antibody to the nuclear protein Lamin D confirms the separation of soluble nuclear and cytoplasmic proteins (Figure 4C, bottom panel). Immunoblot analysis of total lysates prior to immunoprecipitation reveals the expected nuclear enrichment of Nab2 and cytoplasmic enrichment of dFMRP, but also detects pools of each protein in the reciprocal compartment (i.e. dNab2 in the cytoplasm and dFMRP in the nucleus). Significantly, upon anti-Flag immunoprecipitation, dFMRP is detected in association with cytoplasmic dNab2 but not the considerably more abundant pool of nuclear dNab2. The dNab2-dFMRP association is not disrupted by addition of RNAse, indicating that co-immunoprecipitation of the two proteins is not RNA-dependent (Supplemental Figure 1). This biochemical evidence of a dNab2-dFMRP complex in the cytoplasm parallels the co-localization of dNab2 and dFMRP in neurites and provides further a correlate to the genetic evidence that these proteins co-regulate mushroom body development. Thus, dNab2 may be a component of dFMRP-containing RNA-protein granules in the neuronal cytoplasm.

dFMRP and dNab2 co-regulate target RNAs

The conserved requirement for dNab2/ZC3H14 in supporting higher cognitive function (*5, 132, 146*) indicates that the RNAs bound and regulated by this RNA-binding protein are important for neural development and/or function. The spectrum of dNab2-regulated RNAs is not known, but the dNab2-dFMRP association implies that dNab2 could play a role in regulating mRNAs that are also regulated by dFMRP. Two well-conserved mRNA targets of dFMRP/FMRP are *futsch*, the *Drosophila* homolog of *microtubule-associated protein-1B* (*Map1B*) (*59*), and the *Calmodulin-dependent protein Kinase II* (*CaMKII*)

(*60*). dFMRP interacts with the *futsch* and *CamKII* mRNAs and represses their translation (*59, 147*); consequently both proteins are elevated in *Drosophila* neurons lacking dFMRP (*59, 60*). Similarly, FMRP represses translation of CamKIIα and MAP1b mRNAs in mouse brain (*148, 149*)**.**

To assess the requirement for dNab2 in dFMRP-mediated translational repression, we took advantage of the ability of overexpressed dFMRP to repress Futsch protein levels in neurons (*59*). In control cultured brain neurons, Futsch protein is located both in the cell body and distributed along the central shaft of major neuronal processes (Figure 5A). In dFMRP over-expressing neurons (*C155>dfmr1*), Futsch levels drop in the cell body and become nearly undetectable in the neuronal shafts (Figure 5A). When these effects are quantified across all compartments, Futsch levels are reduced by approximately 2-fold in dFMRP-overexpressing neurons (Figure 5C). When we analyzed the requirement for dNab2 in this system, we observed an interesting pattern: although Futsch levels are unaltered in *dNab2* null neurons relative to control neurons, the absence of dNab2 nonetheless effectively suppresses the ability of excess dFMRP to repress Futsch levels (Figures 6B-E). We confirmed that similar levels of exogenous dFMRP are expressed in control and *dNab2* null neurons (Figure 5B,D), indicating that the epistatic effect of dNab2 is not due to differences in *dfmr1* transgene expression between control and *dNab2* null neurons. These genetic data argue that endogenous dNab2 is not strictly required to repress Futsch translation, but that dNab2 is required by exogenous dFMRP to repress Futsch.

We next examined the requirement for dNab2 in control of *CaMKII* mRNA translation in neurons. The *CaMKII* mRNA encodes a post-synaptically localized kinase

involved in synaptic plasticity and learning and memory (*150*) that is repressed by dFMRP *in vivo* (*60*). To assess translational inputs into the *CaMKII* mRNA, we utilized a previously described *CaMKII* translational reporter that contains a Gal4-inducible *eYFP* coding-sequence fused to the *CaMKII* 3'UTR (*151*). This reporter was co-expressed with *dNab2* and *dfmr1* RNAi transgenes in olfactory projection neurons (*GH146-Gal4*) that innervate the antennal lobe (*152, 153*). In control flies, *eYFP:CaMKII-3'UTR* is expressed in the cell bodies and dendrites of *GH146*-positive projection neurons (PNs) of the antennal lobe (Figure 6A). As observed in prior work (*60*), RNAi-mediated depletion of dFMRP in these neurons increases *CaMKII-3'UTR* reporter expression as shown by elevated eYFP fluorescence (Figure 6A). Significantly, RNAi-mediated knockdown of *dNab2* in *GH146* PNs elevates expression of the *CaMKII-3'UTR* reporter to a nearly identical extent as knockdown of *dfmr1* (Figure 6A,C). RNAi knockdown of the unrelated NMDA receptor (NR1) does not affect *CaMKII-3'UTR* reporter expression (Figure 6A), confirming the specificity of the effects of dNab2 and dFMRP knockdown. Moreover, RNAi knockdown of *dNab2* in *GH146* antennal lobe neurons did not affect expression of a second unrelated translational reporter comprised of eGFP fused to the *SV40-3'UTR* (Figure 6B). These *in vivo* data indicate that dNab2 is required in neurons to inhibit expression of a *CaMKII-3'UTR* translational reporter in a manner similar to dFMRP.

ZC3H14 localizes to axons and associates with the translational machinery

Our prior finding that a neuron-specific isoform of human ZC3H14 (isoform1) rescues *dNab2* null fly phenotypes (*23*) implies that vertebrate ZC3H14 may also display properties of a cytoplasmic translational regulator. To test this hypothesis, the

localization of endogenous ZC3H14 was assayed in primary cultured murine hippocampal neurons with an antibody that recognizes ZC3H14-isoform1 (iso1) and the closely related ZC3H14-iso2 and iso3 proteins (*4*). As previously reported (*70, 154*), these ZC3H14 isoforms are located within nuclear speckles (Fig. 7A), but they are also detected in the cytoplasm of neuronal extensions consistent with the finding in cultured *Drosophila* neurons. Importantly, this cytoplasmic anti-ZC3H14 signal is absent from hippocampal neurons cultured from *ZC3H14*$^{\Delta/\Delta}$ mice that were recently generated (*146*) (Figure 7B), confirming that the signal corresponds to endogenous ZC3H14-iso1-3 proteins. As with *Drosophila* dNab2, the cytoplasmic pool of murine ZC3H14 is also detected following biochemical fractionation into nuclear and cytoplasmic lysates (Figure 7D). Nuclear/cytoplasmic fractionation was confirmed with antibodies to the nuclear-specific marker, Histone H3, and the cytoplasmic-specific marker, α-Tubulin (*155*). As a control, we also examined another nuclear RNA-binding protein, THOC1, which aids in the processing and export of polyadenylated mRNA (*156, 157*). As expected, THOC1 was only detected in the nuclear fraction (Figure 7D), which provides evidence that detection of the RNA-binding protein, ZC3H14, in the cytoplasm does not reflect a pattern common to all RNA-binding proteins.

Closer inspection of the anti-ZC3H14 immunofluorescence pattern revealed that the protein is enriched in a single neurite from each hippocampal neuron. To assess the distribution of ZC3H14 in axons and dendrites, antibodies for a dendritic marker, Map2 (*158, 159*), or an axonal marker, Tau (*158, 159*), were used in co-staining experiments. ZC3H14 immunofluorescence is generally excluded from Map2-labeled dendrites but is present throughout the Tau-positive axon, including the growth cone (Figure 7A-C).

These results provide evidence that ZC3H14 is enriched specifically in axonal extensions of cultured hippocampal neurons.

To determine whether ZC3H14 physically associates with translation machinery, we performed a polyribosome fractionation experiment using a linear sucrose density gradient and probed for ZC3H14 by immunoblotting. As shown in Figure 7F, we found that in cytoplasmic brain lysates isolated from P13 mice, ZC3H14 co-sediments with fractions containing monosomes and polyribosomes. To provide additional evidence that ZC3H14 co-sedimentation with polyribosomes is specific to intact translational machinery, we also generated cytoplasmic P13 brain lysates in the presence of the magnesium ion chelator, EDTA, which disrupts ribosomes into large and small ribosomal subunits (*160*). EDTA-mediated disruption of ribosomes is indicated by the absence of polyribosome peaks in the RNA absorption profile and a shift of the ribosomal S6 protein, a component of the 40S subunit (*161*), to the lighter density sucrose fractions (Figure 7G). Following EDTA treatment, ZC3H14 also shifted to the lighter fractions (Figure 7G), indicating that ZC3H14 is specifically associated with intact ribosomes. In aggregate, these data indicate that ZC3H14 isoforms 1-3 are enriched in hippocampal axons and associated with ribosomes in brain lysates, which is consistent with a role in spatial regulation of translation in neurons.

Discussion

Here we report that the dNab2 RNA-binding protein, the sole *Drosophila* ortholog of human ZC3H14, functionally and physically interacts with the homolog of Fragile X Mental Retardation Protein, dFMRP, in the development of the mushroom bodies as well as in the translational repression of mRNA target transcripts. Evidence from both *Drosophila* and mouse reveal a pool of dNab2/ZC3H14 present in the neuronal cytoplasm and associated with the translational machinery. This work suggests that the requirement for this class of protein to support proper brain function could reflect a critical role in the regulation of translation.

The dNab2-dFMRP interaction provides new insight into how dNab2 affects neuronal gene expression, but our data also suggest that the two proteins may not always act in redundant or identical ways on all RNA targets. *dNab2* and *dfmr1* are independently required for proper mushroom body development (*56, 132*) and loss of either factor induces β-lobe overgrowth and α-lobe thinning/loss. However, *dNab2* and *dfmr1* show dosage sensitive interactions only in the context of α-lobe development. One interpretation of these data is that dNab2 and dFMRP may co-regulate RNA transcripts required for proper projection of α-axons, perhaps by acting within common RNP granules, but that these relationships are not conserved in β-lobe projections. Moreover, the observation that dFMRP status determines the phenotypic outcome of *dNab2* alleles in α-lobes implies that dFMRP is, to a degree, epistatic to dNab2: *dNab2* loss leads to α-lobe defects that can be enhanced by *dfmr1* heterozygosity, but *dNab2* heterozygosity rescues α-lobe defects in *dfmr1* null flies. These results imply that dNab2 and dFMRP co-regulate an overlapping set of transcripts, but not in precisely the same manner.

The molecular effects of dNab2 on Futsch and CaMKII reveal additional complexity in the manner in which *dNab2* can modulate translation. Knockdown of *dNab2* is sufficient to increase expression of a *CaMKII* translational reporter to an almost identical degree as knockdown of *dfmr1*, but it is not sufficient to dysregulate steady-state levels of Futsch protein, whose mRNA is bound and regulated by dFMRP (*59*). Rather, dNab2 is required for repression of Futsch by overexpressed *dfmr1*. Thus, dNab2 is independently required to regulate some target transcripts (e.g. *CaMKII)*, while other transcripts *(*e.g. *futsch)* appear to be regulated in a manner that is dependent on dFMRP, implying that dNab2 may be required for dFMRP to properly regulate some target RNAs.

The genetic and biochemical evidence linking dNab2/ZC3H14 to translational repression in the cytoplasm of neurons does not distinguish the molecular process these RNA-binding proteins use to control bound RNAs. Although there are a number of mechanisms through which this regulation could occur, the interaction of dNab2 and dFMRP in fly cells raises the possibility that dNab2-dependent repression might involve dFMRP. dFMRP physically interacts with the RNA-induced silencing complex (RISC) in the cytoplasm of cultured *Drosophila* neurons that is closely linked with miRNA-mediated repression (*162*). Notably, the *CaMKII 3'UTR* GFP sensor which responds to dNab2 loss is also a target of the miRNA pathway (*60, 151*), and multiple miRNA-RISC components, including *Ago1, Dcr1,* and *gawky* (GW182), were recovered in our *GMR-dNab2* rough eye screen. One explanation of these genetic links is that dNab2 loss extends poly(A) tails (*5*), which in turn facilitates enhanced recruitment of the RISC component GW182 by the poly(A) binding protein PABP (*163*). Alternatively, dNab2 may interact with dFMRP and block translation-coupled circularization of mRNAs.

Poly(A) binding proteins are also emerging as important regulators of local translation in the cytoplasm of neurons (*164*). Yet while most cytoplasmic PABPs enhance polyadenylation of their bound mRNAs, dNab2/ZC3H14 appears to repress this process, suggesting that antagonism between two types of cytoplasmic PABPs may directly affect the translation of key neuronal mRNAs.

Consistent with the apparent role of dNab2 in translational regulation in *Drosophila*, the orthologous protein ZC3H14 localizes to axons and the growth cone in cultured murine hippocampal neurons and co-sediments with polyribosomes in the mouse brain, suggesting a potential role in regulation of local protein synthesis. FMRP is localized to polysomes as well, and has been suggested to inhibit translation by polysome stalling (*147*)**.** Intriguingly, CamKIIa is one of a group of synaptic proteins that increase in abundance in the hippocampus of *Zc3h14* knockout mice compared to control $Zc3h14^{+/+}$ mice (*146*), implying that CamKIIa is a conserved target of dNab2/ZC3H14. *CamKIIa* mRNA is also a well-validated target of FMRP (*46*). FMRP localizes to both axons and dendrites (*49*), and two other mammalian FMRP family members Fxr1 and Fxr2 are enriched pre-synaptically in axons (*69, 145*). We speculate that the dNab2-dFMRP interaction observed in flies may be conserved in mammals as a ZC3H14-Fxr1 or Fxr2 interaction. In support of this hypothesis, Fxr1 co-precipitates with the zinc-finger domain of ZC3H14 (*165*). Although functional and biochemical studies will be required to confirm the significance of this interaction in mammals, the significant body of genetic, biochemical and functional data in fly neurons, together with the findings that murine ZC3H14 is enriched in hippocampal axons and co-sediments with polyribosomes

supports a model in which a newly defined cytoplasmic pool of dNab2/ZC3H14 plays a required role in the translational repression of key neuronal target mRNAs.

Here we show that the dNab2 and ZC3H14 poly(A) RNA-binding proteins localize to the nucleus and cytoplasm of neurons, that the cytoplasmic pools of these proteins interact with both dFMRP and polyribosomes, and that dNab2/ZC3H14 modulates neuronal translation. Given the clear link between FMRP and intellectual disease in humans, these interactions raise the question of whether defects in translational silencing of mRNAs transported to distal sites within neuronal processes contribute to intellectual disability in humans lacking ZC3H14.

Experimental Procedures:

Drosophila stocks and genetics. All crosses and stocks were maintained in standard conditions at 27^{o} C. The *dNab2^{ex3}* loss of function mutant, *dNab2^{pex41}* precise excision isogenic control, and UAS-*Flag-dNab2* stocks were described previously (*5, 23*). The following Gal4 drivers were utilized to drive expression of UAS transgenes: *GMR-Gal4* (expresses in the eye cells behind the morphogenic furrow, BL#1350), *C155-Gal4* (pan-neuronal expression, BL#458), *OK107-Gal4* (expresses in all lobes of the mushroom body, BL#854), and *GH146-Gal4* (expresses in antennal lobe projection neurons). The following alleles and transgenic stocks were also used in this study: *dfmr1$^{\Delta 50}$* (BL#6930), *dfmr1$^{\Delta 113M}$* (BL#6929), *UAS-CD8-GFP* (*105*), *UAS-eYFP-CAMKII 3′ UTR*(*151*), *UAS-dNab2^{IR}* (obtained from the Vienna *Drosophila* Research Center), and *dfmr1^{IR}* (BL#35200). The *UAS-dfmr1* transgenic stock was a gift from Thomas A. Jongens. The *eYFP-CaMKII* reporters (*151*) were a gift from Dr. Sam Kunes.

Brain dissection and immunohistochemistry. Brain dissections were performed as previously described (*132*). Briefly, brains were dissected from adult flies in PBT (1x PBS , 0.1% Triton X-100) and immediately transferred to PBS at 4^{o} C. Brains were fixed in 4% paraformaldehyde at room temperature and then washed 3 times in 1x PBS. Subsequently, brains were permeablized in 0.3% PBS-T (1xPBS, 0.3% Triton X-100), incubated in blocking solution (0.1% PBS-T, 5% normal goat serum) for 1 hour, followed by an overnight incubation in blocking solution and primary antibodies. After a series of 5x washes in PBT, brains were incubated in blocking solution for 1 hour and then incubated for 3 hours in blocking solution plus secondary antibodies. The brains were then washed 5x in PBT and mounted in Vectashiel (Vector Labs). The FasII antibody

clone 1D4 hybridoma used to label the mushroom bodies at a 1:20 dilution was obtained from the Developmental Studies Hybridoma Bank (DSHB).

Primary culture of *Drosophila* brain neurons and immunohistochemistry. Brains were dissected from pupae 24 hours after puparium formation (APF), disassociated with the Liberase enzyme blend (following the manufacturer's instructions), and plated on #1.5 35mm glass coverslips coated with Laminin and Concanavalin A. Plated neurons were incubated in Schenider's Medium, 10% FBS and 0.05 mg/mL insulin for three days at 27^{o} C. Cells were washed 3x with Rinaldi's Saline before fixing in 4% paraformaldehyde. Fixed cells were dehydrated with an ethanol gradient and stored in 70% ethanol prior to antibody staining. Primary antibodies were incubated for 1 hour at room temperature, and secondary antibodies were incubated for 40 minutes. The polyclonal dNab2 antibody has been described previously (*5*), was pre-absorbed with fixed *Drosophila* embryos and used at a final concentration of 1:1000. Anti-dFMRP monoclonal antibody 6A15 was used at a 1:400. Anti-HRP FITC (Jackson ImmunoResearch Laboratories, Inc.) was used at a concentration of 1:500.

Microscopy and image processing. Drosophila eye images were collected with a Leica DFC500 charge-coupled device digital camera. All other images were collected with the Zeiss LSM 510 confocal microscope. Whole brain images were captured with a 20x objective, and cultured neurons were captured at 63x. Image Processing: Maximum intensity projections of brain images were obtained by combining serial optical sections with the Zeiss Zen software suite. Images of primary *Drosophila* brain neurons were processed with the Gaussian Blur filter, then background removed using the subtract function in Fiji.

Immunoprecipitation: Immunoprecipitation *Drosophila* neuronal tissue was adapted from Yang et al. (*144*). Briefly, heads from 5 day old adult flies were isolated and lysed in 400 µl of Nuclear Lysis Buffer: 50mM Tris HCl, pH 8.1, 10 mM EDTA, 150mM NaCl,1%SDS. Heads were incubated on ice for 20 minutes, then mixed with 800 µl of IP Dilution buffer: 50mM Tris HCl, pH 8.1, 10 mM EDTA, 50mM NaCl. The diluted homogenate were cleared by centrifugation at 12,000 RPMs for 10 minutes. FLAG-dNab2 lysates were then immunoprecipitated using anti-FLAG-M2 affinity agarose beads (Sigma) for 3 hours at 4^{o} C. After a series of 5 washes with IP Dilution Buffer, beads were eluted at 65^{o} C for 30 minutes with Elution buffer: 50 mM Tris HCl, pH 7.0, 10 mM EDTA, 1.3% SDS. All buffers were treated with RNaseIN and complete protease inhibitor tablets immediately before use.

Nucleocytoplasmic fractionation of *Drosophila* tissue. Five flies of each genotype were homogenized in 250 µl of cold nuclear isolation buffer (10 mM Tris•Cl, pH 7.4, 10 mM NaCl, 3 mM MgCl2, 0.5% (v/v) NP-40, 1 x complete protease inhibitor cocktail). The homogenate was transferred to a fresh tube and incubated on ice for 5 minutes followed by centrifugation for 5 minutes at 500xg. The supernatant was collected as the cytosolic fraction and the pellet contained nuclei. Pelleted nuclei were washed once by gently resuspending in nuclear isolation buffer, collected by centrifugation for 5 minutes at 500xg and lysed by sonication in 250 µl of nuclear isolation buffer.

Western Blot Analysis. 25 µl of immunoprecipitates were mixed with 5 µl of 6x laemmli sample buffer and boiled for 5 min. Equal amounts of protein were loaded onto a 5% SDS-PAGE gel, then transferred to a PVDF membrane (Immuno-Blot, Bio-Rad). The membrane was subsequently blocked with 5% NFDM, 1x TBS-T and probed with

primary antibodies. To detect FLAG-tagged proteins, membranes were incubated the M2 antibody (Sigma-Aldrich) at a concentration of 1:1000. The anti-dFMR1 monoclonal antibody 6A15 was obtained from Abcam and used at a 1:1500 dilution. The anti-Lamin antibody was used at a concentration of 1:2000 and was obtained from the DSHB.

Primary hippocampal culture. Hippocampi were dissected and cultured from postnatal day 1 *Zc3h14*$^{+/+}$ control and *Zc3h14*$^{\Delta/\Delta}$ mutant mice and repeated using at least three independent litters for each genotype. Neuronal isolation and culture were performed as previously described (*166, 167*). Briefly, dissociated neurons were plated on poly-L-lysine coated coverslips (1.0 mg/ml). Neurons were attached to the substrate in minimal essential medium with FBS (10%) for 3 h, inverted onto dishes containing astroglia previously isolated from the appropriate corresponding control *Zc3h14*$^{+/+}$ or mutant *Zc3h14*$^{\Delta/\Delta}$ pups, and grown in defined Neurobasal Medium (Invitrogen, Eugene, OR) with Glutamax (Invitrogen) and B-27 supplements (Invitrogen). Neurons were cultured for 5 days *in vitro* and fixed with 4% PFA in 1× PBS at room temperature for 15 min.

Immunofluorescence staining of mouse primary hippocampal neurons. Anti-ZC3H14 (1:500 (*154*)), Map2 (1:500; Sigma-Aldrich M 1406), Tau (1:500; Millipore MAB3420), β-Tubulin E7a (1:2000; Developmental Studies Hybridoma Bank, University of Iowa) antibodies were incubated overnight at 4°C. Fluorescein (FITC)- and Texas Red-conjugated secondary antibodies (1:500; Jackson ImmunoResearch 711-096-152 and 111-076-047, respectively) were incubated for 1 h at room temperature. Fluorescent images were visualized using a 63X oil objective on a Leica TCS SP8 MP multiphoton confocal microscope. Images were captured using LAS-AF (Leica) software.

Nucleocytoplasmic fractionation of mouse tissue. Brains were collected from control and *Zc3h14*$^{\Delta/\Delta}$ mice and homogenized in CLB buffer (10 mM HEPES, 10 mM NaCl, 1 mM KH2PO4, 5 mM NaHCO3, 5 mM EDTA, 1 mM CaCl2, 0.5 mM MgCl2). 10% of the sample was removed as the whole cell fraction and resuspended in RIPA-2 (150 mM NaCl, 1% IgePal or NP-40, 0.5% sodium deoxycholate, 0.1% SDS, 50 mM Tris pH 8.0). Cytoplasmic and nuclear fractions were then isolated as previously described (*168*). All fractions were sonicated on ice 5 times at 0.5% output for 10 seconds and then centrifuged at 13,000 x RPM for 10 minutes at 4°C. The pellet was then discarded, and the supernatant was subjected to SDS-PAGE and immunoblotting as described above.

Polyribosome fractionation. Analysis was performed as previously described (*169, 170*). Briefly, age P13 mice were sacrificed by isoflurane anesthesia and decapitation. The brain was removed and placed in ice-cold, freshly prepared dissection buffer (10 mM HEPES, pH 7.3, 150 mM KCl, 5 mM $MgCl_2$, 100 ug/ml cycloheximide). Each cortex was dissected and manually homogenized with 12 strokes in 1 ml of lysis buffer (10 mM HEPES, pH 7.3, 150 mM KCl, 5 mM $MgCl_2$, 100 ug/ml cycloheximide, 1 tablet of Complete EDTA-free protease inhibitor cocktail (Roche), 100 U/ml SUPERase-In (RNase inhibitor, Life technologies)). For EDTA treated samples, lysis buffer included 0.030 M EDTA. The homogenate was spun at 2000 x g for 10 min at 4°C. The supernatant (S1) was transferred to new Eppendorf tubes. Igepal was added to S1 for a final concentration of 1% IgePal and mixed by inverting 8 times, followed by incubation on ice for 5 min and centrifugation at 20,000 x g for 10 min at 4°C. The resulting supernatant (S2) was loaded onto a 15-45% wt/wt linear density gradient of sucrose in 10 mM HEPES, pH 7.3, 150 mM KCl, 5 mM $MgCl_2$, 100 ug/ml cycloheximide, 100 U/ml

SUPERase-In. Gradients were centrifuged at 38,000 x RPM for 2 hr at 4°C in a Beckman SW41 rotor and fractionated into 10 x 1.1-ml fractions with continuous monitoring at OD_{254}. Fractions were processed for immunoblotting using standard techniques, without need for further concentration of samples.

Figures

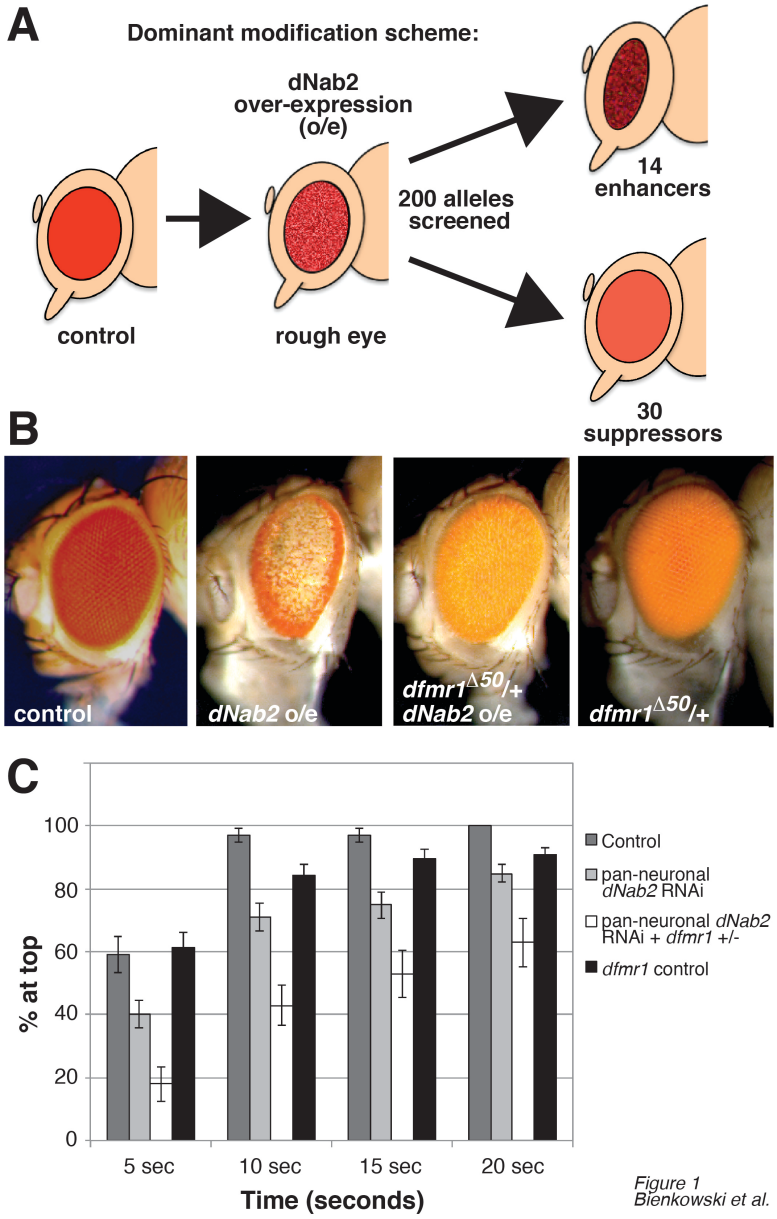

Figure 3-1. Genetic interactions between *dNab2* and *dfmr1*. (**A**) Schematic of the screen for genetic modifiers of a *dNab2* gain-of-function phenotype. *GMR-Gal4* driven overexpression (o/e) of dNab2 from the $dNab2^{EP3716}$ allele (*GMR>dNab2*) in the developing eye field leads to a "rough" adult eye phenotype that was screened against a pre-selected group of 200 candidate alleles. Of these, 14 enhanced and 30 suppressed *GMR>dNab2* rough eyes. (**B**) Light microscopic images of eyes from control (*GMR-*

Gal4/+), *dNab2* transgenic (*GMR-Gal4/+;dNab2*^{EP3716}/+), *dNab2* transgenic+*dfmr1* heterozygous (*GMR-Gal4/+;+,dfmr1*$^{\Delta 50}$/ *dNab2*^{EP371},+), and *dfmr1* heterozygous (*GMR-Gal4/+;dfmr1*$^{\Delta 50}$/+) adult females. (**C**) Quantitation of a negative geotaxis assay among groups of 5-day old adult control flies (*C155-Gal4*), flies with pan-neuronal dNab2 RNAi (*C155-Gal4,UAS-dNab2-IR*), flies with pan-neuronal dNab2 RNAi in combination with *dfmr1* heterozygosity (*C155-Gal4,UAS-dNab2-IR,dfmr1*$^{\Delta 113M}$/+) or *dfmr1* heterozygotes alone (*C155-Gal4,dfmr1*$^{\Delta 113}$/+). Data are presented as the percentage of flies that reach the top of a cylinder at each time interval. Flies were assayed in groups of 10 and measured in at least 10 independent trials. Error bars represent SD.

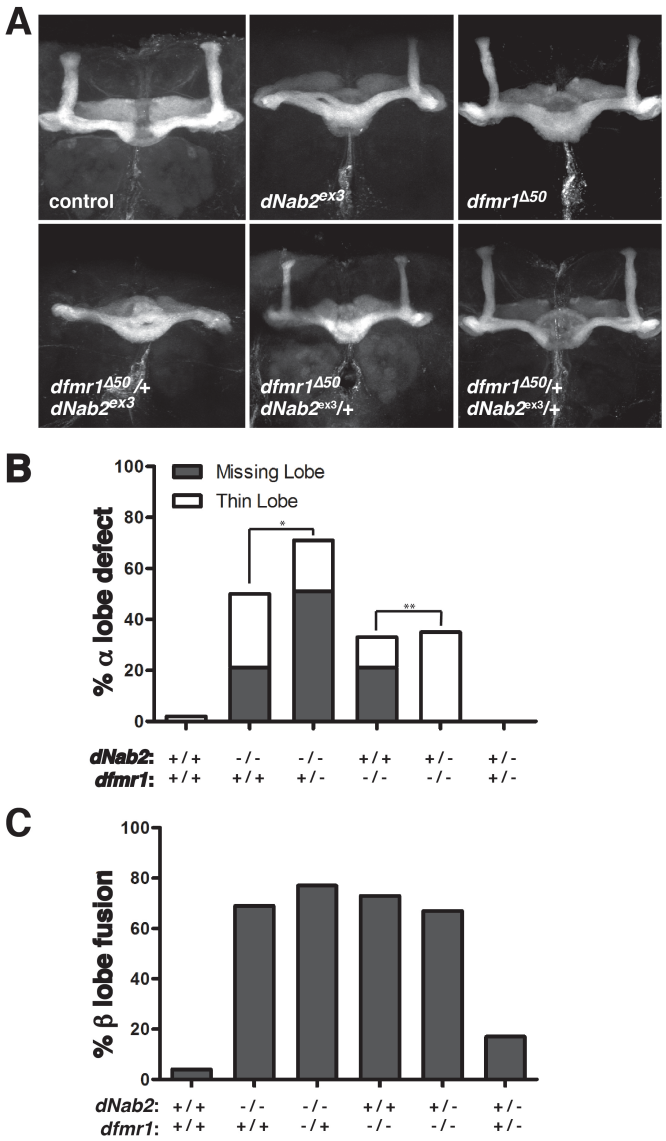

Figure 3-2. *dNab2* and *dfmr1* interact genetically in the process of mushroom body (MB) α-lobe development. (**A**) Maximum intensity projections of a *dNab2* wildtype brain (*pex41/pex41* isogenic control), a *dNab2* null brain (*ex3/ex3* null homozygotes), a *dfmr1* null brain (Δ*50*/Δ*50* null homozygotes), a *dNab2* null brain lacking on copy of *dfmr1* (*ex3*,Δ*50/ex3,*+), an *dfmr1* null lacking one copy of *dNab2* (*ex3*,Δ*50/*+,Δ*50*), or a *trans*-heterozygote brain (*ex3,* Δ*50/*+). Quantitation of (**B**) the percentage of α-lobe defects (missing or thinned) and (**C**) fused β-lobe defects in the same genotypes as in (**A**)

with individual lobes counted as discrete events. At least 24 brains of each genotype were examined. Significance was determined via the Chi-squared test (* p=0.000482 and ** p=0.0000150).

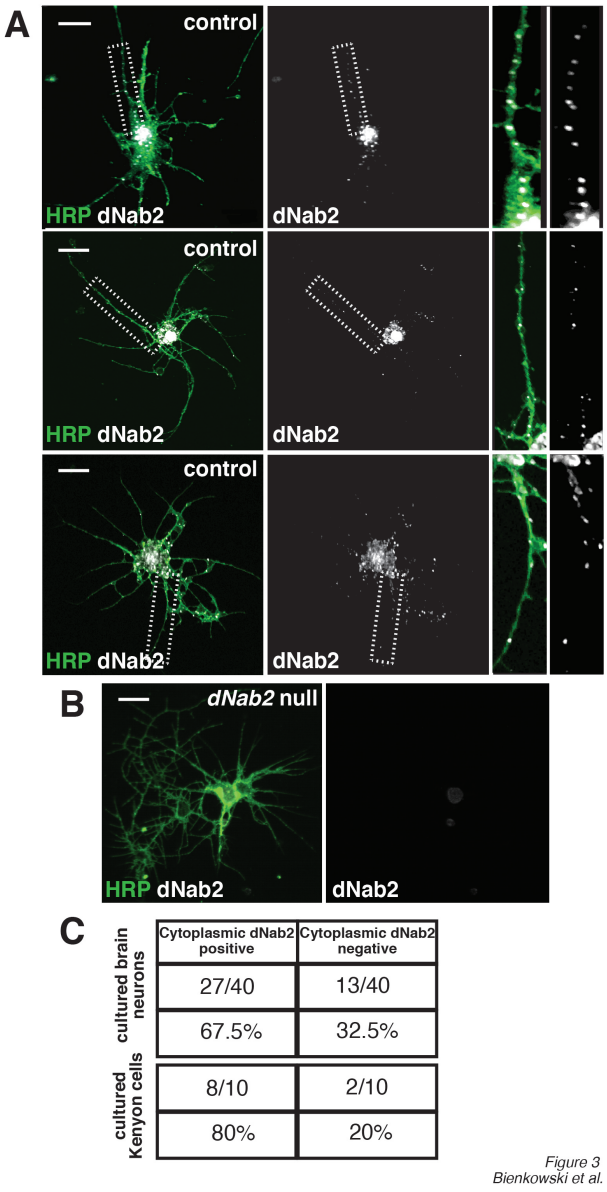

Figure 3-3. dNab2 localizes to neurites of primary brain neurons. Confocal images of representative (**A**) control (*pex41*) or (**B**) dNab2 null (*ex3*) brain neurons from 24h APF pupae cultured 72h *in vitro* and labeled with anti-HRP (green) to highlight neuronal membranes, and anti-dNab2 protein (grey). Rightmost panels in (**A**) show magnified views of dNab2 puncta in HRP-positive neurites (dotted boxes). (**C**) Quantification of the frequency of cytoplasmic dNab2 in neurites of wild type (*pex41*) brain neurons (top) or

Kenyon cells (bottom) labeled CD8:GFP expression (*CD8-GFP/+ ;;OK107>Gal4/+)*. Scale bars=10μm.

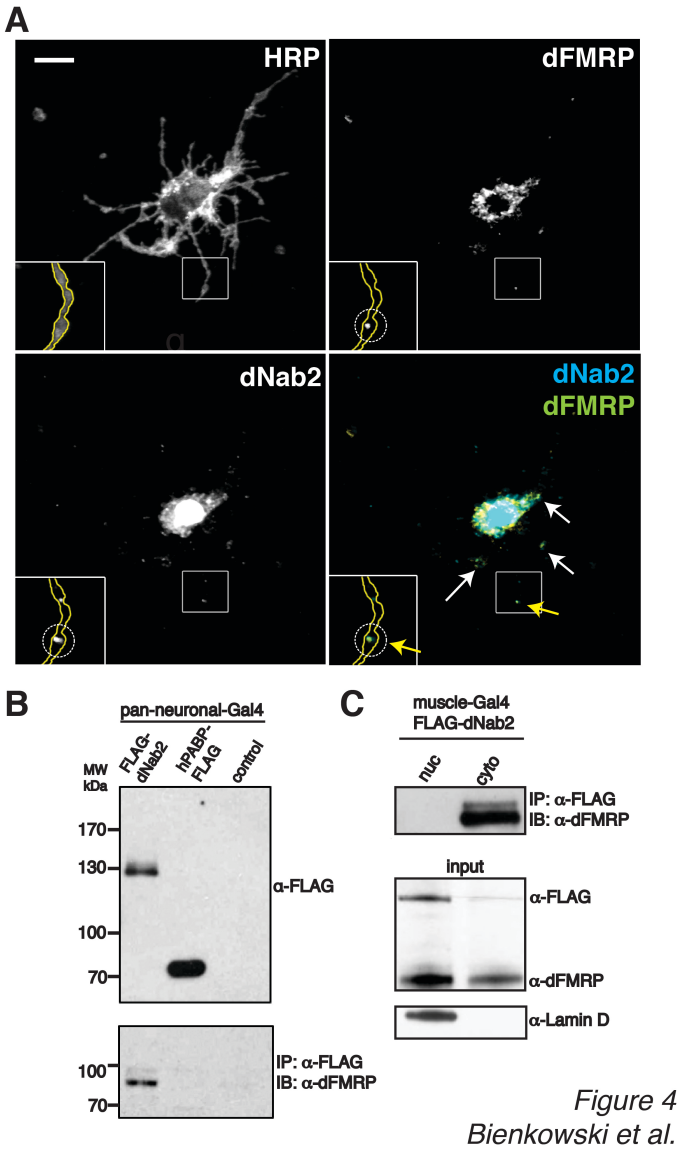

Figure 3-4. dNab2 physically associates with dFMRP in the neuronal cytoplasm. (**A**) Confocal image of a single control (*pex41*) 24h APF brain neuron labeled with anti-HRP to mark membranes (top left panel), anti-dFMRP (top right panel), anti-dNab2 (bottom left panel), and double labeled with anti-dFMRP (green) and anti-dNab2 (blue) (bottom right panel). White arrows denote dNab2/dFMRP-double positive puncta. Boxed insert shows a high magnification view of a dNab2/dFMRP-positive speckle localized to a distal neurite (yellow arrow & dotted circle). Scale bars=10μm. (**B**) Anti-Flag (top panel)

or anti-dFMRP (bottom panel) Western blot analysis of anti-Flag immunoprecipitates (IPs) from adult heads expressing neuronal Flag-dNab2 (*C155-Gal4;;UAS-Flag-dNab2/+*), hPABP-Flag (*C155-Gal4;UAS-hPABP-Flag/+*), or Gal4 alone (*C155-Gal4*). Note that endogenous dFMRP is only enriched in Flag-dNab2 precipitates. (**C**) Bulk lysates of adults expressing Flag-dNab2 from the muscle-specific driver *Mhc-Gal4* were separated into nuclear (nuc) and cytoplasmic (cyto) fractions and subject to anti-Flag IP/anti-dFMRP Western blot (upper panel). Input lysates were blotted to detect nuclear and cytoplasmic distribution of Flag-dNab2 and endogenous dFMRP. An antibody to nuclear Lamin was used to assess biochemical fractionation.

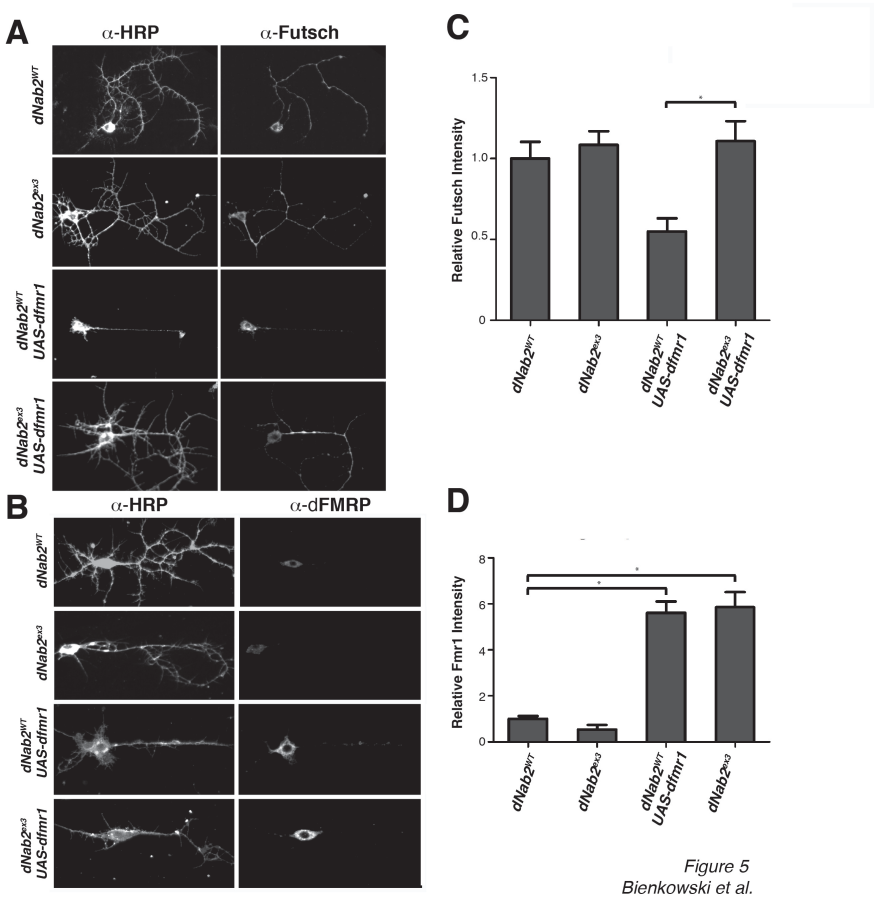

Figure 3-5. dNab2 is required for translational suppression of *futsch* by exogenous dFMRP. Paired confocal images of (**A**) anti-Futsch or (**B**) anti-dFMRP stained 24h APF brain neurons co-stained with anti-HRP to illuminate neuronal membranes. Indicated genotypes: wildtype Nab2 (*dNab2*^{wt}), mutant dNab2 (*dNab2*^{ex3}), transgenic dFMRP (*UAS-dfmr1;dNab2*^{wt}), or mutant dNab2 + transgenic dFMRP (*UAS-dfmr1;dNab2*^{ex3}). The *C155-Gal4* neuronal driver is present in all neurons. Quantitation of (**C**) Futsch or (**D**) dFMRP protein levels presented as mean fluorescence intensity among the same genotypes as in (**A)** and (**B**). Data are normalized to *C155-Gal4;dNab2*^{wt} (lane 1) (n=15 in **C**; n=12 in **D**). Error bars represent SEM ($*$ $p<0.05$)

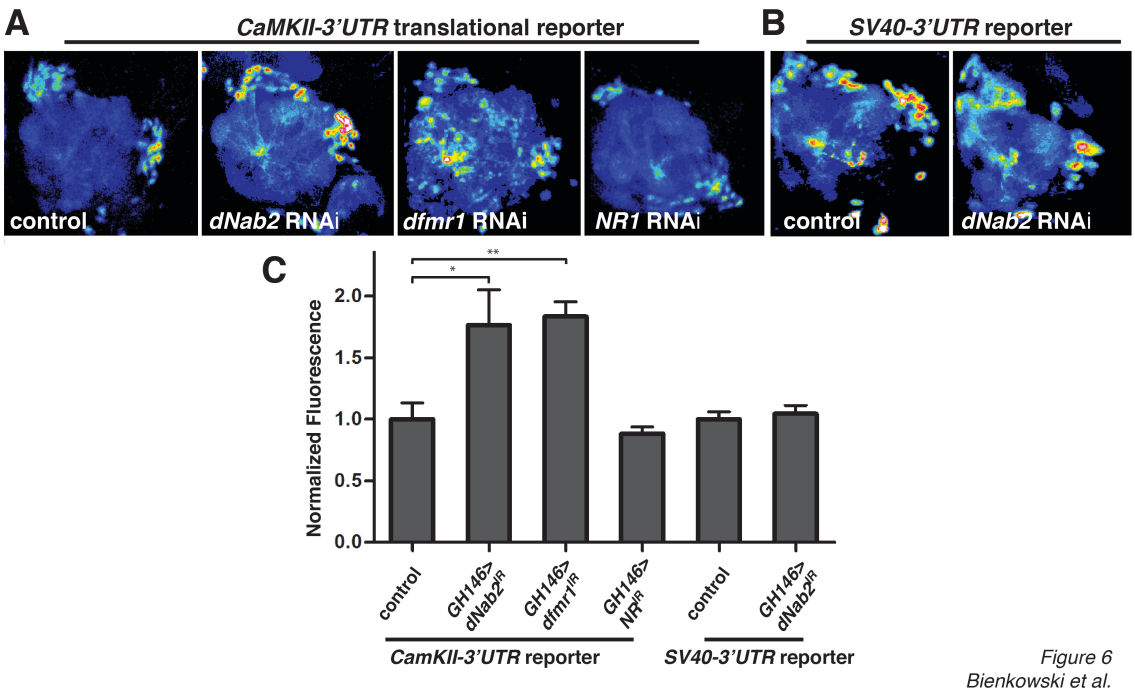

Figure 3-6. *dNab2* regulates expression of a CaMKII translational reporter. Confocal images of (**A**) *UAS-eYFP:CaMKII-3'UTR* and (**B**) *UAS-eYFP:SV40-3'UTR* expression in *GH146-Gal4* antennal lobe neurons expressing the indicated RNAi transgenes. Expression levels are represented as a 16-color intensity scale. RNAi genotypes: no RNAi (*control*), *UAS-dNab2-RNAi* (*dNab2* RNAi), *UAS-dfmr1-RNAi* (*dfmr1* RNAi), *UAS-NMDA Receptor-1-RNAi* (*NR1* RNAi). (**C**) Mean eYFP fluorescence from the *CaMKII-3'UTR* and *SV40-3'UTR* reporters for each indicated genotype. Data are normalized to the mean fluorescence of control (*GH146-Gal4,UAS-eYFP:CaMKII-3'UTR* or *GH146-Gal4,UAS-eYFP:SV40-3'UTR*) antennal lobes. Error bars represent SEM. $*$ $p<0.05$, $**p<0.01$.

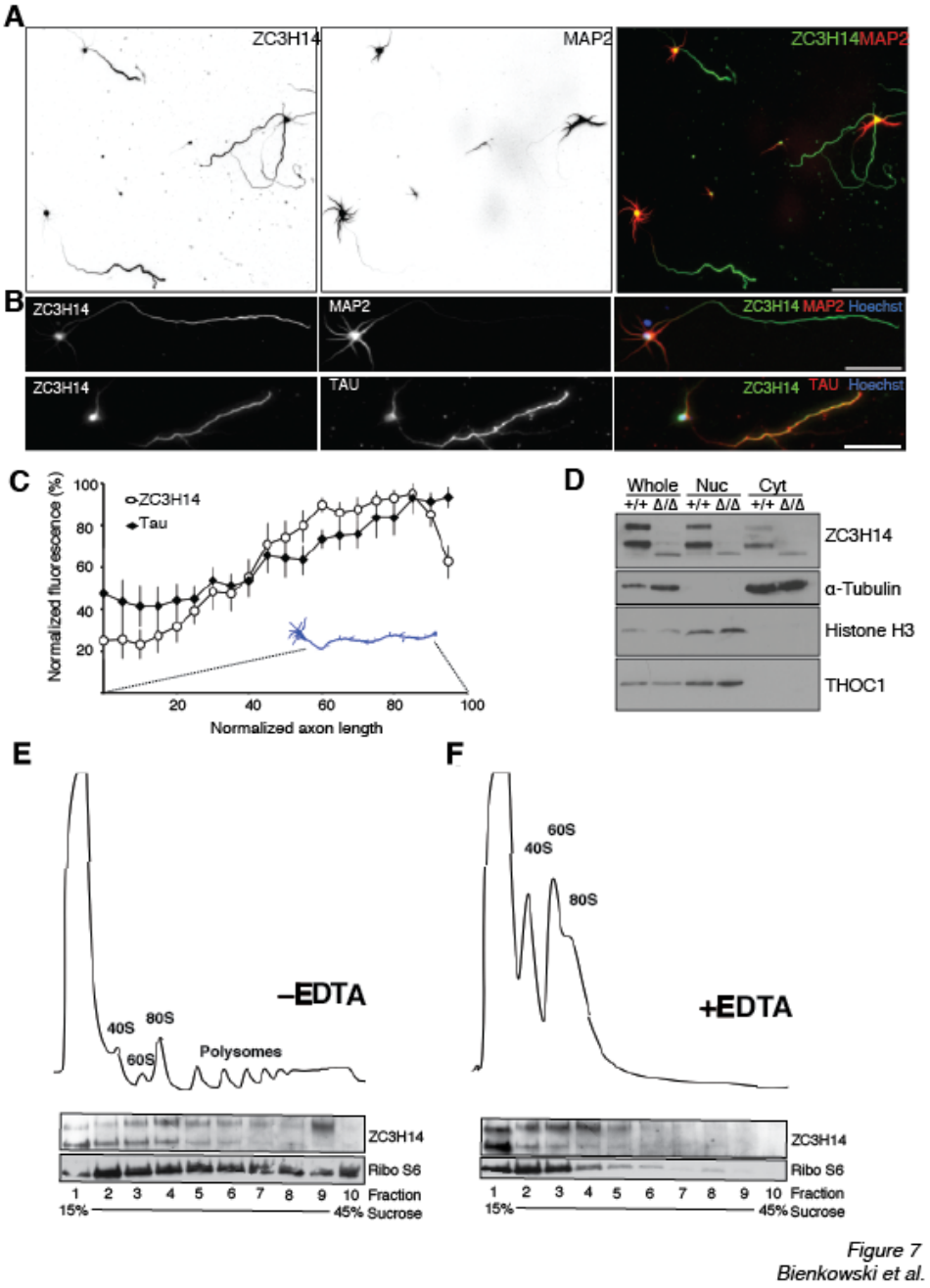

Figure 3-7. ZC3H14 localizes to axons in primary hippocampal neurons and associates with polyribosomes in mouse cortical lysates. (**A**,**B**) Immunofluorescence images of 5 days *in vitro* (DIV) cultures of primary hippocampal neurons collected from P1 (**A**) *Zc3h14*$^{+/+}$ or (**B**) *Zc3h14*$^{\Delta/\Delta}$ pups and stained with anti-ZC3H14 (green), anti-β-tubulin (red), and Hoechst to detect DNA (blue). Scale bars=50 µm. (**C**) Distribution of

Tau and ZC3H14 fluorescence quantified as a function of axon length. (**D**) Nuclear and cytoplasmic fractions of *Zc3h14*$^{+/+}$ and *Zc3h14*$^{\Delta/\Delta}$ brains immunoblotted to detect the ZC3H14 RNA-binding proteins, α-tubulin (cytoplasmic marker), Histone H3 (nuclear marker), and THOC1, a second RNA-binding protein that localizes exclusively in nuclei. (**E**,**F**) Polysome profiles across a 15-45% linear sucrose gradient of cytoplasmic extracts of the P13 brain cortex of wildtype mice prepared in the (**E**) absence or (**F**) presence of EDTA, which dissociates the 40S and 60S ribosomal subunits. Linear traces denote 254nm absorption profiles (RNA) of representative gradients, with the positions of ribosome peaks and polysomes indicated. Lower panels show the distribution of ZC3H14 and the S6 ribosomal protein (Ribo S6) across the indicated fractions as detected by immunoblot.

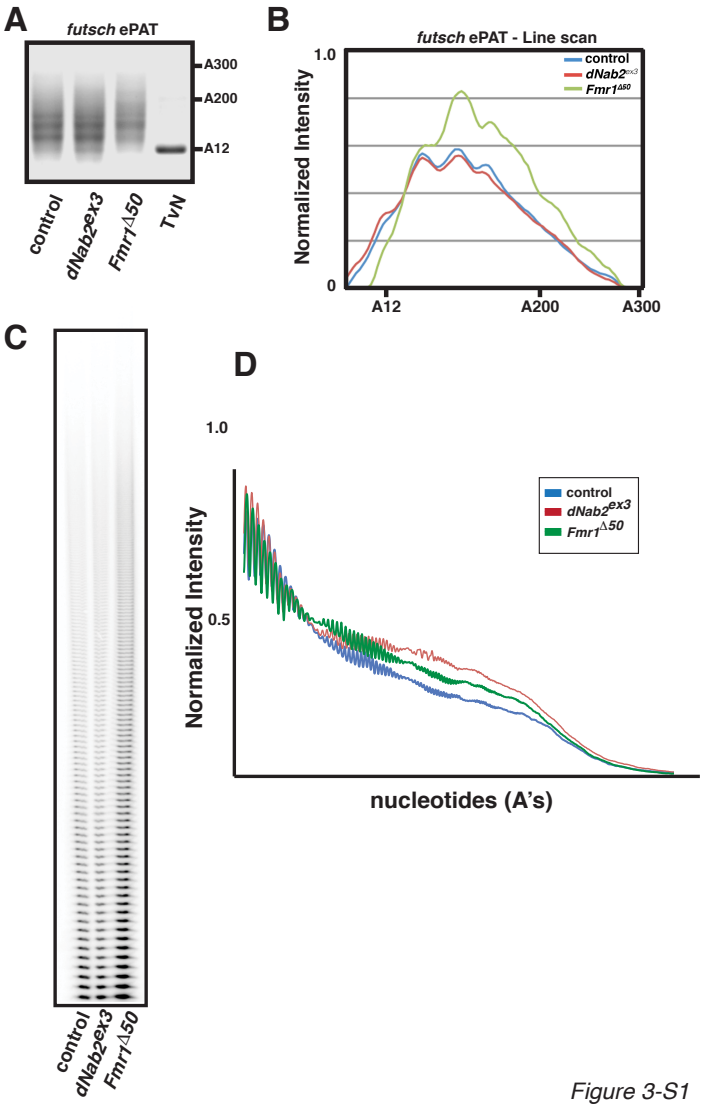

Figure 3-S1

Figure 3-S1: dFMRP regulates poly(A) tail length of the *futsch* mRNA transcript and of bulk RNA. (A) The extension poly(A) tail test specifically amplifies the poly(A) tails of *futsch* transcripts in RNAs extracted from the heads of isogenic control flies (control), dNab2 null flies (dNab2^{ex3}), Fmr1 null flies (Fmr1$^{\Delta 50}$). The TvN lane represents a fixed-length control band in which the first 12 adenosines of the poly(A) tail of the *futsch* transcript are amplified. **(B)** Line scans of the ePAT agarose gel pictured in (A). The TvN band was used to delineate the base of the poly(A) tail (0A-12A). **(C)** Bulk poly(A) tail assay performed of RNAs extracted from the heads of isogenic control flies (control), dNab2 null flies (dNab2^{ex3}), and Fmr1 null flies (Fmr1$^{\Delta 50}$). **(D)** Line scan of the gel pictured in (C), normalized in each lane such that the signal at the bottom of each lane is set to 1.

Table 3-S1. Alleles tested for genetic interaction with *dNab2* in a dNab2 overexpression eye screen.

Bloomington #	Allele	Modification (E or S)
	Pabp2^{EP2264}	S++
22407	*robo2^{ey206209}*	S++
1507	*stau^{1}*	S++
--	*UAS-puc*	S++
31788	*paip2^{epG4716}*	S +
11388	*ago1^{04845}*	S
21645	*Atx2^{DG08112}*	S
10063	*bel^{NEO30}*	S
29401	*CaMKII^{TRiP}-P{TRiP.JF03336}attP2*	S
11531	*cpo^{1432}*	S
32067	*Dcr-1[Q1147X]*	S
15364	*EF1alpha ^{ey010605}*	S
11720	*eIF-4E^{7238}*	S
6929	*Fmr1^{D113M}*	S
6930	*Fmr1^{D50M}*	S
18062	*Hel25E^{e02545}*	S
10654	*hoip^{K07104}*	S
14915	*mRpS29^{KG07362}*	S
11624	*mub^{4093}*	S
36127	*Pabp IR*	S
14276	*Pur-α^{KG05743}*	S
25775	*Rbp9[delta1]*	S
28669	*Rbp9^{TRIP}*	S
19858	*Rm62^{EY06795}*	S
32418	*Rps6^{Trip}*	S
11295	*spen^{3350}*	S
16659	*Trf4-2^{EY05585}*	S
58708	*UAS-Timp*	S
33615	*Akt^{TRIP}*	lethal: no interaction (Akt TRiP is lethal alone)
--	*UAS-Fmr1.Z§*	lethal (GMR>UAS- Fmr1.Z is lethal alone)
8161	*hrg^{10}*	E+++

--	*Pabp2*^{55}	E+++
17023	*qkr58E-2*^{EP2103}	E+++
34796	*gawky*^{TRIP}	E++
34809	*Rrp6*^{TRIP}	E++
5930	*smg*^{1}	E++
--	*UAS Pabp-flag*	E++
17117	*Dscam4*$^{[EP3362]}$	E
28784	*fne*^{IR}	E
1676	*fz*^{1}	E
38391	*Pabp2*^{6}	E
9126	*sif*^{ES11}	E
25789	*sif*^{TRiP} *- P{TRiP.JF01795}attP2*	E
--	*UAS-fne.C 4-10B§*	E
7125	*UAS-lark-3HA 23A§*	E
8565	*Abl*^{2}	-
11504	*abs*^{00620}	-
21172	*abs*^{EY015915}	-
18459	*abs*^{f01698}	-
12712	*Adar*^{BG02235}	-
16608	*AGO2*^{EY04479}	-
11688	*Atx2*^{06490}	-
8517	*aub*^{HN}	-
14001	*aub*^{KG05389}	-
4968	*aub*^{QC42}	-
25933	*babo*^{TRIP} *(P{TRiP.JF01953}attP2)*	-
4024	*bel*^{6}	-
11778	*bel*^{CAP1}	-
4553	*BicD*^{r5}	-
--	*bl*^{EY09813}	-
--	*bl*^{KG02524}	-
22296	*bru-2*^{EY18918}	-
18300	*bru-2*^{f00171}	-
27190	*bru-2*^{G5819}	-
22797	*bru-2*^{MB00431}	-
201401	*CCR4/twin*^{8115}	-
--	*CCR4*^{0115}	-
--	*CenG1A*^{EY01217}	-
--	*Clp*^{G2556}	-
38294	*CyFip*^{TRIP}	-

12164	*dco*^{J3B9}	-
6020	*dnc*^{1}	-
--	*Dp1*^{BG0145B}	-
12855	*Dp1*^{BG02288}	-
2070	*dpp*$^{(d12)}$	-
2065	*dpp*$^{(s11)}$	-
7363	*drl*^{exc21}	-
22419	*EF1alpha100E* ^{ey20719}	-
16341	*EF1beta*^{ep}	-
--	*EF1beta*^{ep} *(#271921)*	-
11034	*Ef1α48D*^{1275}	-
10506	*eIF-4a*^{K01501}	-
12240	*elav[G0319] arg[G0319] w[67c23]/FM7c*	-
--	*fasII*^{e7}	-
--	*fasII*^{EB112}	-
28990	*fasII*^{RNAi}	-
8794	*futsch*^{K68}	-
8805	*futsch*^{N94}	-
34898	*gbb*^{TRIP}	-
--	*GluRIIA*^{AD9}	-
--	*GluRIIA*^{Sp16}	-
9564	*homer*^{R102}	-
12151	*how*^{J5B5}	-
11204	*Hrb27C*^{2647}	-
14414	*Hrb87F*^{KG02089}	-
6822	*Hrb98DE*^{ZCL0558}	-
8162	*hrg*^{1}	-
8160	*hrg*^{p1}	-
41590	*Ime4*^{TRIP}	-
17294	*Imp*^{EP760}	-
8263	*InR .A1325D*	-
8252	*InR.K1409A*	-
8250	*InR.R418P*	-
--	*lark*^{DG23107}	-
--	*lark*^{EY00297}	-
--	*lark*^{EY23084}	-
16006	*mael*^{EY08554}	-
13015	*mael*^{KG03309}	-
8516	*mael*^{R20}	-

7318	*mbl*^{E27}	-
4160	*msi*^{1}	-
5945	*msn*^{102}	-
5947	*msn*^{172}	-
125	*nonA*^{4B18}	-
3285	*nos*^{L7}	-
21033	*Nxt1*^{DG05102}	-
18809	*Nxt1*^{f04855}	-
12812	*orb2*^{BG02373}	-
27050	*orb2*^{TRiP}*-P{TRiP.JF02376}attP2*	-
--	*orb*^{dec}	-
--	*orb*^{EY08547}	-
17261	*pAbp*^{EP310}	-
20684	*pAbp*^{EY11561}	-
10970	*pAbp*^{K10109}	-
4759	*pan*^{2}	-
--	*park*^{25}	-
28728	*pde1c*^{TRIP}	-
10236	*ps*^{10615}	-
23562	*ps*^{MB04043}	-
9756	*Ptpmeg[1]*	-
16420	*pUf68*^{EY07952}	-
3260	*pum*^{13}	-
3332	*pum*^{13}	-
6782	*pum*^{BEM}	-
14653	*qkr58E-2*^{KG07766}	-
15086	*qkr58E-3*^{EY02038}	-
6677	*rac1,rac2*	-
6674	*rac1*$^{[J11]}$	-
25778	*Rbp9*^{P2690}	-
27	*Rd*^{1}	-
7326	*Rho1*^{72F}	-
32417	*RhoGAP71E*^{TRIP}	-
31167	*RhoGAP93B*^{TRIP}	-
--	*Rm62 (excision L3)*	-
11520	*Rm62*^{1086}	-
--	*Rm62*^{DG12402}	-
20644	*Rm62*^{EY10915}	-
8755	*robo*^{1}	-

(harvard collection	*Rrp42*^{c02320}	-
16981	*Rrp42*^{EY}	-
9404	*rut*^{1}	-
32552	*S6k*$^{l-1}$	-
94	*sbr*^{1}	-
23660	*sbr*^{Magellan}	-
12904	*SC35*^{KG02986}	-
4095	*sgg*^{1}	-
17211	*Slbp*^{EP1045}	-
11177	*snRNP-U1-70K*^{2107}	-
8735	*spen*^{3}	-
12133	*sqd*^{J6E3}	-
7379	*Src64B [Pi/Pid]*	-
24071	*Src64B*^{MB03494}	-
41776	*stan*^{e59}	-
6967	*stau*^{192}	-
40875	*tau*^{TRIP}	-
20801	*TBPH* ^{EY10530}	-
14737	*TBPH*^{KG08578}	-
-	*Tis11*^{BG00309}	-
--	*Tis11*^{EY09107}	-
-	*Tis11*^{EY09433}	-
29517	*Tis11*^{TRIP}	-
14718	*tra2*^{KG08361}	-
27732	*trio*^{TRiP}*-P{TRiP.JF02815}attP2*	-
14737	*tsr*^{N121}	-
6597	*tsu*^{EP567}	-
14097	*tsu*^{KG04415}	-
15237	*tud*^{KG10175}	-
15863	*twin*^{EY02330}	-
32901	*twin*^{TRiP}*- P{TRiP.HMS00690}attP2*	-
32490	*twin*^{TRiP}*-P{TRiP.HMS00493}attP2*	-
--	*UAS-AvrA*	-
--	*UAS-bsk*^{DN}	-
--	*UAS-pde1c*	-
8477	*UAS-Src64B*	-

17408	*vig*^{EY07816}	-
2978	*Wg*^{1}	-
2980	*Wg*$^{l-17}$	-
4613	*wisp*$^{12-3147}$	-
16467	*wisp*^{KG05287}	-
6651	*Wnt4*^{C1}	-
28534	*wnt5*^{TRIP}	-
12863	*Zn72D*^{BG02677}	-
36512	*AGO2*^{454}*/TM3, Sb1*	-
28269	*ago3*^{t2}	-
33657	*drosha*^{TRIP}	-
--	*fne*$^{[KO26]}$	-
10970	*Pabp* $^{[K10109]}$	-
8653	*paip2-HA*	-
18987	*PBac{WH}Dcr-2*^{f06544}*/CyO*	-
29517	*TBPH* ^{TRIP}	-

Acknowledgements

The authors thank the Bloomington Drosophila Stock Center (Indiana, USA) and the Developmental Studies Hybridoma Bank (Iowa, USA) for providing stocks and antibodies. We are grateful to Seth Kelly for technical assistance and guidance in brain dissection and neuronal culture experiments. We would also like to thank Thomas A. Jongens and Sam Kunes for sharing fly reagents. Financial support was provided by the National Institutes of Health grants: R01MH10730501 (to K.H.M. and A.H.C.), R01MH085617 (G.J.B.), U54NS091859 (S.T.W.) and F31HD07922601 (to R.S.B.).

Chapter 4: The polyadenosine RNA-binding protein dNab2 interacts with the Rho-GEF *still life* to promote viability and proper development of the mushroom bodies in *Drosophila melanogaster.*

Introduction:

Rho GTPases coordinate the polymerization of filamentous actin (F-actin) and control the organization of the actin cytoskeleton (*171*). Regulation of actin dynamics by Rho GTPases has been linked to a diverse set of cellular processes, including cell proliferation, vesicular trafficking, migration, and cell polarity (*172, 173*). Rac1, one of the most investigated Rho GTPases, provides a clear example the importance of this family of proteins for normal cellular function. Rac1 is directly implicated in the regulation of adhesion and migration of cells across extracellular substrates (*174*). In neurons, Rac1 is required for axon growth and guidance (*175*), stimulates the formation and growth of dendritic spines (*176*) and has been linked to maintenance of synapses (*177, 178*). The proper control of Rac1 activity is therefore predicted to be critical for neuronal architecture and function.

At a molecular level, Rho GTPases act like "molecular switches" that are active when bound by GTP, and inactive when bound by GDP (*179*). The "molecular switch" is controlled by two separate classes of regulatory proteins, Guanine nucleotide exchange factors (GEFs) and GTPase-activating proteins (GAPs) (*179*). GEFs activate Rho GTPases by facilitating exchange of the bound GDP for GTP, and GTPase-activating proteins (GAPs) inhibit Rho function by stimulating it's intrinsic GTPase activity, which hydrolyzes of GTP to GDP (*179*). The proper balance of this GEF-GAP cycle is critical to tuning Rho GTPase activity and F-actin assembly in cells. Indeed inactivation of Rho GEFs dysregulates F-actin polymerization *in vivo* (*180*). Mutations in Rho GEFs are associated with human disease, including amyotrophic lateral sclerosis and other

neurodegenerative diseases (*181, 182*), thus highlighting the importance of the strict regulation of Rho GTPases.

Still life (sif) encodes a putative Rac1-GEF in *Drosophila melanogaster (183)*. Here, I will provide evidence that dNab2, a CCCH-type polyadenosine RNA-binding protein that is lost in a form of intellectual disability (*5*), regulates the *sif* mRNA transcript. I show that neuronal phenotypes caused by the loss of dNab2 protein are in part mediated by the overexpression of the *sif* transcript, and I show that lowering *sif* gene dosage is sufficient to partially rescue the viability, neuronal function, and axon projection defects found in *dNab2* null flies.

Results:

Still life (Sif) is the *Drosophila* ortholog of human Tiam1 and Tiam2 (Figure 1). These proteins contain conserved functional domains, including two pleckstrin homology domains (PH), a Ras binding domain (RBD), a PDZ domain, and a RhoGEF/Dbl-homologous domain. Human Tiam1 can directly activate Rac1 (*184*), and a crystal structure of murine Tiam1 reveals that the adjacent RhoGEF/PH domains bind directly to Rac1 to facilitate GEF activity (*185*). (Figure 1). Sif protein is highly expressed in *Drosophila* neurons and can be localized to synapses (*183*). Additionally, expression of a truncated Sif protein gives rise to defects in actin polymerization in *Drosophila* cells (*183*). The molecular properties of *Drosophila* Sif have not been well studied; however, given its homology to Tiam1, Sif is predicted to have Rho GEF activity.

I identified *sif* in a candidate-based genetic screen for modifiers of dNab2 overexpression in retinal neurons (Chapter 3-S1). This overexpression of *dNab2* causes

small adult eyes with pockets of pigment loss and disorganized ommatidia, known as a "rough eye" phenotype [Figure 2A.]. I found that knockdown of *sif* with a short-hairpin (shRNA) construct that specifically targets *sif* for RNAi-mediated degradation (*186*) leads to strong enhancement of the rough eye. This enhancement includes further shrinkage of the eye and the appearance of areas of localized necrosis [Figure 2A iii]. However, this effect of Sif loss is unique to the *GMR-dNab2* background: when *sif* is RNAi-depleted alone, the adult eye is unaffected and indistinguishable from control wildtype eyes, suggesting a specific functional link between dNab2 and Sif.

To determine whether *sif* and *dNab2* alleles interact in other genetic contexts, I turned to measuring the effect of a *sif* allele on the rate of eclosion of dNab2 null flies. dNab2 zygotic nulls are partially viable, with only about 5% of flies surviving to adulthood [(*5*) Figure 2B]. dNab2 null flies also homozygous for the sif^{ES11} hypomorphic allele (i.e. $dNab2^{ex3}/dNab2^{ex3};sif^{ES11}/sif^{ES11}$) have a significantly increased rate of eclosion, and survive to adulthood 27% of the time [Figure 2B]. Similarly, when Sif is knocked down by pan-neuronal expression of the *sif* shRNA in dNab2 null flies ($dNab2^{ex3}/dNab2^{ex3}$*;C155>UAS-sif-IR*), the rate of eclosion increases to 41% [Figure 2B]. Interestingly, this pan-neuronal knockdown of Sif also partially suppresses the dNab2 null wings-held-out phenotype originally documented in Pak et al, 2011(*5*). Importantly, flies heterozygous for the sif^{ES11} allele rescue $dNab2^{ex3}$ null eclosion in a manner similar to the *sif* shRNA, indicating that the RNAi rescue is specifically due to the modulation of *sif* expression and not due to any RNAi off-target effects. The knockdown of *sif* in these experiments was limited to neuronal tissue, revealing that the

Sif Rho-GEF is active in *Drosophila* neurons, and dNab2 and Sif interact functionally in neurons

So far, my genetic data establish that RNAi knockdown of Sif enhances phenotypes caused by the overexpression of dNab2, and rescues phenotypes caused by the zygotic loss of dNab2. These data support the hypothesis that dNab2 may be negatively regulating the expression of Sif in neurons. To test this hypothesis, I extracted RNA from isolated *Drosophila* head lysates and measured the steady-state levels of *sif* mRNA by qPCR. This analysis identified the *sif* mRNA as one of four transcripts that are up-regulated upon loss of dNab2 (Figure 3A). The *sif* transcript is 2.5x more abundant in the dNab2 null mutant RNAs than control RNAs harvested from wild type heads (Figure 3A). Furthermore, we were able to identify stretches of polyadenosine-rich sequence in the 3' UTRs of the *sif* mRNA and a second transcript affected by dNab2 loss, *pde1c* (Figure 3B). To test the hypothesis that dNab2 may bind these 3'UTR polyadenosine tracts, I performed RNA-immunoprecipitation to assess whether the *sif* and *pde1c* transcripts are enriched in dNab2-immunoprecipitates from adult brains. I found that *pde1c* and *sif* were enriched in dNab2 immunoprecipitates, but that two transcripts that lack polyadenosine-rich stretches in their *3' UTRs*, *scb* or *Kmn1*, were not. These data suggest dNab2 directly associates with the *sif* transcript; my current untested hypothesis is that this interaction occurs through the polyadenosine-rich sequence found in the *3'UTR* of s*if*.

dNab2 acts cell-autonomously within the mushroom bodies to promote proper axon projection and guidance (*132*). In the absence of dNab2, the β-lobe axons misproject across the midline of the brain, and the α-lobes are thinned or missing (*132*).

As Rho GEFs are known to affect axon guidance in other contexts (*187*), I hypothesized that loss of *sif* repression in dNab2 null neurons may contribute to these axon defects. Remarkably, dNab2 null brains that are also heterozygous for *sif* with the sif^{ES11} allele show dramatically reduced rates of β-lobe and α-lobe defects (Figure 4A,B). The RNAi-mediated knockdown of *sif* in dNab2 null mushroom bodies also rescues α-lobe defects but led to a new guidance defect in the β-lobes: 25% of the time β-lobes were missing, or misprojected and tracked alongside the α-lobes (Figure 4B). Critically, heterozygosity for the sif^{ES11} allele or RNAi knockdown of *sif* had no effect on α-lobe or β-lobe development in wild type mushroom bodies (Figure 4A,B), suggesting that dNab2 and Sif are closely linked in the projection and guidance of the α and β-lobe axons.

Discussion:

In this chapter, I have presented preliminary evidence that the putative Rho-GEF Sif exhibits properties of a transcript that is bound and repressed by dNab2. I showed that *sif* and *dNab2* alleles show patterns of interaction in retinal neurons and the entire CNS that are consistent with dNab2 repressing Sif activity in these contexts. At a molecular level, I showed that steady state levels of the *sif* mRNA are elevated in dNab2 null brain neurons and that the *sif* transcript co-precipitates with dNab2 from brain lysates, suggesting that this transcript may be directly bound and regulated by dNab2. Additionally, I showed that either a null allele of *sif* or RNAi-mediated depletion of *sif* can rescue mushroom body defects found in *dNab2* null flies. However, the combination of dNab2 loss and shRNAi of *sif* can also produce more severe pathfinding defects in which β-lobe axons project along the α-lobe route. This enhancement is not consistent with a simple working model

that dNab2 represses *sif* mRNA stability or expression. Notably, the medial β-lobe defect is not seen with the sif^{ES11} allele, and could thus be an artifact of the *sif* shRNAi cassette. Alternatively, it could suggest that the rescue of the sif^{ES11}/+ allele on α /β-lobe structure is due to a non-cell autonomous effect. Finally, it may be that the functional relationship between dNab2 and Sif is not as simple as initially hypothesized. This preliminary work thus establishes a strong foundation for the further study of Sif and the F-actin cytoskeleton in axonogenesis defects in dNab2 mutant neurons.

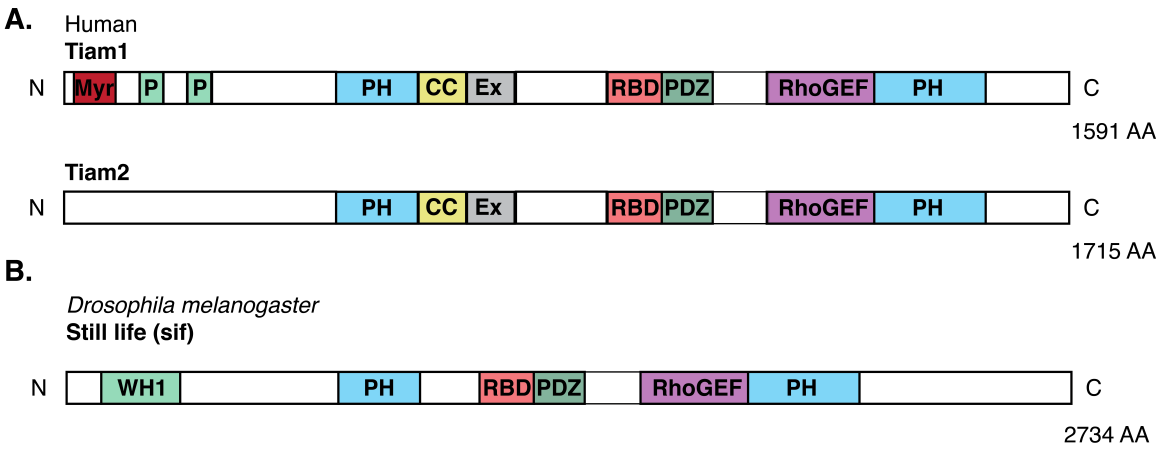

Figure 4-1. sif is the *Drosophila melanogaster ortholog* of human Tiam1 and Tiam2. Protein domain layouts found in Human Tiam1 and Tiam 2 (**A)** and *Drosophila melanogaster still life* **(B)**. Myr: Myristoylation Signal, P: PEST domain, PH: Pleckstrin homology domain, PH-CC-Ex: monomeric membrane-associated and protein scaffold-associated domain, RBD: Ras binding domain, PDZ: PDZ domain, RhoGEF: Dbl-homologous domain, WH1- Wasp homology domain.

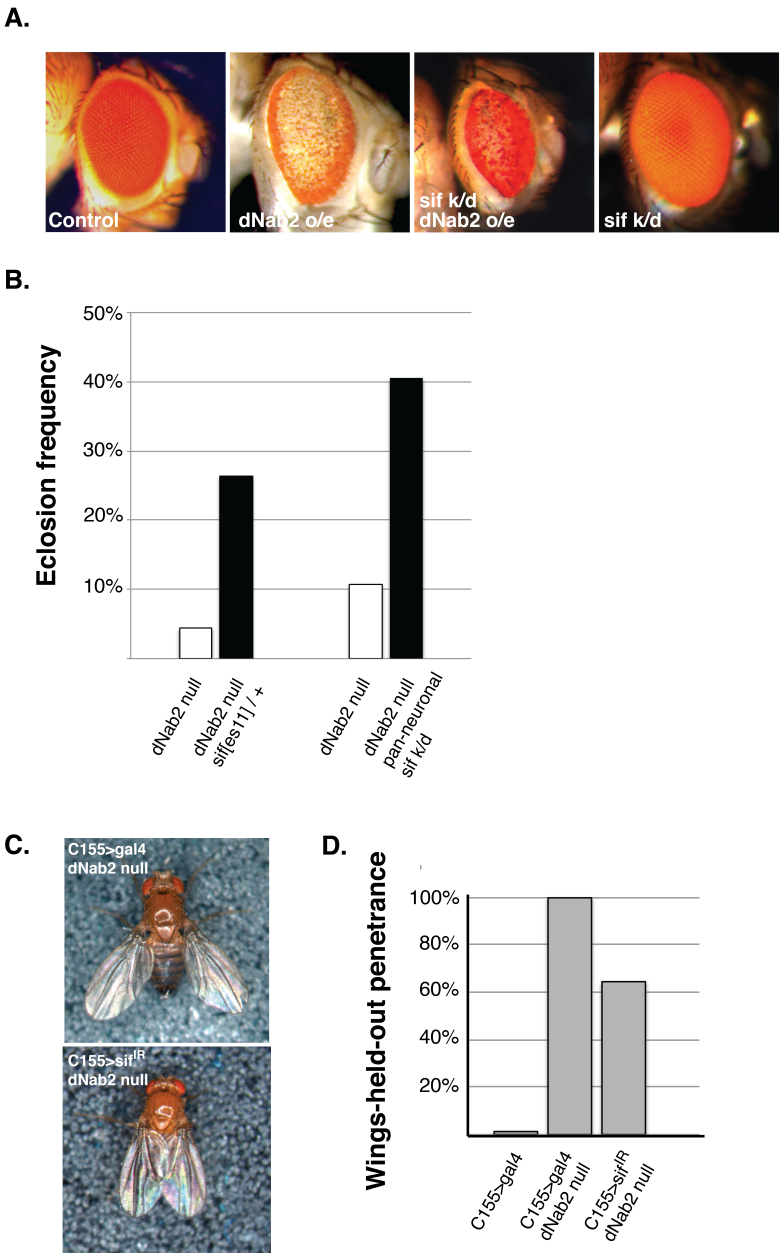

Figure 4-2. Genetic interactions between *sif* and dNab2. (A) Images of control (*GMR-Gal4*/+), dNab2 overexpression (GMR- Gal4/+;dNab2^{EP3716}/+), dNab2 overexpression with *sif* RNAi (GMR-Gal4/+;+,*sif*^{TRiP}/ dNab2^{EP371}), and *sif* RNAi alone (GMR-Gal4/+;+,*sif*^{TRiP} /+) adult female eyes. **(B)** Comparison of eclosion rates between dNab2 null (*dNab2*^{ex3}/ *dNab2*^{ex3}) to dNab2 null, sif heterozygote (*sif*^{es11,}*dNab2*^{ex3}/ *dNab2*^{ex3}), and dNab2 null (C155/+;; (*dNab2*^{ex3}/ *dNab2*^{ex3}) to dNab2 null+ neuronal-specific sif RNAi

(C155/+;; (sif^{TRiP},$dNab2^{ex3}$/ $dNab2^{ex3}$). **(C)** Light microscopy images of a dNab2 null ($dNab2^{ex3}$/ $dNab2^{ex3}$) adult fly displaying the wings-held-out phenotype, and a dNab2 null+ neuronal-specific sif RNAi (C155;; (sif^{TRiP}, $dNab2^{ex3}$/ $dNab2^{ex3}$) fly with wings normally folded. **(D)** Quantification of the wings-held-out phenotype in control (C155/C155), dNab2 null (C155/+;; ($dNab2^{ex3}$/ $dNab2^{ex3}$), and dNab2 null + neuronal-specific sif RNAi (C155/+;; (sif^{TRiP},$dNab2^{ex3}$/ $dNab2^{ex3}$).

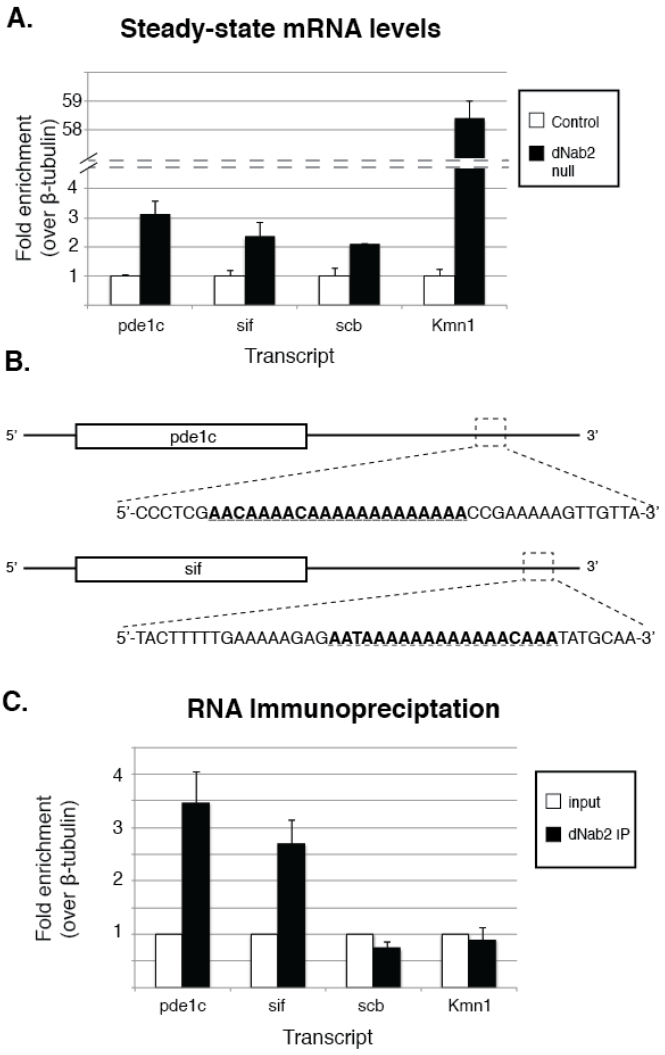

Figure 4-3. The *sif* mRNA transcript is regulated by dNab2. (A) Steady-state levels of mRNA extracted from the heads of adult flies aged to 5 days after eclosion. **(B)** The identification of poly(A) stretches found in the 3' UTR of the pde1c and sif mRNA transcripts. No such poly(A) stretches were found in the 3'UTR of the scb or Kmn1 mRNAs. **(C)** Enrichment of transcripts after RNA-immunoprecipitation. Flag-dNab2 was expressed specifically in the neurons (C155>dNab2-flag), and lysates incubated in anti-flag beads. Fold enrichment was calculated as fold increase over beta-tubulin.

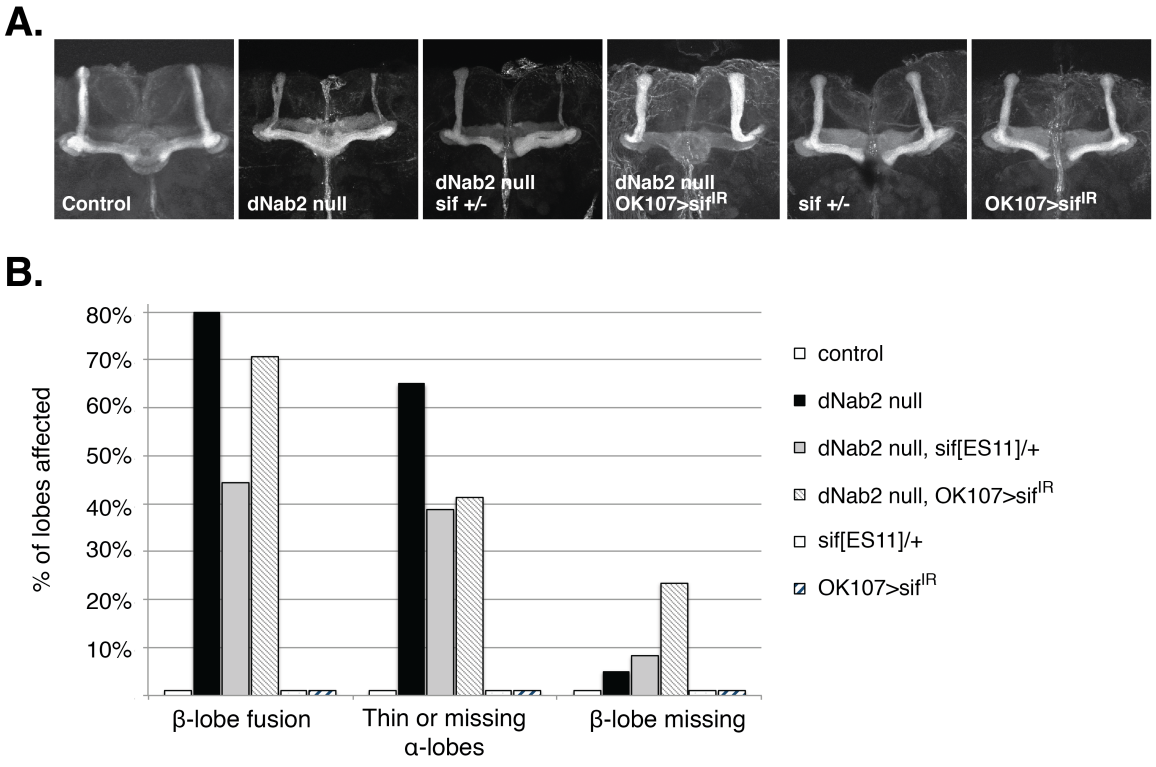

Figure 4-4. *sif* and dNab2 interact in the developing mushroom bodies.

(A) Maximum intensity projections of a *dNab2* wildtype brain (*pex41/pex41* control), a *dNab2* null brain (*ex3/ex3* homozygotes), a *dNab2* null brain lacking a copy of *sif* (*ex3*,*sif*^{es11}*/ex3,+*), a *dNab2* null brain with RNAi-mediated sif depletion in the mushroom bodies (OK107>sif^{IR}, *ex3/ex3*), a *dNab2* wildtype brain lacking a copy of *sif* (*sif*^{es11}*/+*), and a *dNab2* wildtype brain with sif depleted specifically in the mushroom bodies (OK107>sif^{IR}). **(B)** Quantitation of the percentage of fused ß-lobe defects, α-lobe defects (missing or thinned) missing ß-lobe defects in the same genotypes as in (A) with individual lobes counted as discrete events. At least 20 brains of each genotype were examined.

Chapter 5: Discussion and Conclusion

Discussion and Conclusion:

I. Summary:

The development of the vertebrate brain is extremely complex, requiring the coordination of billions of neurons to form functional neural circuits. Although it is unclear how higher-order cognitive processes emerge from neural circuits, we do know that the strict control of post-transcriptional regulation by RNA-binding proteins is essential in neurons, the fundamental unit of the neural circuit. RNA-binding proteins are crucial for the trafficking of mRNP granules to distal subcellular compartments and for the local translation of proteins. These processes mediate synaptic plasticity and are thought to form the foundation of the molecular basis for learning and memory (*39, 40*).

Here we show that dNab2, the *Drosophila melanogaster* ortholog of a human protein that is lost in intellectual disability (*5*), is required for proper axon projection in the brain and for normal learning and memory (Chapter 2). We describe a network of physical and genetic interactions between dNab2 and the fragile X protein homolog dFMRP that demonstrate the cooperation of these proteins during the development of the brain and identify mRNA targets that are negatively regulated by both proteins (Chapter 3). This finding is particularly significant since it links dNab2 and ZC3H14-associated disability to the pathology of fragile X syndrome. Furthermore, polyribosome profile analysis reveals ZC3H14 co-fractionates with 80S ribosomes and polysomes suggesting that dNab2/ZC3H14 may play a role in local protein translation (Chapter 3). We then go on to provide preliminary evidence that dNab2 directly regulates the *still life (sif)* mRNA transcript, which encodes a putative GEF for the Rho/Rac GTPases, and show that the regulation of Sif by dNab2 may be important for the proper development of mushroom

bodies (Chapter 4). In sum, these studies have leveraged our *Drosophila melanogaster* model to further reveal the molecular function of dNab2/ZC3H14 in neurons and provide insight into how the loss of this protein can lead to intellectual disability in humans.

II. A Model of dNab2 Function in Neurons

Although the precise molecular role of dNab2 in neurons is not fully defined, the findings in this dissertation offer significant new insights into dNab2 function. In addition to the previously defined role in limiting the length of poly(A) tails(*5*), our data lead us to hypothesize that dNab2 participates in the trafficking of mRNAs to distal neuronal sub-compartments and negatively regulates the translation of these target mRNA transcripts (Figure 5-1). In this model, we propose that dNab2 regulates mRNA transcripts in conjunction with dFMRP, and that regulation occurs in the dNab2-dFMRP positive RNPs described earlier in this thesis (Figure 5-1). This model is based on the following observations: (1) dNab2 localizes to distinct puncta in neurite extensions and can be co-localized with dFMRP, (2) dNab2 physically interacts with dFMR1 in the neuronal cytoplasm, (3) alleles of *dNab2* and *dFMR1* exhibit strong dominant interactions in the brain, and (4) mammalian ZC3H14 co-fractionates with polysomes and is enriched in the neuronal cytoplasm of hippocampal neurons. Taken together, these data suggest a model in which dNab2/ZC3H14 directly participates in the regulation of local mRNA translation in the neuronal cytoplasm. However, our data do not exclude a significant role for dNab2/ZC3H14 in the processing and polyadenylation of mRNAs in the nucleus, and also suggest that only a subset of dNab2-regulated transcripts are also bound and regulated by dFMRP. This latter hypothesis is supported by the facts that: (1) the overlap

of co-localization between dNab2 and dFMRP puncta in cultured neurons only comprise 25% of the total signal, (2) dNab2 regulates the steady-state levels of the two dFMRP targets *futsch* and *CaMKII*, but apparently utilizes distinct modes of regulation to regulate each transcript, and (3) alleles of *dNab2* and *dFMR1* interact in the development of mushroom body α-lobes, but not β-lobes. This selective interaction between dNab2 and dFMRP in the α-lobes suggests either that dNab2-dFMRP granules are localized to particular sub-compartments of mushroom body neurons (e.g. α- lobe axons and not β-lobe axons), or that the mRNAs co-regulated by dNab2 and dFMRP encode factors that act primarily in α-lobe development (e.g. the α-lobe specific role of the Formin DAMM;(*188*)). Our discovery of functional dNab2-dFMRP interactions alongside the role of dNab2 in translational repression informs models of how loss of ZC3H14 could cause intellectual disability. However, many open questions about the function of dNab2 and ZC3H14 remain. Here, I will identify open questions and suggest future directions for the investigation of ZC3H14 and dNab2 function.

III. Open Questions and Future Directions

Is the dNab2-dFMRP interaction conserved in humans?

One of the most exciting findings in this dissertation is that dNab2 and dFMRP proteins physically and functionally interact. In Chapter 3, we show that flies that are null for *dFMR1* are sensitive to the dose of *dNab2* and reducing the expression of *dNab2* can reduce the severity of neurodevelopmental defects caused by the lack of dFMRP in these flies. If this interaction is conserved in humans with the ZC3H14 and FMRP proteins, it implies that the pathology of fragile X syndrome may in part involve the dysregulation of

ZC3H14 and the improper elongation of poly(A) tails. In *Drosophila,* we found that *dFMR1* null flies display an increased length of bulk poly(A) RNA similar to dNab2 flies (Figure 3-S1). However, it is currently unclear whether the amelioration of *dFMR1*-null phenotypes in flies made heterozygous for *dNab2* is due to the reduction of dNab2 expression, or because of a general increase in poly(A) tail length in these flies.

Preliminary evidence shows that FXR2, a paralog of FMRP (*66*), co-precipitates with ZC3H14 from cultured human cell lysates (Morris; unpublished 2015) and from murine brain lysates ((Rha, Morris; unpublished 2016). FXR2 is an essential component of FMRP-containing fragile x granules (*66*) that localizes to presynaptic and postsynaptic sites, (*67*) and shows a similar patterns of distribution to ZC3H14 in the axons of cultured neurons (*69*). The conserved physical interaction between mammalian ZC3H14 and FXR2 proteins suggests that genetic interactions between *dNab2* and *dFMR1* in *Drosophila* may be conserved between *ZC3H14* and *FXR2* in mammalian tissues. This finding paves the way for studies in mice, and the investigation of whether the down-regulation of ZC3H14 expression can rescue the severity of neuronal phenotypes seen in the murine model of fragile X syndrome.

In parallel, we could investigate whether the rescue of the neurodevelopment and neuronal function of dFMRP null flies is specific to modulation of *dNab2* expression, or whether it extends to other proteins known to modulate poly(A) tail length in flies. By rapidly introducing alleles of other poly(A) tail modulating factors into dFMRP null flies, we could measure the extent of neuronal rescue and determine whether dFMR1 interacts with general factors that affect poly(A) tail length. Experiments that continue to utilize *Drosophila* as a model for human disease will further our understanding of ZCH14 and

FMRP, and could one day reveal new molecular targets for pharmacological intervention in fragile X syndrome.

Which mRNA transcripts are regulated by dNab2?

One of the ultimate goals of these studies is to identify the dNab2 target transcripts that are critical for proper neuronal function and development. A first step in this process would be to identify the full breadth of transcripts that are regulated by dNab2. Though we have made significant advances in identifying dNab2-regulated RNA transcripts and gene networks, we have relied solely on a dominant-modification genetic screen to identify genetic interactors. The *GMR-dNab2* "rough eye" screen has been successful in identifying a number of genes that interact with *dNab2*; however, this screen is not without drawbacks. First, it relies on the overexpression of *dNab2* to levels that could create artifact interactions that do not occur in endogenous tissues, and cannot be recapitulated with genomic alleles of *dNab2*. Second, "hits" in the genetic screen do not necessarily correspond to direct mRNA targets of dNab2. These candidate modifier "hits" could potentially encode an mRNA target of dNab2, a protein that interacts with dNab2, a gene that regulates dNab2 expression, or a factor that acts within a pathway that dNab2 itself also modulates. Thus the results of the eye screen could be interpreted in many different ways, and any follow-up experiments assessing "hits" found through the eye screen can be time consuming and difficult to plan.

To bypass the concerns listed above, I propose that next-generation RNA sequencing be utilized to identify dysregulated transcripts (*189*). Using a transcriptome-wide approach would allow for the identification of transcripts that are important for

neurodevelopment and neuronal function, if mRNAs are extracted and sequenced from the brains of adult flies with the following four genotypes: control (*dNab2*^{pex41}), dNab2 null (d*Nab2*^{ex3}), dNab2 null with dNab2 re-expressed only in neuronal tissue ("dNab2 neuronal rescue"; *C155>dNab2, dNab2*^{ex3}) and dNab2 null with ZC3H14-iso1 expressed only in neuronal tissue ("ZC3H14 neuronal rescue"; *C155>ZC3H14-iso1, dNab2*^{ex3}). Comparing the levels of RNAs across these four genotypes would allow us to identify putative roles for dysregulated transcripts in *dNab2* null neurons. The neuronal expression of ZC3H14 rescues adult viability and restores normal locomotor function to dNab2 null flies, but does not rescue brain morphology defects (*23*). Identifying the transcripts that become dysregulated upon the loss of dNab2 but are rescued upon expression of ZC3H14 expression would help us identify the mRNAs that contribute to the rescue of adult viability and locomotion. The neuronal re-expression of dNab2 in otherwise *dNab2* null flies rescues viability, locomotor, brain morphology and learning and memory defects (*5, 23*). Therefore, identifying the transcripts that are dysregulated in *dNab2* null neurons and are restored in the dNab2 neuronal rescue will may reveal transcripts critical for the rescue of proper axon guidance and learning. Additionally, the RNA-seq dataset can be analyzed (*190*) to determine whether the loss of dNab2 leads to defects in alternative splicing (as predicted from the eye screen data, discussed below).

The workflow above describes only one method of identifying dNab2-regulated transcripts. However, given the putative role of dNab2 as a negative regulator of neuronal translation, directly assessing changes in steady-state levels of protein in the brain might be more appropriate. This could be achieved with a proteomic mass-spectrometry approach, comparing the proteomes of dNab2 null brains to control brains. If mass

spectrometry is paired with a dNab2 RIP-seq experiment, transcripts that both associate with dNab2 and encode a protein whose steady-state levels become dysregulated upon dNab2 loss could be identified. In the Moberg laboratory, Chris Rounds is currently optimizing conditions to perform these two experiments in parallel. Mass spectrometry and RIP-seq combine to form a powerful technique that can elucidate the targets directly regulated by dNab2 in neurons.

Which dNab2-target transcripts cause neuronal-specific phenotypes when dysregulated?

The phenotypes observed upon depletion of dNab2 are undoubtedly the culmination of pleiotropic effects from the dysregulation of many mRNA transcripts. However, in some cases, many of the phenotypes observed upon loss of an RNA-binding protein can be explained through the dysregulation of a few key pathways. For example, in the *Drosophila melanogaster* model of fragile X syndrome, viability and learning and memory defects can be rescued by down-regulating the mGluR signaling pathway (*191, 192*), and defects in brain morphology can be rescued by down-regulating excess PI3K signaling (*193*).

The list of transcripts generated from the RNA-seq experiments outlined above could be utilized to identify the putative dNab2-regulated transcripts that may play a role in neuronal function. If flies carrying alleles of these putative transcripts are available, we could then rapidly screen these alleles in our *GMR-dNab2* "rough eye" screen and negative locomotor assay and determine whether these alleles genetically interact with

dNab2. Alleles that can dominantly modify *dNab2*-mediated phenotypes will be candidate alleles for further study.

In Chapter 3, we presented evidence that CaMKII expression is regulated by dNab2. Interestingly, CaMKII is a conserved target of ZC3H14, and has found to be dysregulated in the brains of ZC3H14 null mice (*146*). The strict regulation of CaMKII is essential for learning and memory in flies (*150, 194*) and in mice (*195, 196*). The dysregulation of local CaMKII translation could represent one of these key pathways disrupted by loss of *dNab2,* and provide a molecular basis for impaired learning and memory in *dNab2* mutant flies and *ZC3H14* null mice.

Which proteins are required for the dNab2-mediated regulation of mRNA?

dNab2 has no known catalytic activity and it is likely that dNab2 regulates mRNA through protein-protein interactions. Therefore, to fully understand the molecular role of dNab2 in neurons we will have to identify the proteins with which dNab2 interacts. As a first step, the data collected from our *GMR-dNab2* "rough eye" screen can be leveraged to identify the major regulatory pathways that mediate improper development of the eye in the context of dNab2 overexpression. Our genetic screen detected 44 dominant modifiers of the eye phenotype (Chapter 3, Table S1), suggesting that these alleles may be closely linked to dNab2 function. Looking at all of the genetic modifiers as a whole, I have identified six functional groups of genes that account for 31 of these 44 modifiers: .

- **a.** PABPs and poladenylation machinery (*Pabp, Pabp2, Paip2, hrg, GLD2, Trf4-2*)
- **b.** General translation factors (*eIF-4E, EF1alpha, mRpS29*)
- **c.** Deadenylase activity and the exosome degradation pathway (*Rrp6, Rrp41, CCR4, smg*)
- **d.** Regulation of alternative splicing (*hoip, Hel25E,qkr58E-2, Rm62, mub*)

e. Fragile X-associated genes (*dFMR1, stau, Dcr1, ago1, Timp, Atx-2, CaMKII, gawky*)
f. Wnt-planar cell polarity (PCP) signaling (*fz, dsh, puc*)

These six clusters can be used to make inferences about dNab2 function. First, based on the genes in group a, dNab2 interacts with factors that modulate poly(A) tail length and with proteins that bind directly to the poly(A) tail. This observation confirms that the dysregulation of poly(A) tail length is relevant to downstream phenotypes *in vivo*, and that at least some of these phenotypes can be rescued by restoring the length of the poly(A) tail to their appropriate size, or by modulating the levels of other poly(A) binding proteins. Second, the overexpression of *dNab2* can potentially dysregulate post-transcriptional regulation through at least three distinct mechanisms. Alleles of genes that regulate splicing, RNA turnover, and translational regulation all dominantly modify the dNab2 overexpression phenotype. I have already begun to explore the link between dNab2 and translational regulation in Chapter 3, and these genetic data suggest that dNab2 may play a role in alternative splicing of mRNA transcripts in the nucleus, and that the eventual turnover of mRNAs by the exosome may be part of the dNab2 regulatory pathway. Recently, a role for Nab2 in the splicing of pre-mRNA has been defined in S. cerevisiae. Yeast mutant for *Nab2* improperly retain unspliced RNA transcripts in the nucleus (*197*). This retention is also dependent on the exosome (*197*), linking these two classes of "hits" found in our eye screen together. These data indicate that *dNab2* may also be a factor required for the correct removal of introns from pre-mRNA, and provide a new direction for the study the regulation of mRNA of in the fly and mouse models of *ZC3H14*-associated intellectual disability.

How does dNab2 achieve target specificity?

Poly(A) binding proteins, such as PABPN1 and PABPC, are thought to indiscriminately bind the poly(A) tails of mRNA transcripts (*16*). However, evidence from multiple lines of experimentation suggests that dNab2 only regulates a smaller subset of polyadenylated mRNA. In unpublished work, the knockdown of dNab2 in S2 cells disrupts the steady-state levels of only 94 mRNA transcripts (Pak, Corbett and Moberg, unpublished 2009). Similarly, a preliminary RNA-sequencing experiment with ~8x coverage suggested that the steady-state levels of only a few hundred RNA transcripts change significantly (>2x increased or decreased) among mRNAs extracted from the heads of *dNab2* null flies. (Kelly; unpublished 2011). Moreover, in Chapter 3, I showed that loss of *dNab2* is sufficient to upregulate the expression a YFP translational reporter fused to the *CaMKII 3' UTR*, but has no effect a YFP reporter with the *SV40 3'UTR*, the *sdt* 3'UTR, or on the levels of endogenous Futsch protein. Taken together, these data suggest that dNab2 regulates only a specific subset of mRNA transcripts *in vivo*, but the mechanism that affords this specificity is unknown.

Proceeding from the hypothesis that dNab2 regulates a subset of mRNAs expressed in the cell, one must ask how polyadenosine RNA-binding proteins achieve target specificity? Here I present two competing models demonstrating how dNab2 might bind and regulate specific transcripts (Figure 5-2). In Chapter 5, I propose that dNab2 may achieve specificity by binding polyadenosine-rich sequences found in the *3'UTR* of target transcripts. Supporting this hypothesis, *sif* and *Pde1c,* both transcripts which harbor poly(A) tracts of 15 adenosines in their 3' UTR, are enriched in anti-Flag-dNab2 immunoprecipitates from brains, suggesting that the these target transcripts directly

interact with *dNab2* (Chapter 4). This model is supported by a crystal structure of yeast Nab2 that shows the zinc fingers of Nab2 can bind to adenosine-rich RNA sequences that have adenosines placed in critical positions(*198*), and previous RNA-immunopreciptation experiments in yeast have identified that Nab2 interacts with internal adenosine-rich motifs that includes a stretch of 11 adjacent adenosines (*199*). In my alternative model, dNab2 can bind directly to poly(A) tails, but achieves target specificity through protein-protein interactions with other RNA-binding proteins that stabilize its interaction with some poly(A) tails.

Testing my first hypothesis that dNab2 binds to A-rich tracts in the *3' UTR* of target transcripts could be easily done through the use of crosslinking immunoprecipitation (CLIP). CLIP could be utilized in conjunction with the expression of a *UAS-FLAG-dNab2* construct in S2 cells to cross-link RNA to protein with UV-light, shear the RNA to an average length of about 200 nucleotides, and immunoprecipitating cell lysates with anti-FLAG antibody. The RNAs recovered from the CLIP can be analyzed by qPCR using primer pairs that probe polyadenosine stretches in *3'UTRs* of interest. If this method were unsuccessful, one alternative method would be to synthesize and sequence a cDNA library from the RNAs obtained in the CLIP. However, if dNab2 does bind to poly(A) tails not inside the 3'UTR, we will not be able to be map these using next-generation sequencing.

On the other hand, testing my second hypothesis that dNab2 can bind all polyadenylated RNAs but is only stabilized on some through protein-protein interactions with other RNA-binding protiens bound to the same transcript is somewhat harder to accomplish. The extent to which the PWI, NLS and zinc-finger motifs in dNab2 (Figure

1-4) interact with other proteins is not well defined. Therefore, testing the hypothesis that dNab2 interacts with other sequence-specific RNA-binding proteins would likely begin with a mass-spectrometry based proteomic analysis of proteins that co-purify with dNab2 from fly brain lysates. This approach is further justified by my finding that dFMRP co-purifies with dNab2. Experiments are currently underway in the Moberg-Corbett laboratories to apply proteomic tools to identify the full repertoire of dNab2-associated proteins *in vivo.*

What other dFMRP-associated proteins does dNab2 interact with?

Multiple lines of evidence to suggest that dNab2 only associates with a subset of the cytoplasmic pool of dFMRP to regulate translation. For example, *dNab2* and *dFMR1* interact in the formation of the mushroom body α-lobes, but not the β-lobes. Depletion of dNab2 dysregulates the expression of *CaMKII*, an established target of dFMRP repression, but depletion of dNab2 is not sufficient to dysregulate the expression of *futsch*, another dFMRP target. Lastly, phenotypes in dFMRP null flies can be ameliorated by genetically dampening mGluR or PI3K signaling (*192, 193*), but manipulating these pathways has no effect on *dNab2* null phenotypes (Pak, Bienkowski; unpublished). These observations highlight the need to define the extent of overlap between the dNab2 and dFMRP interactomes in neurons. dFMR1 interacts with Orb2, the cytoplasmic CPEB in *Drosophila* (*200*), and dFMRP can be co-localized to Orb2, PABP, Rm62/Dmp68, and Sm protein positive RNP granules (*138*). Does dNab2 also interact with these components of the cytoplasmic poly(A) polymerase pathways? In a previous iteration of the *GMR-dNab2* screen, *dNab2* did not interact with *wispy*, a cytoplasmic poly(A)

polymerase (Pak, 2011; unpublished). However, a more recent version of this screen found that an allele of GLD-2, another cytoplasmic poly(A) polymerase, does modify the *GMR-dNab2* phenotype (Bienkowski, 2015; unpublished). GLD-2 is thought to interact with Orb2 to mediate cytoplasmic polyadenylation in neurons (*201*). GLD2 can also localize to the dendrites, where it forms polyadenylation complex that includes the deadenylase PARN and the translational inhibitor Ngd (*202*). Thus, GLD-2 may participate in a cytoplasmic polyadenylation pathway that also involves the cytoplasmic pool of dNab2 I discovered in fly brain neurons (Chapter 3).

The hypothesis that dNab2 and dFMRP function are linked through the cytoplasmic polyadenylation complex is appealing. As a first test of this hypothesis, I propose an anti-FLAG-dNab2 immunoprecipitation assay similar to the one I applied in Chapter 3 coupled with western blotting for cytoplasmic polyadenylation factors (e.g. GLD-2) using specific antibodies. In parallel, one could test whether dNab2 co-localizes with the Orb2/PABP/Rm62/Sm protein granules that FMRP localizes to in cultured neurons.

Do dNab2 null flies have defects in actin polymerization?

The *still life* mRNA encodes a putative Rho/Rac guanine exchange factor (GEF), and I have provided preliminary evidence in Chapter 4 that the *sif* mRNA transcript is regulated by dNab2. In support of this hypothesis, levels of *sif* transcript are increased when dNab2 is depleted, suggesting that dNab2 normally acts to repress *sif* expression. The *sif* transcript also associates with Flag-dNab2 precipitates, which implies that the regulation of *sif* by dNab2 may be direct. Additionally, I demonstrated that an allele of

sif and RNAi-mediated depletion of *sif* both dominantly modify mushroom body defects found in *dNab2* null flies, suggesting that this axon guidance defect may be dependent on actin dynamics.

One avenue for further analysis of the dNab2-Sif interaction would be to assess whether dNab2 loss alters the cytoskeleton in a Sif-dependent manner. Our lab currently has flies bearing a UAS-inducible transgene that expresses Lifeact-GFP, a transgenic protein that binds specifically to F-actin (*203*). To investigate whether loss of *dNab2* has any effect on steady-state F-actin, we could image Lifeact-GFP in wild type and *dNab2* null brains or cultured neurons. Alternatively, we could use live imaging of Lifeact-GFP in *dNab2* null cultured neurons to assess the effect of dNab2 loss on F-actin dynamics. Both approaches could be complemented by testing whether alleles of *sif* can dominantly modify any defects in F-actin polymerization that are found in the context of *dNab2*-null neurons.

Moving forward with the investigation of the *sif* mRNA as a dNab2-bound and regulated transcript, I propose developing an antibody specific to the Sif protein to measure steady-state levels of Sif *in vivo*. In addition to measuring protein levels in wild type and *dNab2* null brains, an anti-Sif antibody would allow us to measure the abundance and localization of Sif protein in cultured wild type and *dNab2* null neurons. A putative Rac-GEF could potentially localize to the growth cone of growing axons or to dendrites (*187*). We could also test whether the localization of Sif protein is dysregulated upon loss of *dNab2.* The regulation of the *sif* transcript is a new route of investigation for our lab, and is an exciting opportunity to investigate the extent to which changes of the F-actin cytoskeleton underlie dNab2-associated neuronal defects.

III. Conclusion

Our studies utilizing the *Drosophila melanogaster* model of ZC3H14-associated disability have led to significant progress in modeling how loss of ZC3H14 may lead to intellectual disability in humans. However, many unanswered questions remain about the function of ZC3H14 and dNab2 within neurons. My work has uncovered an interaction between dNab2 and dFMRP that hints at common disease-causing mechanisms underlying ZC3H14-associated disability and fragile X syndrome. This connection implies that dNab2 participates in dFMRP-associated translational repression, and that loss of dFMRP may dysregulate the bulk poly(A) tail length of RNA. However, the connection between these two proteins is still not fully understood and necessitates further research in model systems.

My study of dNab2 underscores a theme introduced in the opening section of this thesis: the prevalence of human diseases caused by defects in RNA-binding proteins illustrates the key role that post-transcriptional mechanisms play in eukaryotic cells. Additionally, this dissertation highlights the critical role that RNA-binding proteins play in the localized regulation of protein synthesis in neurons. Continued study of dNab2 will help unravel the complex regulatory networks that underlie brain function and reveal the underpinnings of *ZC3H14*-associated intellectual disability.

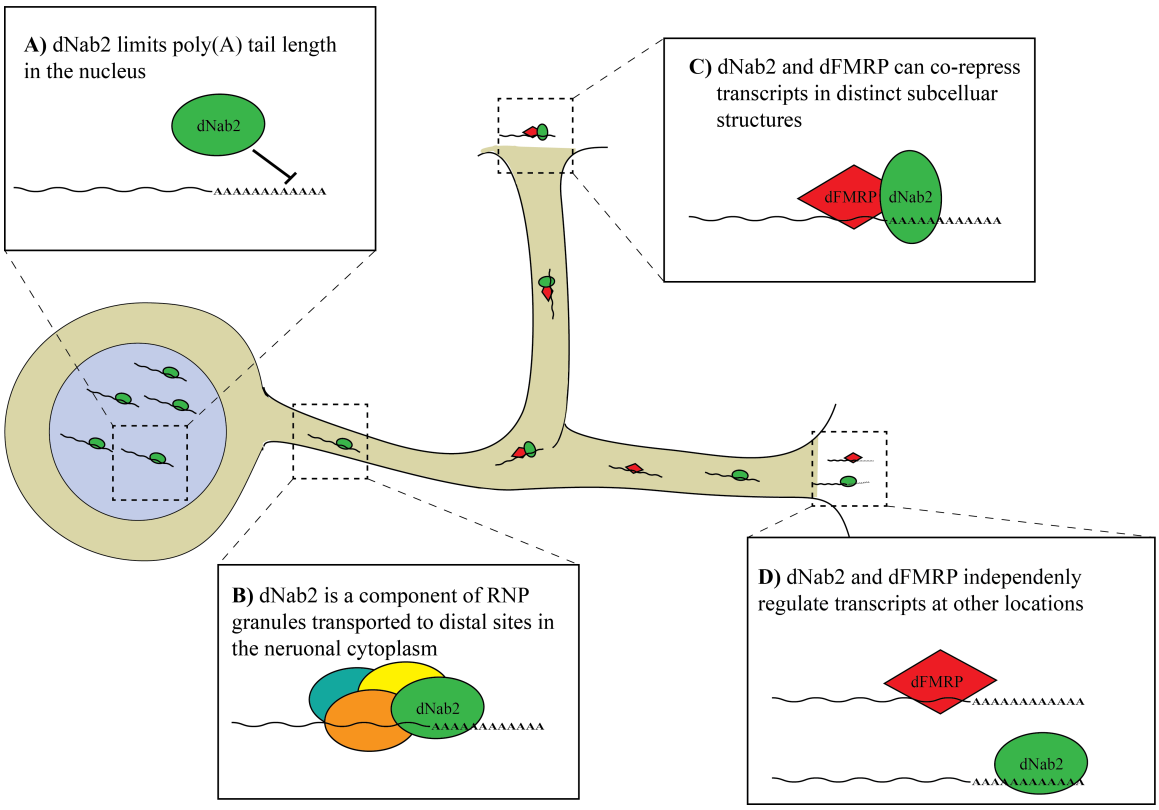

Figure 5-1. A comprehensive model of dNab2 function in neurons. dNab2 can regulate different aspects of post-transcriptional regulation. **(A)** dNab2 limits the length of poly(A) tails in the cytoplasm, affecting the downstream processes regulated by other poly(A) binding proteins. **(B)** dNab2 is a component of translationally repressed RNP granules that are trafficked to distal subcellular compartments. **(C)** dNab2 and dFMRP interact to repress a specific subset of transcripts in distinct RNP granules that may be localized to specific cellular structures. **(D)** dNab2 and FMRP also act independently at other sites in the neuronal cytoplasm.

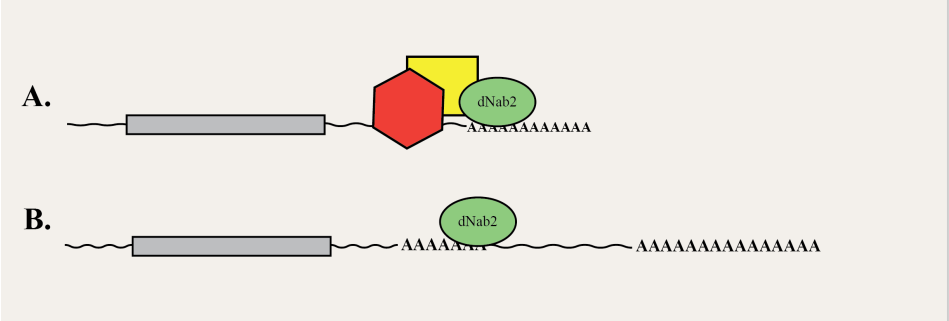

Figure 5-2. Models of dNab2 binding specificity. (A) dNab2 may bind directly to the poly(A) tails of target transcripts, and achieve specificity through selective protein-protein interactions. **(B)** dNab2 could potentially achieve specificity by binding particular polyadenosine-rich motifs found in the 3' UTRs of target transcripts.

References:

1. F. Crick, Central dogma of molecular biology. *Nature* **227**, 561-563 (1970).
2. M. J. Moore, From birth to death: the complex lives of eukaryotic mRNAs. *Science* **309**, 1514-1518 (2005).
3. K. E. Lukong, K. W. Chang, E. W. Khandjian, S. Richard, RNA-binding proteins in human genetic disease. *Trends Genet* **24**, 416-425 (2008).
4. S. W. Leung *et al.*, Splice variants of the human ZC3H14 gene generate multiple isoforms of a zinc finger polyadenosine RNA binding protein. *Gene* **439**, 71-78 (2009).
5. C. Pak *et al.*, Mutation of the conserved polyadenosine RNA binding protein, ZC3H14/dNab2, impairs neural function in Drosophila and humans. *Proceedings of the National Academy of Sciences of the United States of America* **108**, 12390-12395 (2011).
6. A. E. McKee, P. A. Silver, Systems perspectives on mRNA processing. *Cell Res* **17**, 581-590 (2007).
7. S. Rodriguez-Navarro, Nuclear transport and RNA processing. *Biochim Biophys Acta* **1819**, 467 (2012).
8. P. Fechter, G. G. Brownlee, Recognition of mRNA cap structures by viral and cellular proteins. *J Gen Virol* **86**, 1239-1249 (2005).
9. D. A. Mangus, M. C. Evans, A. Jacobson, Poly(A)-binding proteins: multifunctional scaffolds for the post-transcriptional control of gene expression. *Genome Biol* **4**, 223 (2003).
10. S. F. Newbury, Control of mRNA stability in eukaryotes. *Biochem Soc Trans* **34**, 30-34 (2006).
11. T. V. Pestova *et al.*, Molecular mechanisms of translation initiation in eukaryotes. *Proceedings of the National Academy of Sciences of the United States of America* **98**, 7029-7036 (2001).
12. S. Meyer, C. Temme, E. Wahle, Messenger RNA turnover in eukaryotes: pathways and enzymes. *Crit Rev Biochem Mol Biol* **39**, 197-216 (2004).
13. E. Wahle, Poly(A) tail length control is caused by termination of processive synthesis. *The Journal of biological chemistry* **270**, 2800-2808 (1995).
14. A. O. Subtelny, S. W. Eichhorn, G. R. Chen, H. Sive, D. P. Bartel, Poly(A)-tail profiling reveals an embryonic switch in translational control. *Nature* **508**, 66-71 (2014).
15. S. W. Eichhorn *et al.*, mRNA poly(A)-tail changes specified by deadenylation broadly reshape translation in Drosophila oocytes and early embryos. *Elife* **5**, (2016).
16. C. P. Wigington, K. R. Williams, M. P. Meers, G. J. Bassell, A. H. Corbett, Poly(A) RNA-binding proteins and polyadenosine RNA: new members and novel functions. *Wiley interdisciplinary reviews. RNA* **5**, 601-622 (2014).

17. M. C. Daugeron, F. Mauxion, B. Seraphin, The yeast POP2 gene encodes a nuclease involved in mRNA deadenylation. *Nucleic Acids Res* **29**, 2448-2455 (2001).
18. C. Y. Chen *et al.*, AU binding proteins recruit the exosome to degrade ARE-containing mRNAs. *Cell* **107**, 451-464 (2001).
19. J. D. Richter, Cytoplasmic polyadenylation in development and beyond. *Microbiol Mol Biol Rev* **63**, 446-456 (1999).
20. M. J. Moore, N. J. Proudfoot, Pre-mRNA processing reaches back to transcription and ahead to translation. *Cell* **136**, 688-700 (2009).
21. F. Tritschler, E. Huntzinger, E. Izaurralde, Role of GW182 proteins and PABPC1 in the miRNA pathway: a sense of deja vu. *Nat Rev Mol Cell Biol* **11**, 379-384 (2010).
22. L. Zekri, D. Kuzuoglu-Ozturk, E. Izaurralde, GW182 proteins cause PABP dissociation from silenced miRNA targets in the absence of deadenylation. *EMBO J* **32**, 1052-1065 (2013).
23. S. M. Kelly *et al.*, A conserved role for the zinc finger polyadenosine RNA binding protein, ZC3H14, in control of poly(A) tail length. *RNA* **20**, 681-688 (2014).
24. J. Merkin, C. Russell, P. Chen, C. B. Burge, Evolutionary dynamics of gene and isoform regulation in Mammalian tissues. *Science* **338**, 1593-1599 (2012).
25. A. Kalsotra, T. A. Cooper, Functional consequences of developmentally regulated alternative splicing. *Nat Rev Genet* **12**, 715-729 (2011).
26. J. A. Calarco, M. Zhen, B. J. Blencowe, Networking in a global world: establishing functional connections between neural splicing regulators and their target transcripts. *RNA* **17**, 775-791 (2011).
27. J. Schwerk, R. Savan, Translating the Untranslated Region. *J Immunol* **195**, 2963-2971 (2015).
28. V. Balagopal, R. Parker, Polysomes, P bodies and stress granules: states and fates of eukaryotic mRNAs. *Curr Opin Cell Biol* **21**, 403-408 (2009).
29. C. J. Decker, R. Parker, P-bodies and stress granules: possible roles in the control of translation and mRNA degradation. *Cold Spring Harb Perspect Biol* **4**, a012286 (2012).
30. P. Anderson, N. Kedersha, RNA granules. *The Journal of cell biology* **172**, 803-808 (2006).
31. G. J. Bassell *et al.*, Sorting of beta-actin mRNA and protein to neurites and growth cones in culture. *The Journal of neuroscience : the official journal of the Society for Neuroscience* **18**, 251-265 (1998).
32. G. Singh, G. Pratt, G. W. Yeo, M. J. Moore, The Clothes Make the mRNA: Past and Present Trends in mRNP Fashion. *Annu Rev Biochem* **84**, 325-354 (2015).
33. J. R. Buchan, R. Parker, Eukaryotic stress granules: the ins and outs of translation. *Mol Cell* **36**, 932-941 (2009).
34. Z. Li *et al.*, The fragile X mental retardation protein inhibits translation via interacting with mRNA. *Nucleic Acids Res* **29**, 2276-2283 (2001).
35. Y. Feng *et al.*, Translational suppression by trinucleotide repeat expansion at FMR1. *Science* **268**, 731-734 (1995).

36. L. N. Antar, R. Afroz, J. B. Dictenberg, R. C. Carroll, G. J. Bassell, Metabotropic glutamate receptor activation regulates fragile x mental retardation protein and FMR1 mRNA localization differentially in dendrites and at synapses. *J. Neurosci.* **24**, 2648-2655 (2004).
37. O. Penagarikano, J. G. Mulle, S. T. Warren, The pathophysiology of fragile x syndrome. *Annu Rev Genomics Hum Genet* **8**, 109-129 (2007).
38. P. K. Todd, K. J. Mack, J. S. Malter, The fragile X mental retardation protein is required for type-I metabotropic glutamate receptor-dependent translation of PSD-95. *Proceedings of the National Academy of Sciences of the United States of America* **100**, 14374-14378 (2003).
39. M. A. Sutton, E. M. Schuman, Dendritic protein synthesis, synaptic plasticity, and memory. *Cell* **127**, 49-58 (2006).
40. J. D. Richter, E. Klann, Making synaptic plasticity and memory last: mechanisms of translational regulation. *Genes Dev* **23**, 1-11 (2009).
41. A. Castello, B. Fischer, M. W. Hentze, T. Preiss, RNA-binding proteins in Mendelian disease. *Trends Genet* **29**, 318-327 (2013).
42. B. M. Edens, S. Ajroud-Driss, L. Ma, Y. C. Ma, Molecular mechanisms and animal models of spinal muscular atrophy. *Biochim Biophys Acta* **1852**, 685-692 (2015).
43. A. Banerjee, L. H. Apponi, G. K. Pavlath, A. H. Corbett, PABPN1: molecular function and muscle disease. *FEBS J* **280**, 4230-4250 (2013).
44. P. Jin, S. T. Warren, Understanding the molecular basis of fragile X syndrome. *Hum Mol Genet* **9**, 901-908 (2000).
45. A. R. Santos, A. K. Kanellopoulos, C. Bagni, Learning and behavioral deficits associated with the absence of the fragile X mental retardation protein: what a fly and mouse model can teach us. *Learn Mem* **21**, 543-555 (2014).
46. G. J. Bassell, S. T. Warren, Fragile X syndrome: loss of local mRNA regulation alters synaptic development and function. *Neuron* **60**, 201-214 (2008).
47. A. Lee *et al.*, Control of dendritic development by the Drosophila fragile X-related gene involves the small GTPase Rac1. *Development* **130**, 5543-5552 (2003).
48. T. A. Comery *et al.*, Abnormal dendritic spines in fragile X knockout mice: maturation and pruning deficits. *Proceedings of the National Academy of Sciences of the United States of America* **94**, 5401-5404 (1997).
49. L. N. Antar, C. Li, H. Zhang, R. C. Carroll, G. J. Bassell, Local functions for FMRP in axon growth cone motility and activity-dependent regulation of filopodia and spine synapses. *Mol Cell Neurosci* **32**, 37-48 (2006).
50. L. N. Antar, G. J. Bassell, Sunrise at the synapse: the FMRP mRNP shaping the synaptic interface. *Neuron* **37**, 555-558 (2003).
51. L. Hou *et al.*, Dynamic translational and proteasomal regulation of fragile X mental retardation protein controls mGluR-dependent long-term depression. *Neuron* **51**, 441-454 (2006).
52. E. D. Nosyreva, K. M. Huber, Metabotropic receptor-dependent long-term depression persists in the absence of protein synthesis in the mouse model of fragile X syndrome. *J Neurophysiol* **95**, 3291-3295 (2006).

53. J. B. Dictenberg, S. A. Swanger, L. N. Antar, R. H. Singer, G. J. Bassell, A direct role for FMRP in activity-dependent dendritic mRNA transport links filopodial-spine morphogenesis to fragile X syndrome. *Dev Cell* **14**, 926-939 (2008).
54. I. Napoli *et al.*, The fragile X syndrome protein represses activity-dependent translation through CYFIP1, a new 4E-BP. *Cell* **134**, 1042-1054 (2008).
55. E. Chen, M. R. Sharma, X. Shi, R. K. Agrawal, S. Joseph, Fragile X mental retardation protein regulates translation by binding directly to the ribosome. *Mol Cell* **54**, 407-417 (2014).
56. C. I. Michel, R. Kraft, L. L. Restifo, Defective neuronal development in the mushroom bodies of Drosophila fragile X mental retardation 1 mutants. *The Journal of neuroscience : the official journal of the Society for Neuroscience* **24**, 5798-5809 (2004).
57. A. C. McMahon *et al.*, TRIBE: Hijacking an RNA-Editing Enzyme to Identify Cell-Specific Targets of RNA-Binding Proteins. *Cell* **165**, 742-753 (2016).
58. J. C. Darnell *et al.*, Kissing complex RNAs mediate interaction between the Fragile-X mental retardation protein KH2 domain and brain polyribosomes. *Genes Dev* **19**, 903-918 (2005).
59. Y. Q. Zhang *et al.*, Drosophila fragile X-related gene regulates the MAP1B homolog Futsch to control synaptic structure and function. *Cell* **107**, 591-603 (2001).
60. I. P. Sudhakaran *et al.*, FMRP and Ataxin-2 function together in long-term olfactory habituation and neuronal translational control. *Proceedings of the National Academy of Sciences of the United States of America* **111**, E99-E108 (2014).
61. G. Deshpande, G. Calhoun, P. Schedl, The drosophila fragile X protein dFMR1 is required during early embryogenesis for pole cell formation and rapid nuclear division cycles. *Genetics* **174**, 1287-1298 (2006).
62. E. Chen, S. Joseph, Fragile X mental retardation protein: A paradigm for translational control by RNA-binding proteins. *Biochimie* **114**, 147-154 (2015).
63. M. C. Siomi, Y. Zhang, H. Siomi, G. Dreyfuss, Specific sequences in the fragile X syndrome protein FMR1 and the FXR proteins mediate their binding to 60S ribosomal subunits and the interactions among them. *Mol Cell Biol* **16**, 3825-3832 (1996).
64. F. Tamanini *et al.*, Differential expression of FMR1, FXR1 and FXR2 proteins in human brain and testis. *Hum Mol Genet* **6**, 1315-1322 (1997).
65. E. J. Mientjes *et al.*, Fxr1 knockout mice show a striated muscle phenotype: implications for Fxr1p function in vivo. *Hum Mol Genet* **13**, 1291-1302 (2004).
66. S. B. Christie, M. R. Akins, J. E. Schwob, J. R. Fallon, The FXG: a presynaptic fragile X granule expressed in a subset of developing brain circuits. *The Journal of neuroscience : the official journal of the Society for Neuroscience* **29**, 1514-1524 (2009).
67. M. R. Akins, H. F. Leblanc, E. E. Stackpole, E. Chyung, J. R. Fallon, Systematic mapping of fragile X granules in the mouse brain reveals a potential role for

presynaptic FMRP in sensorimotor functions. *J Comp Neurol* **520**, 3687-3706 (2012).
68. M. R. Akins, H. E. Berk-Rauch, J. R. Fallon, Presynaptic translation: stepping out of the postsynaptic shadow. *Front Neural Circuits* **3**, 17 (2009).
69. E. E. Stackpole, M. R. Akins, J. R. Fallon, N-myristoylation regulates the axonal distribution of the Fragile X-related protein FXR2P. *Mol Cell Neurosci* **62**, 42-50 (2014).
70. C. R. Guthrie, L. Greenup, J. B. Leverenz, B. C. Kraemer, MSUT2 is a determinant of susceptibility to tau neurotoxicity. *Hum Mol Genet* **20**, 1989-1999 (2011).
71. S. Kelly *et al.*, New kid on the ID block: neural functions of the Nab2/ZC3H14 class of Cys(3)His tandem zinc-finger polyadenosine RNA binding proteins. *RNA biology* **9**, 555-562 (2012).
72. R. E. Hector *et al.*, Dual requirement for yeast hnRNP Nab2p in mRNA poly(A) tail length control and nuclear export. *EMBO J* **21**, 1800-1810 (2002).
73. D. C. Lee, J. D. Aitchison, Kap104p-mediated nuclear import. Nuclear localization signals in mRNA-binding proteins and the role of Ran and Rna. *The Journal of biological chemistry* **274**, 29031-29037 (1999).
74. S. M. Kelly *et al.*, Recognition of polyadenosine RNA by the zinc finger domain of nuclear poly(A) RNA-binding protein 2 (Nab2) is required for correct mRNA 3'-end formation. *The Journal of biological chemistry* **285**, 26022-26032 (2010).
75. L. Kaufman, M. Ayub, J. B. Vincent, The genetic basis of non-syndromic intellectual disability: a review. *J Neurodev Disord* **2**, 182-209 (2010).
76. A. V. Buescher, Z. Cidav, M. Knapp, D. S. Mandell, Costs of autism spectrum disorders in the United Kingdom and the United States. *JAMA Pediatr* **168**, 721-728 (2014).
77. P. K. Maulik, M. N. Mascarenhas, C. D. Mathers, T. Dua, S. Saxena, Prevalence of intellectual disability: a meta-analysis of population-based studies. *Res Dev Disabil* **32**, 419-436 (2011).
78. B. L. Thompson, P. Levitt, G. D. Stanwood, Prenatal exposure to drugs: effects on brain development and implications for policy and education. *Nat Rev Neurosci* **10**, 303-312 (2009).
79. J. A. Vorstman, R. A. Ophoff, Genetic causes of developmental disorders. *Curr Opin Neurol* **26**, 128-136 (2013).
80. A. Rzhetsky *et al.*, Environmental and state-level regulatory factors affect the incidence of autism and intellectual disability. *PLoS Comput Biol* **10**, e1003518 (2014).
81. A. Rauch *et al.*, Diagnostic yield of various genetic approaches in patients with unexplained developmental delay or mental retardation. *Am J Med Genet A* **140**, 2063-2074 (2006).
82. A. H. Brand, N. Perrimon, Targeted gene expression as a means of altering cell fates and generating dominant phenotypes. *Development* **118**, 401-415 (1993).
83. D. B. Sattelle, S. D. Buckingham, Invertebrate studies and their ongoing contributions to neuroscience. *Invert Neurosci* **6**, 1-3 (2006).

84. A. Androschuk, B. Al-Jabri, F. V. Bolduc, From Learning to Memory: What Flies Can Tell Us about Intellectual Disability Treatment. *Front Psychiatry* **6**, 85 (2015).
85. T. Guven-Ozkan, R. L. Davis, Functional neuroanatomy of Drosophila olfactory memory formation. *Learn Mem* **21**, 519-526 (2014).
86. T. Tully, W. G. Quinn, Classical conditioning and retention in normal and mutant Drosophila melanogaster. *J Comp Physiol A* **157**, 263-277 (1985).
87. L. Wan, T. C. Dockendorff, T. A. Jongens, G. Dreyfuss, Characterization of dFMR1, a Drosophila melanogaster homolog of the fragile X mental retardation protein. *Mol Cell Biol* **20**, 8536-8547 (2000).
88. A. Bettencourt da Cruz *et al.*, Disruption of the MAP1B-related protein FUTSCH leads to changes in the neuronal cytoskeleton, axonal transport defects, and progressive neurodegeneration in Drosophila. *Mol Biol Cell* **16**, 2433-2442 (2005).
89. S. M. McBride *et al.*, Pharmacological rescue of synaptic plasticity, courtship behavior, and mushroom body defects in a Drosophila model of fragile X syndrome. *Neuron* **45**, 753-764 (2005).
90. M. W. Waung, K. M. Huber, Protein translation in synaptic plasticity: mGluR-LTD, Fragile X. *Curr Opin Neurobiol* **19**, 319-326 (2009).
91. C. Gross *et al.*, Increased expression of the PI3K enhancer PIKE mediates deficits in synaptic plasticity and behavior in fragile X syndrome. *Cell Rep* **11**, 727-736 (2015).
92. H. J. Bellen *et al.*, The BDGP gene disruption project: single transposon insertions associated with 40% of Drosophila genes. *Genetics* **167**, 761-781 (2004).
93. J. R. Crittenden, E. M. Skoulakis, K. A. Han, D. Kalderon, R. L. Davis, Tripartite mushroom body architecture revealed by antigenic markers. *Learn Mem* **5**, 38-51 (1998).
94. M. Heisenberg, Mushroom body memoir: from maps to models. *Nat Rev Neurosci* **4**, 266-275 (2003).
95. J. S. de Belle, M. Heisenberg, Associative odor learning in Drosophila abolished by chemical ablation of mushroom bodies. *Science* **263**, 692-695 (1994).
96. M. Heisenberg, A. Borst, S. Wagner, D. Byers, Drosophila mushroom body mutants are deficient in olfactory learning. *J Neurogenet* **2**, 1-30 (1985).
97. T. A. Cooper, L. Wan, G. Dreyfuss, RNA and disease. *Cell* **136**, 777-793 (2009).
98. M. R. Santoro, S. M. Bray, S. T. Warren, Molecular Mechanisms of Fragile X Syndrome: A Twenty-Year Perspective. *Annu Rev Pathol*, (2011).
99. C. P. Wigington, K. R. Williams, M. P. Meers, G. J. Bassell, A. H. Corbett, Poly(A) RNA-binding proteins and polyadenosine RNA: new members and novel functions. *Wiley interdisciplinary reviews. RNA*, (2014).
100. D. J. Goss, F. E. Kleiman, Poly(A) binding proteins: are they all created equal? *Wiley interdisciplinary reviews. RNA* **4**, 167-179 (2013).
101. A. Charlesworth, H. A. Meijer, C. H. de Moor, Specificity factors in cytoplasmic polyadenylation. *Wiley interdisciplinary reviews. RNA* **4**, 437-461 (2013).

102. S. M. Kelly *et al.*, Recognition of polyadenosine RNA by zinc finger proteins. *Proc Natl Acad Sci U S A* **104**, 12306-12311 (2007).
103. H. H. Ropers, Genetics of early onset cognitive impairment. *Annu Rev Genomics Hum Genet* **11**, 161-187 (2010).
104. C. R. Guthrie, G. D. Schellenberg, B. C. Kraemer, SUT-2 potentiates tau-induced neurotoxicity in Caenorhabditis elegans. *Hum Mol Genet* **18**, 1825-1838 (2009).
105. T. Lee, L. Luo, Mosaic analysis with a repressible cell marker for studies of gene function in neuronal morphogenesis. *Neuron* **22**, 451-461 (1999).
106. J. S. Wu, L. Luo, A protocol for dissecting Drosophila melanogaster brains for live imaging or immunostaining. *Nat Protoc* **1**, 2110-2115 (2006).
107. G. Grenningloh, E. J. Rehm, C. S. Goodman, Genetic analysis of growth cone guidance in Drosophila: fasciclin II functions as a neuronal recognition molecule. *Cell* **67**, 45-57 (1991).
108. A. Ejima, L. C. Griffith, Assay for courtship suppression in Drosophila. *Cold Spring Harb Protoc* **2011**, pdb prot5575 (2011).
109. R. W. Siegel, J. C. Hall, Conditioned responses in courtship behavior of normal and mutant Drosophila. *Proc Natl Acad Sci U S A* **76**, 3430-3434 (1979).
110. T. Lee, A. Lee, L. Luo, Development of the Drosophila mushroom bodies: sequential generation of three distinct types of neurons from a neuroblast. *Development* **126**, 4065-4076 (1999).
111. J. D. Armstrong, J. S. de Belle, Z. Wang, K. Kaiser, Metamorphosis of the mushroom bodies; large-scale rearrangements of the neural substrates for associative learning and memory in Drosophila. *Learn Mem* **5**, 102-114 (1998).
112. K. Fushima, H. Tsujimura, Precise control of fasciclin II expression is required for adult mushroom body development in Drosophila. *Dev Growth Differ* **49**, 215-227 (2007).
113. X. Zheng *et al.*, Baboon/dSmad2 TGF-beta signaling is required during late larval stage for development of adult-specific neurons. *EMBO J* **25**, 615-627 (2006).
114. Y. Aso *et al.*, The mushroom body of adult Drosophila characterized by GAL4 drivers. *J Neurogenet* **23**, 156-172 (2009).
115. J. E. Shin, A. DiAntonio, Highwire regulates guidance of sister axons in the Drosophila mushroom body. *J Neurosci* **31**, 17689-17700 (2011).
116. H. H. Yu, C. H. Chen, L. Shi, Y. Huang, T. Lee, Twin-spot MARCM to reveal the developmental origin and identity of neurons. *Nat Neurosci* **12**, 947-953 (2009).
117. T. Lee, L. Luo, Mosaic analysis with a repressible cell marker (MARCM) for Drosophila neural development. *Trends Neurosci* **24**, 251-254 (2001).
118. Y. C. Wu, C. H. Chen, A. Mercer, N. S. Sokol, Let-7-complex microRNAs regulate the temporal identity of Drosophila mushroom body neurons via chinmo. *Dev Cell* **23**, 202-209 (2012).
119. A. Ishizuka, M. C. Siomi, H. Siomi, A Drosophila fragile X protein interacts with components of RNAi and ribosomal proteins. *Genes Dev* **16**, 2497-2508 (2002).

120. B. Laggerbauer, D. Ostareck, E. M. Keidel, A. Ostareck-Lederer, U. Fischer, Evidence that fragile X mental retardation protein is a negative regulator of translation. *Hum Mol Genet* **10**, 329-338 (2001).
121. K. Keleman *et al.*, Dopamine neurons modulate pheromone responses in Drosophila courtship learning. *Nature* **489**, 145-149 (2012).
122. H. Ishimoto, Z. Wang, Y. Rao, C. F. Wu, T. Kitamoto, A novel role for ecdysone in Drosophila conditioned behavior: linking GPCR-mediated non-canonical steroid action to cAMP signaling in the adult brain. *PLoS Genet* **9**, e1003843 (2013).
123. H. Zhu, L. Luo, Diverse functions of N-cadherin in dendritic and axonal terminal arborization of olfactory projection neurons. *Neuron* **42**, 63-75 (2004).
124. X. L. Zhan *et al.*, Analysis of Dscam diversity in regulating axon guidance in Drosophila mushroom bodies. *Neuron* **43**, 673-686 (2004).
125. J. Wang *et al.*, Transmembrane/juxtamembrane domain-dependent Dscam distribution and function during mushroom body neuronal morphogenesis. *Neuron* **43**, 663-672 (2004).
126. J. Wang, C. T. Zugates, I. H. Liang, C. H. Lee, T. Lee, Drosophila Dscam is required for divergent segregation of sister branches and suppresses ectopic bifurcation of axons. *Neuron* **33**, 559-571 (2002).
127. T. Goossens *et al.*, The Drosophila L1CAM homolog Neuroglian signals through distinct pathways to control different aspects of mushroom body axon development. *Development* **138**, 1595-1605 (2011).
128. M. Boyle, A. Nighorn, J. B. Thomas, Drosophila Eph receptor guides specific axon branches of mushroom body neurons. *Development* **133**, 1845-1854 (2006).
129. J. Ng, Wnt/PCP proteins regulate stereotyped axon branch extension in Drosophila. *Development* **139**, 165-177 (2012).
130. K. Shimizu, M. Sato, T. Tabata, The Wnt5/planar cell polarity pathway regulates axonal development of the Drosophila mushroom body neuron. *J Neurosci* **31**, 4944-4954 (2011).
131. N. Grillenzoni, A. Flandre, C. Lasbleiz, J. M. Dura, Respective roles of the DRL receptor and its ligand WNT5 in Drosophila mushroom body development. *Development* **134**, 3089-3097 (2007).
132. S. M. Kelly *et al.*, The Drosophila ortholog of the Zc3h14 RNA binding protein acts within neurons to pattern axon projection in the developing brain. *Developmental neurobiology*, (2015).
133. B. Lu, H. Vogel, Drosophila models of neurodegenerative diseases. *Annu Rev Pathol* **4**, 315-342 (2009).
134. C. Li, G. J. Bassell, Y. Sasaki, Fragile X Mental Retardation Protein is Involved in Protein Synthesis-Dependent Collapse of Growth Cones Induced by Semaphorin-3A. *Front Neural Circuits* **3**, 11 (2009).
135. P. Rorth, A modular misexpression screen in Drosophila detecting tissue-specific phenotypes. *Proceedings of the National Academy of Sciences of the United States of America* **93**, 12418-12422 (1996).

136. S. S. Siller, K. Broadie, Neural circuit architecture defects in a Drosophila model of Fragile X syndrome are alleviated by minocycline treatment and genetic removal of matrix metalloproteinase. *Dis Model Mech* **4**, 673-685 (2011).
137. S. A. Barbee *et al.*, Staufen- and FMRP-containing neuronal RNPs are structurally and functionally related to somatic P bodies. *Neuron* **52**, 997-1009 (2006).
138. A. M. Cziko *et al.*, Genetic modifiers of dFMR1 encode RNA granule components in Drosophila. *Genetics* **182**, 1051-1060 (2009).
139. P. Jin *et al.*, Biochemical and genetic interaction between the fragile X mental retardation protein and the microRNA pathway. *Nat Neurosci* **7**, 113-117 (2004).
140. D. C. Zarnescu *et al.*, Fragile X protein functions with lgl and the par complex in flies and mice. *Dev Cell* **8**, 43-52 (2005).
141. Y. Feng *et al.*, Fragile X mental retardation protein: nucleocytoplasmic shuttling and association with somatodendritic ribosomes. *The Journal of neuroscience : the official journal of the Society for Neuroscience* **17**, 1539-1547 (1997).
142. D. M. Green *et al.*, Nab2p is required for poly(A) RNA export in Saccharomyces cerevisiae and is regulated by arginine methylation via Hmt1p. *The Journal of biological chemistry* **277**, 7752-7760 (2002).
143. M. Kim, M. Bellini, S. Ceman, Fragile X mental retardation protein FMRP binds mRNAs in the nucleus. *Mol Cell Biol* **29**, 214-228 (2009).
144. Z. Yang, H. J. Edenberg, R. L. Davis, Isolation of mRNA from specific tissues of Drosophila by mRNA tagging. *Nucleic Acids Res* **33**, e148 (2005).
145. J. Morales *et al.*, Drosophila fragile X protein, DFXR, regulates neuronal morphology and function in the brain. *Neuron* **34**, 961-972 (2002).
146. J. Rha *et al.*, The RNA-binding protein, ZC3H14, is required for proper polyadenylation and brain function in mice. *Submitted*, (2016).
147. J. C. Darnell *et al.*, FMRP stalls ribosomal translocation on mRNAs linked to synaptic function and autism. *Cell* **146**, 247-261 (2011).
148. R. Lu *et al.*, The fragile X protein controls microtubule-associated protein 1B translation and microtubule stability in brain neuron development. *Proceedings of the National Academy of Sciences of the United States of America* **101**, 15201-15206 (2004).
149. F. Zalfa *et al.*, The fragile X syndrome protein FMRP associates with BC1 RNA and regulates the translation of specific mRNAs at synapses. *Cell* **112**, 317-327 (2003).
150. B. R. Malik, J. J. Hodge, CASK and CaMKII function in Drosophila memory. *Front Neurosci* **8**, 178 (2014).
151. S. I. Ashraf, A. L. McLoon, S. M. Sclarsic, S. Kunes, Synaptic protein synthesis associated with memory is regulated by the RISC pathway in Drosophila. *Cell* **124**, 191-205 (2006).
152. R. F. Stocker, G. Heimbeck, N. Gendre, J. S. de Belle, Neuroblast ablation in Drosophila P[GAL4] lines reveals origins of olfactory interneurons. *J Neurobiol* **32**, 443-456 (1997).

153. T. Komiyama, W. A. Johnson, L. Luo, G. S. Jefferis, From lineage to wiring specificity. POU domain transcription factors control precise connections of Drosophila olfactory projection neurons. *Cell* **112**, 157-167 (2003).
154. S. W. Leung *et al.*, Splice variants of the human ZC3H14 gene generate multiple isoforms of a zinc finger polyadenosine RNA binding protein. *Gene* **439**, 71-78 (2009).
155. K. M. Ahmed, M. Fan, D. Nantajit, N. Cao, J. J. Li, Cyclin D1 in low-dose radiation-induced adaptive resistance. *Oncogene* **27**, 6738-6748 (2008).
156. A. G. Rondón, S. Jimeno, A. Aguilera, The interface between transcription and mRNP export: from THO to THSC/TREX-2. *Biochim Biophys Acta* **1799**, 533-538 (2010).
157. J. I. Piruat, A. Aguilera, A novel yeast gene, THO2, is involved in RNA pol II transcription and provides new evidence for transcriptional elongation-associated recombination. *EMBO J* **17**, 4859-4872 (1998).
158. K. S. Kosik, E. A. Finch, MAP2 and tau segregate into dendritic and axonal domains after the elaboration of morphologically distinct neurites: an immunocytochemical study of cultured rat cerebrum. *J Neurosci* **7**, 3142-3153 (1987).
159. H. Togashi *et al.*, Interneurite affinity is regulated by heterophilic nectin interactions in concert with the cadherin machinery. *J Cell Biol* **174**, 141-151 (2006).
160. G. Stefani, C. E. Fraser, J. C. Darnell, R. B. Darnell, Fragile X Mental Retardation Protein Is Associated with Translating Polyribosomes in Neuronal Cells. *The Journal of Neuroscience* **24**, 7272-7276 (2004).
161. P. P. Roux *et al.*, RAS/ERK signaling promotes site-specific ribosomal protein S6 phosphorylation via RSK and stimulates cap-dependent translation. *J Biol Chem* **282**, 14056-14064 (2007).
162. Y. Li, L. Lin, P. Jin, The microRNA pathway and fragile X mental retardation protein. *Biochim Biophys Acta* **1779**, 702-705 (2008).
163. M. R. Fabian *et al.*, Mammalian miRNA RISC recruits CAF1 and PABP to affect PABP-dependent deadenylation. *Mol Cell* **35**, 868-880 (2009).
164. M. R. Khan *et al.*, Amyloidogenic Oligomerization Transforms Drosophila Orb2 from a Translation Repressor to an Activator. *Cell* **163**, 1468-1483 (2015).
165. J. Hu, S. Gao, Mutant of RNA Binding Protein Zc3h14 Causes Cell Growth Delay/Arrest through Inducing Multinucleation and DNA Damage. *JSM Biochem Mol Biol* **2**, (2014).
166. S. Kaech, G. Banker, Culturing hippocampal neurons. *Nature protocols* **1**, 2406-2415 (2006).
167. G. M. Beaudoin *et al.*, Culturing pyramidal neurons from the early postnatal mouse hippocampus and cortex. *Nature protocols* **7**, 1741-1754 (2012).
168. I. Guillemin, M. Becker, K. Ociepka, E. Friauf, H. G. Nothwang, A subcellular prefractionation protocol for minute amounts of mammalian cell cultures and tissue. *Proteomics* **5**, 35-45 (2005).

169. L. K. Myrick *et al.*, Independent role for presynaptic FMRP revealed by an FMR1 missense mutation associated with intellectual disability and seizures. *Proc Natl Acad Sci U S A* **112**, 949-956 (2015).
170. J. B. Zang *et al.*, A mouse model of the human Fragile X syndrome I304N mutation. *PLoS Genet* **5**, e1000758 (2009).
171. S. T. Sit, E. Manser, Rho GTPases and their role in organizing the actin cytoskeleton. *J Cell Sci* **124**, 679-683 (2011).
172. A. Boureux, E. Vignal, S. Faure, P. Fort, Evolution of the Rho family of ras-like GTPases in eukaryotes. *Mol Biol Evol* **24**, 203-216 (2007).
173. X. R. Bustelo, V. Sauzeau, I. M. Berenjeno, GTP-binding proteins of the Rho/Rac family: regulation, effectors and functions in vivo. *Bioessays* **29**, 356-370 (2007).
174. A. J. Ridley, Rho GTPases and actin dynamics in membrane protrusions and vesicle trafficking. *Trends Cell Biol* **16**, 522-529 (2006).
175. Z. L. Hua, F. E. Emiliani, J. Nathans, Rac1 plays an essential role in axon growth and guidance and in neuronal survival in the central and peripheral nervous systems. *Neural Dev* **10**, 21 (2015).
176. A. Y. Nakayama, M. B. Harms, L. Luo, Small GTPases Rac and Rho in the maintenance of dendritic spines and branches in hippocampal pyramidal neurons. *The Journal of neuroscience : the official journal of the Society for Neuroscience* **20**, 5329-5338 (2000).
177. K. Um *et al.*, Dynamic control of excitatory synapse development by a Rac1 GEF/GAP regulatory complex. *Dev Cell* **29**, 701-715 (2014).
178. K. F. Tolias, J. G. Duman, K. Um, Control of synapse development and plasticity by Rho GTPase regulatory proteins. *Prog Neurobiol* **94**, 133-148 (2011).
179. A. Hall, C. D. Nobes, Rho GTPases: molecular switches that control the organization and dynamics of the actin cytoskeleton. *Philos Trans R Soc Lond B Biol Sci* **355**, 965-970 (2000).
180. Y. Bai, X. Xiang, C. Liang, L. Shi, Regulating Rac in the nervous system: molecular function and disease implication of Rac GEFs and GAPs. *Biomed Res Int* **2015**, 632450 (2015).
181. D. R. Cook, K. L. Rossman, C. J. Der, Rho guanine nucleotide exchange factors: regulators of Rho GTPase activity in development and disease. *Oncogene* **33**, 4021-4035 (2014).
182. C. A. Droppelmann, D. Campos-Melo, K. Volkening, M. J. Strong, The emerging role of guanine nucleotide exchange factors in ALS and other neurodegenerative diseases. *Front Cell Neurosci* **8**, 282 (2014).
183. M. Sone *et al.*, Still life, a protein in synaptic terminals of Drosophila homologous to GDP-GTP exchangers. *Science* **275**, 543-547 (1997).
184. G. Bollag, A. M. Crompton, D. Peverly-Mitchell, G. G. Habets, M. Symons, Activation of Rac1 by human Tiam1. *Methods Enzymol* **325**, 51-61 (2000).
185. D. K. Worthylake, K. L. Rossman, J. Sondek, Crystal structure of Rac1 in complex with the guanine nucleotide exchange region of Tiam1. *Nature* **408**, 682-688 (2000).

186. J. Q. Ni *et al.*, A Drosophila resource of transgenic RNAi lines for neurogenetics. *Genetics* **182**, 1089-1100 (2009).
187. J. G. Duman, S. Mulherkar, Y. K. Tu, X. C. J, K. F. Tolias, Mechanisms for spatiotemporal regulation of Rho-GTPase signaling at synapses. *Neurosci Lett* **601**, 4-10 (2015).
188. R. Gombos *et al.*, The Formin DAAM Functions as Molecular Effector of the Planar Cell Polarity Pathway during Axonal Development in Drosophila. *The Journal of neuroscience : the official journal of the Society for Neuroscience* **35**, 10154-10167 (2015).
189. F. Ozsolak, P. M. Milos, RNA sequencing: advances, challenges and opportunities. *Nat Rev Genet* **12**, 87-98 (2011).
190. Y. Han, S. Gao, K. Muegge, W. Zhang, B. Zhou, Advanced Applications of RNA Sequencing and Challenges. *Bioinform Biol Insights* **9**, 29-46 (2015).
191. J. C. Darnell, E. Klann, The translation of translational control by FMRP: therapeutic targets for FXS. *Nat Neurosci* **16**, 1530-1536 (2013).
192. S. Chang *et al.*, Identification of small molecules rescuing fragile X syndrome phenotypes in Drosophila. *Nat Chem Biol* **4**, 256-263 (2008).
193. C. Gross *et al.*, Selective role of the catalytic PI3K subunit p110beta in impaired higher order cognition in fragile X syndrome. *Cell Rep* **11**, 681-688 (2015).
194. B. R. Malik, J. M. Gillespie, J. J. Hodge, CASK and CaMKII function in the mushroom body alpha'/beta' neurons during Drosophila memory formation. *Front Neural Circuits* **7**, 52 (2013).
195. J. Lisman, H. Schulman, H. Cline, The molecular basis of CaMKII function in synaptic and behavioural memory. *Nat Rev Neurosci* **3**, 175-190 (2002).
196. S. De Rubeis, C. Bagni, Regulation of molecular pathways in the Fragile X Syndrome: insights into Autism Spectrum Disorders. *J Neurodev Disord* **3**, 257-269 (2011).
197. S. Soucek *et al.*, The Evolutionarily-conserved Polyadenosine RNA Binding Protein, Nab2, Cooperates with Splicing Machinery to Regulate the Fate of pre-mRNA. *Mol Cell Biol*, (2016).
198. S. I. Kuhlmann, E. Valkov, M. Stewart, Structural basis for the molecular recognition of polyadenosine RNA by Nab2 Zn fingers. *Nucleic Acids Res* **42**, 672-680 (2014).
199. K. Kim Guisbert, K. Duncan, H. Li, C. Guthrie, Functional specificity of shuttling hnRNPs revealed by genome-wide analysis of their RNA binding profiles. *RNA* **11**, 383-393 (2005).
200. S. Kimura *et al.*, The Drosophila lingerer protein cooperates with Orb2 in long-term memory formation. *J Neurogenet* **29**, 8-17 (2015).
201. J. E. Kwak *et al.*, GLD2 poly(A) polymerase is required for long-term memory. *Proceedings of the National Academy of Sciences of the United States of America* **105**, 14644-14649 (2008).
202. T. Udagawa *et al.*, Bidirectional control of mRNA translation and synaptic plasticity by the cytoplasmic polyadenylation complex. *Mol Cell* **47**, 253-266 (2012).

203. J. Riedl *et al.*, Lifeact: a versatile marker to visualize F-actin. *Nat Methods* **5**, 605-607 (2008).